RESTWES

October, 1999

Contents

1 Introduction

1.1 Background

Currently, the Western Scheldt estuary is the focus of much infrastructural activity with potential impacts to water quality and ecology: Specifically, construction of a tunnel under the estuary, linking Terneuzen in Zeeuwsch-Vlaanderen and Ellewoutsdijk in Midden-Zeeland is beginning (mid 1999). As a result, an estimated 1.5 million m^3 of fine material will be dumped in the estuary over a period of several years, potentially affecting Suspended Particulate Matter (SPM)[1] concentrations (turbidity) and the composition of the bed sediment in tidal flats. This can further affect the habitat suitability for various species. Additionally, dredging activities to deepen the shipping channel to Antwerp Harbour will result in additional dumping of dredged bottom sediment.

The existing monitoring infrastructure (facilities and programmes) for the Western Scheldt are not appropriate for following the potential detailed changes resulting from the dumping of the tunnel boring material. There is a need for monitoring information with a detailed spatial and temporal resolution.

The existing conditions of turbidity and suspended concentrations in the estuary are highly dynamic due to the significant amount of silt that is naturally brought into suspension due to tidal forces. Thus it is not certain to what extent the dumping of the tunnel boring material will be 'visible'. However, there is desire and legal responsibility for the Directorate Zeeland to monitor the environmental effects of the construction activities. The Directorate Zeeland is busy setting up a monitoring program and has established two monitoring stations for continuous measurement of turbidity and fluorescence.

Additionally, the use of optical remote sensing and water quality models is being considered for operational monitoring. The interlinked use of remote sensing, in-situ information and modelling to improve knowledge of water quality and ecology has been investigated in recent years using the RESTWAQ (Remote Sensing as Tool for improved knowledge on WAter Quality and ecology) methodology. Through applications to the Southern North Sea, the Dutch Coastal zone and the Frisian lakes, RESTWAQ has proved to be a very valuable method to improve knowledge on water quality (especially SPM and light climate). The use of the RESTWAQ methodology for monitoring the Western Scheldt estuary is expected to provide a more complete picture of the spatial and temporal developments in the estuary water system. With the methodology, the chance of observing changes in the system will be increased, and resolution of any spatial changes due to dumping will be much higher.

[1] *Many different terms are used to indicate particulate matter: Suspended Particulate Matter (SPM), Total Suspended Matter (TSM), seston, silt, etc. In this report, the term Suspended Particulate Matter is used, and is defined as inorganic and organic material that is <63 μ.*

Potential effects from the sediment dumping can be separated into *direct* and *indirect* effects. Expected *direct* effects of the sediment dumping are: increase in sediment concentrations in water (turbidity), changes to flows and bed sediment composition and changes to location/area of tidal flats and channels.

Indirect effects of the sediment dumping are expected on: sedimentation in harbours, dredging activities, sand mining, and ecology.

1.2 Project Objectives

The goals of the project can be summarized as follows:

- to demonstrate the added value of integrated use of in-situ measurements, optical remote sensing data and a water quality model, using the RESTWAQ concept, for assessment of the suspended sediment conditions in the Western Scheldt estuary prior to the dumping of tunnel boring material (T0 situation). This RESTWAQ component of the complete monitoring process will at first be set-up as a prototype due to its innovative character;
- to describe the perspectives for an implementation of the RESTWAQ procedure for monitoring the effects of dumping of the tunnel boring material (T1/T2 phase).

This project, RESTWES (REmote Sensing as Tool for improved management in the WEstern Scheldt) should result in an adequate description of the baseline (T0) situation in the estuary before dumping of the tunnel boring material. The year 1998 has been selected as the 'baseline'. The project should clearly demonstrate the surplus value of the combined use of remote sensing, in-situ and model information for this application.

An additional goal is to extend the RESTWAQ methodology by also classifying tidal flats using remote sensing data. In this component of the project, classification of sand, fine sediment or vegetated areas will be linked to the ecological conditions of the estuary (habitat evaluation).

Perspectives for implementation and operationalization within the RWS environment will be evaluated during the project. The relevant end users are involved in this demonstration so that knowledge transfer can occur efficiently. Additionally, a 'blueprint' defining all the steps and procedures necessary for implementing the methodology is being prepared.

1.3 General Procedure

The following main steps are identified in RESTWES:

1. Acquisition of relevant remote sensing and in situ data over 1998, the period which was chosen to be indicative for the T0 situation in the Western Scheldt.
2. Measurement of optical properties of suspended matter in the Western Scheldt, development of an optical model, and processing of remote sensing images to produce SPM concentration maps;
3. Set-up and initial calibration of a dynamic water quality model for the Western Scheldt.
4. Integration of RS with data from water quality models and in-situ measurement using cost functions, for final calibration of the water quality model;

5. Definition of baseline (T0) conditions of SPM in the Westen Scheldt and production of a number of information products illustrating baseline conditions;
6. Prediction of T1 conditions of SPM in the Westen Scheldt for a dumping scenario of 1 million tons of tunnel silt over 1 year.
7. Classification of tidal flat composition and habitat evaluation for a selected key species (e.g. the Cockle) in the Western Scheldt Estuary for the baseline conditions (see 'RESTWES Ecology' Baptist and Peters, 1999);
8. Specification of the implementation procedures for application of the RESTWAQ methodology (in an operational system) for the Western Scheldt Estuary ('blueprint').

While this project is seen as somewhat of a demonstration of the RESTWAQ methodology for the Western Scheldt, it is hoped that in a following phase, the procedure will be extended for use in operational monitoring once the dumping of the tunnel material has commenced.

1.4 This report

The RESTWES study is being conducted by a team of institutes including RWS-RIKZ, WL|Delft Hydraulics, IvM, RWS-MD, RWS-DZ and KNMI. This report describes the work that has been conducted by WL|Delft Hydraulics and IvM during on the main component of RESTWES corresponding to i.e. analysis of SPM in the water phase of the Western Scheldt through an integration of 3 components information sources, namely:

- In-situ data
- Remote sensing
- Water quality modelling

In Chapters 2-4, the main activities and results for each of these components are presented. In Chapter 5, comparison of results from the different information sources is made. In Chapter 6, the results of model predictions for a T1 scenario are given. In Chapter 7, conclusions of the present study and recommendations for the T1 monitoring are given. Appendix A and B give details of the water quality model set-up and calibration using the cost function.

The development of algorithms for processing remote sensing images, and preparation of SPM maps from remote sensing are described in detail in Peters et al., 1999. The use of remote sensing for classification of tidal flats and for assessing the potential ecological impacts of the tunnel material dumping are presented in Baptist and Peters, 1999.

These studies have all been financed by the BCRS with support from the Programmabureau Meetstrategie 2000+.

2 In-situ data

2.1 Introduction

An overview of available in-situ data for RESTWES has been made by RIKZ (Hoogenboom, 1999). In-situ data of concern for RESTWES consist of continuous monitoring, and project based data of suspended particulate matter and turbidity. These data are one of the main information sources about suspended sediment conditions in the Western Scheldt. Tidal cycle data (water levels) and wind data corresponding to the in-situ measurements are crucial for interpretation of the in-situ measurements and these are also available.

The SPM in-situ values are also necessary for input and calibration of the water quality model, and for validating the processed remote sensing images (conversion of reflectance signal to a concentration).

In this chapter, the available SPM in-situ data is reviewed and a short analysis made of the important trends and patterns which can be seen in the data. Available wind data is also presented, and potential relation between wind and in-situ SPM concentrations are discussed.

2.2 SPM data

A number of sources of in-situ SPM data in the Western Scheldt is available (Hoogenboom, 1999):

- Continuous monitoring stations (Vlissingen, Terneuzen and Baalhoek)
- Project oriented monitoring data (e.g. van Maldegem, ECOFLAT, Life Westerschelde, GEM, MATURE, Borgerhout)
- Rijkswaterstaat MWTL network

These data are not all readily (digitally) available (especially project oriented data), and data cover different time periods, frequencies, and locations. After a review of available data, the following 2 data sets have shown to be the most useful for illustrating important suspended sediment trends and processes, and calibrating and validating the water quality model and the remote sensing processing:

1. Project data from van Maldegem (1992): Long-term monthly averaged SPM concentrations are available at 9 locations in the Western Scheldt for the period 1970-1990, see Figures 2.1 and 2.2.
2. Continuous monitoring data from 3 fixed stations: Vlissingen, Terneuzen and Baalhoek.

Figure 2.1 Locations of 9 monitoring stations for long-term monthly averaged SPM concentrations (1970-1990). Also, the 14 segments of the Western Scheldt SAWES model are shown (van Maldegem, 1992)

Figure 2.2 Monthly averaged SPM concentrations (1970-1990) at 9 locations in the Western Scheldt.

2.2.1 Continuous monitoring stations

Fixed monitoring stations at locations Vlissingen, Terneuzen and Baalhoek recorded on a continuous basis (every 10 minutes) during all or parts of 1998. All stations monitor turbidity (as optical backscattering, OBS) and fluorescence, which must be converted to obtain SPM concentrations in mg/l. The stations have been established and are operated for Directorate Zeeland by RIKZ. Locations are shown in Figure 2.3.

The station at Vlissingen was an existing station and was operating for all of 1998, measuring at one depth of -4.5 m NAP. In November and December, a technical problem with the instrument prevented measurements of high signals, corresponding to concentrations above ~70 mg/l.

The stations at Baalhoek and Terneuzen were established specifically for monitoring SPM conditions in the Western Scheldt prior to dumping of tunnel material. The station Baalhoek was operational starting on 1 October 1998, measuring at one depth of -4.5 m NAP. The station Teurneuzen measures at 3 fixed depths of -4, -11, and -17 m NAP and was operational starting on 26 October 1998.

The locations for these two stations were chosen because there was a previously existing monitoring station (meetpaal) at each point, and thus measuring instruments could be installed relatively easily. The monitoring station at Terneuzen, located at 'steiger DOW', is at the location for dumping the tunnel material, and is actually within the region selected for discharge of the tunnel material by pipeline (Figure 2.4). The monitoring station Baalhoek is approximately 50 km upstream from the dumping location, near Saeftinghe, a region of great ecological importance.

Data from the 3 stations for all of 1998 are presented in Figure 2.5. Data for Terneuzen are from the shallowest depth (-4.5 NAP). A thinning of the data was made for these plots: one data point every 2 hours.

In 1998, stations Terneuzen and Baalhoek were only operational in the period October - December, and the data for this period are presented in Figure 2.6 (one date point every 2 hours). Detailed data for the station Baalhoek for the month of October only are given in Figure 2.7 (one data point every 10 minutes).

A comparison of data from different depths for Station Terneuzen for months October and November is given in Figure 2.8. In October, data were not available at depth -17m NAP.

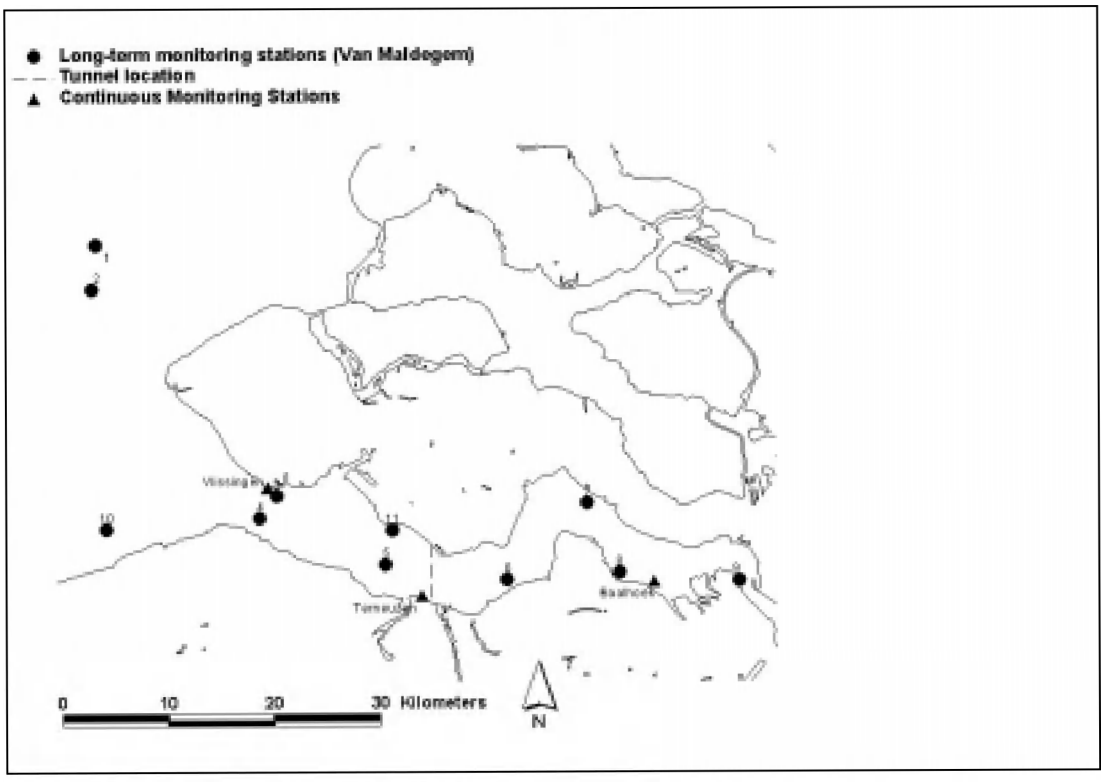

Figure 2.3 Location of continuous monitoring stations together with Van Maldegem stations

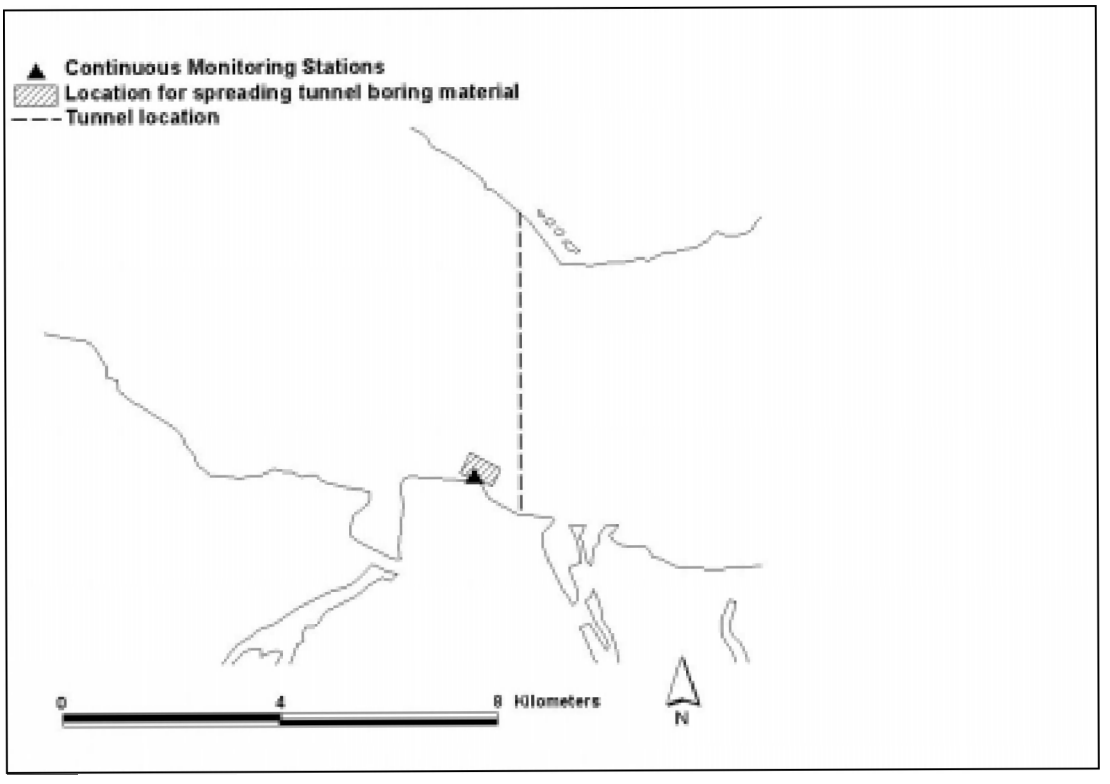

Figure 2.4 Location of continuous monitoring station Terneuzen with respect to the tunnel material 'dumping' location (discharge will most likely be via pipeline)

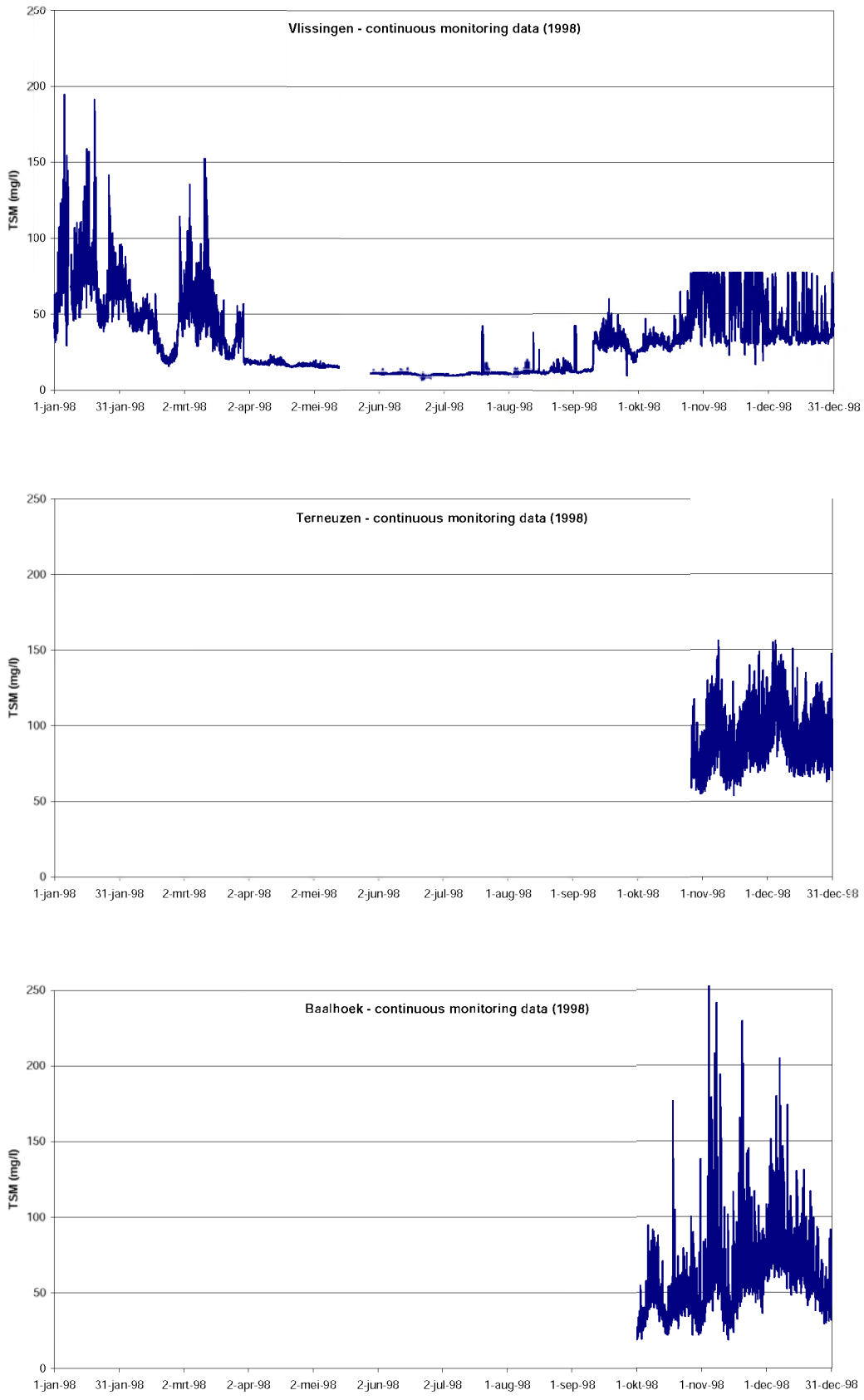

Figure 2.5 Continuous monitoring data of SPM (mg/l) in 1998 (data very 2 hours)

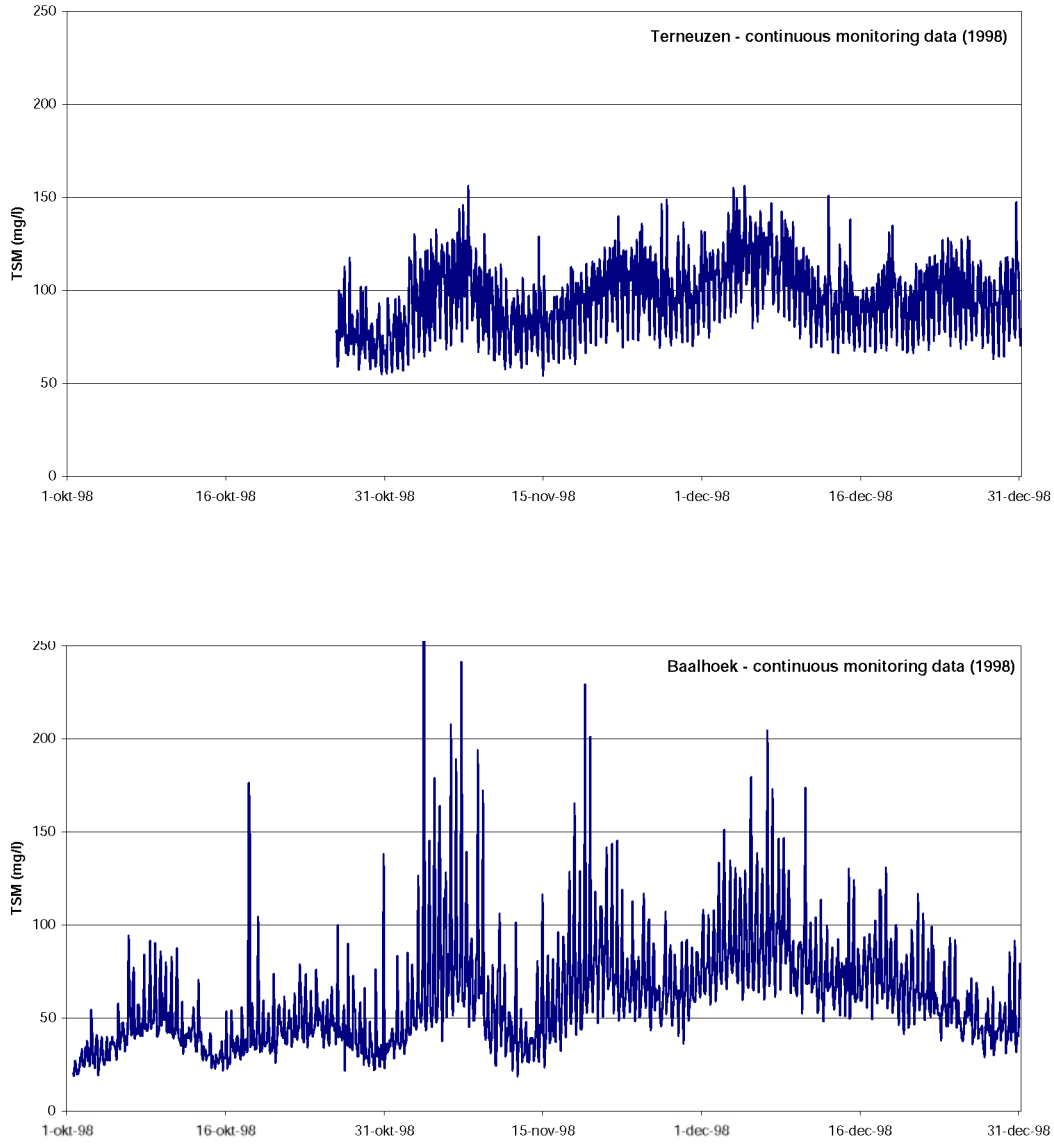

Figure 2.6 Continuous monitoring data at stations Terneuzen and Baalhoek (October - December, 1998; one data point every 2 hours). Here the concentration variation over the spring-neap cycle of ~14.5 days can clearly be seen.

Figure 2.7 Continuous SPM concentrations at Station Baalhoek (October - December, 1998). Here the concentration variation over the tidal cycle can clearly be seen (data every 10 minutes).

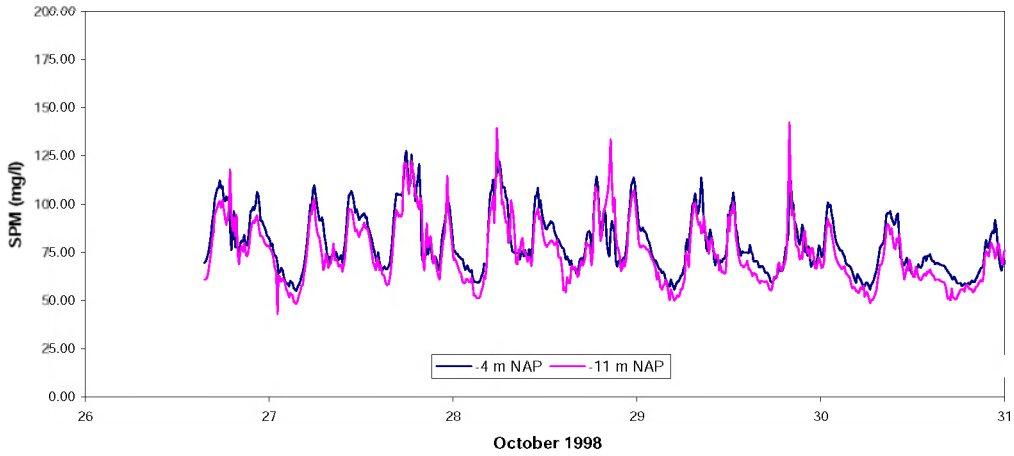

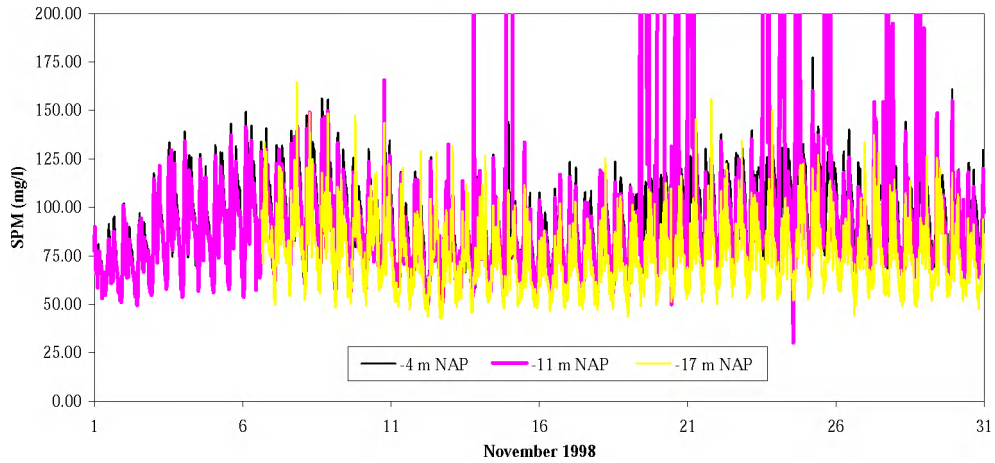

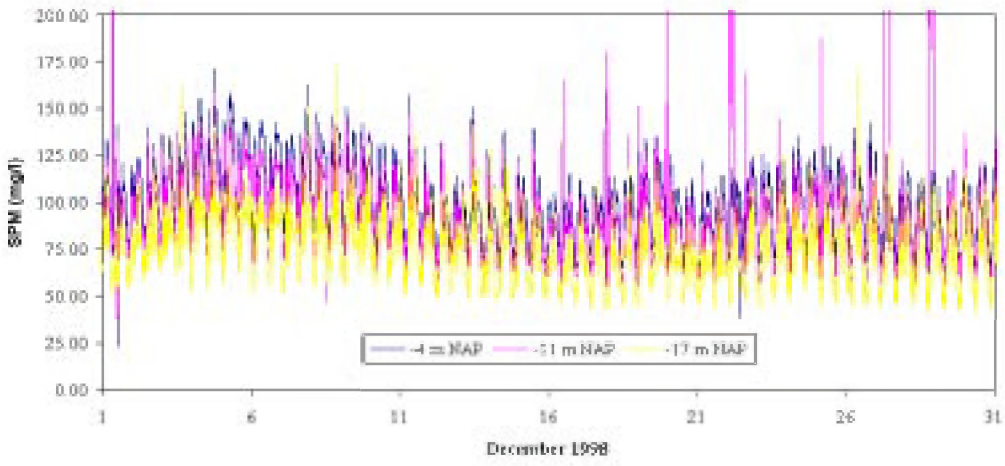

Figure 2.8 SPM concentrations at Station Terneuzen at multiple depths (data every 2 hours)

2.2.2 Trends and patterns in the in-situ data

The selected data sets for SPM measurements show several important trends and patterns in the in-situ data over different time scales.

1. Seasonal cycle over 1 year.
Long-term monthly averaged data (1970-1990) of SPM concentrations in the surface water at 9 locations in the Western Scheldt estuary show a clear seasonal cycle, with the lowest concentrations in the summer months June and July (Figure 2.2). Highest concentrations are seen in December and January. At station Vlissingen, for example, winter concentrations are approximately 50 (± 20) mg/l, while summer concentrations are approximately 15 (± 10) mg/l. Other stations show the same pattern, with different concentration ranges, and varying degrees of variability (standard deviation) over the months. The continuous monitoring data at Vlissingen also shows this seasonal trend (Figure 2.5), though the recording instrument had some disturbance in November-December and could not register any signal corresponding to values above ~70- mg/l.

2. Spring -Neap cycle of 14 days.
The variation in SPM concentrations over the spring-neap tidal cycle can most clearly be seen in the continuous measurements at Terneuzen and Baalhoek in the period October-December 1998 (Figure 2.6). These data show concentrations of SPM which have a cycle over approximately 14.5 days, with highest concentrations at spring tide, and lowest concentrations at neap tide . The concentration range in the cycle is small compared to some of the higher frequency peaks which occur, but is consistent through the measured period.

3. Tidal cycle of 12 hours
Due to the tidal cycle of approximately 12.5 hours, there are SPM concentration peaks corresponding to low water levels (or flood tides), and concentration dips corresponding to high water levels. The result is clear peaks in concentration occurring approximately every 12.5 hours, evenly interspersed with dips in concentration. The peaks in the tidal cycle are extremely regular and clear to see in the continuous monitoring data from station Baalhoek (Figure 2.7) in e.g. the period 3 November to 11 December. The relation between concentration, water level and wind is shown for 11 November 1998, Figure 2.9. The peak concentration (0:00 and ~13:00) correspond with rising water (incoming tide). The low concentrations (04:00 and 17:00) correspond most closely with high water.

4. Variation in SPM concentration with Depth
At continuous monitoring station Terneuzen, measurements are made at 3 depths: -4, -11, and -17 m NAP. A comparison of SPM concentrations at different depths over the period October - December 1998 shows that concentrations are very similar (Figure 2.8). In all three months, data from the 2 upper depths are essentially the same. The data from November and December show that the bottom concentrations (-17 NAP) are somewhat lower. On the whole, it can be concluded that the system is well mixed.

5. Wind effects
Wind has a strong effect on SPM concentrations via waves, and thus wind data for 1998 was also analyzed (see section 2.2.3). Wind waves can create a bottom stress on the tidal

flats which causes resuspension of the bottom sediment. It can be seen that periods of high SPM concentrations correspond to periods of high wind. Storm periods in January and March (i.e. wind >10 m/s) correspond to high SPM concentrations seen in the continuous data at Vlissingen. The high concentrations at Baalhoek in the first half of November are perhaps due to the wind storm in the period 23-31 October. The wind in October does not seem to affect the concentrations at Terneuzen, though unfortunately continuous monitoring data start only at 26 October.

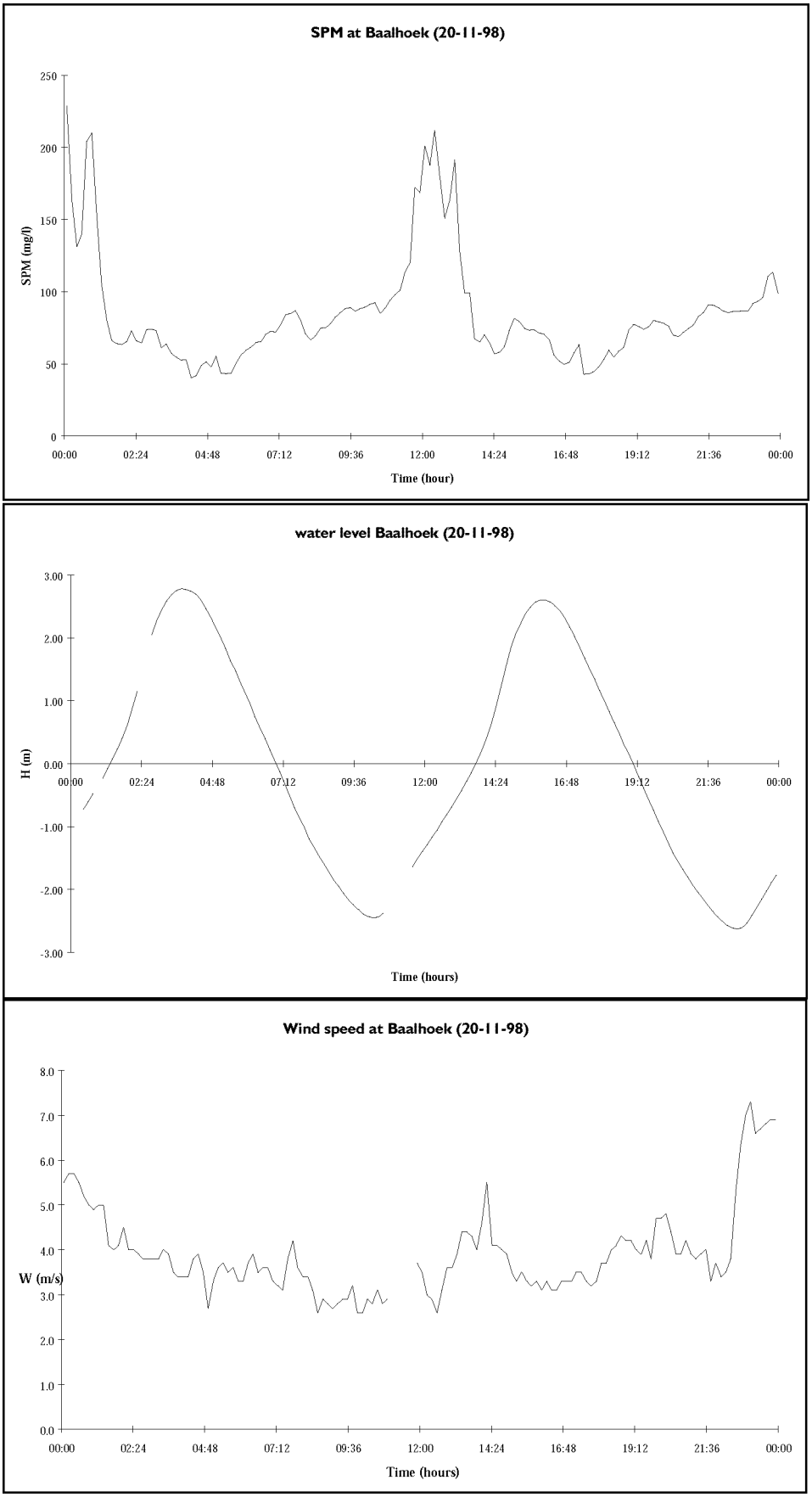

Figure 2.9 SPM concentration, water level and wind at Baalhoek, 20-11-98

2.2.3 Wind data

Because wind can have a significant effect on suspended matter transport (sedimentation and resuspension), some analysis of wind data was made. Wind data from the KNMI are available from Vlissingen on an hourly basis, and from Baalhoek every 10 minutes. Data from Vlissingen are used as input to the water quality model, after they are averaged to daily wind speeds (Figure 2.10). The daily average wind speed is calculated as a quadratic average[2]. Three 'storm' periods of high wind (daily average >10 m/s) can be seen in begin January, begin March and end October-begin November.

To check if there is much spatial difference in the wind over the area of the estuary, a comparison of wind speed as measured at Vlissingen and Baalhoek was made for the period of 21-31 October, 1998, Figure 2.11. The data show that there is no significant difference in wind speed between Vlissingen and Baalhoek. Peak gust and low wind speeds occur at the same time, with similar values. Thus there is no problem in using the Vlissingen data for the whole model area.

The daily averaged values obviously show less variability and less extreme values than the higher frequency data. During the selected period in October, daily averaged values are between 8-17 m/s, while some of the higher frequency wind data measure speeds as high as 23 m/s and as low as 5 m/s. This is not expected to have a significant effect in the model calculation.

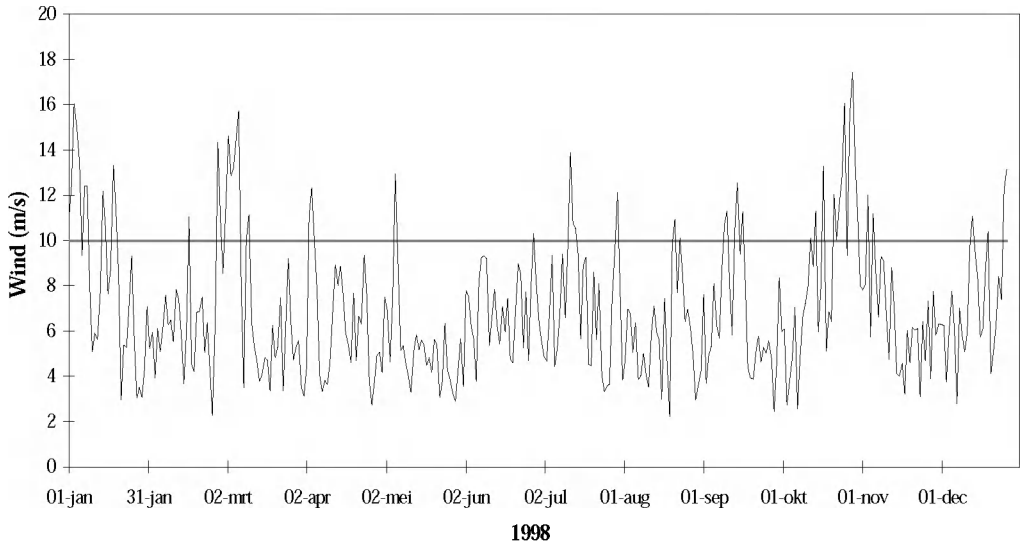

Figure 2.10 Daily average wind speed at Vlissingen. 'Storm' periods of high wind (daily average >10 m/s) can be seen in begin January, begin March and end October-begin November.

[2] *Daily average wind speed calculation from 24 hourly values:*

$$W_{daily\ ave} = \frac{\sqrt{w_1^2 + w_2^2 + \ldots + w_{24}^2}}{24}$$

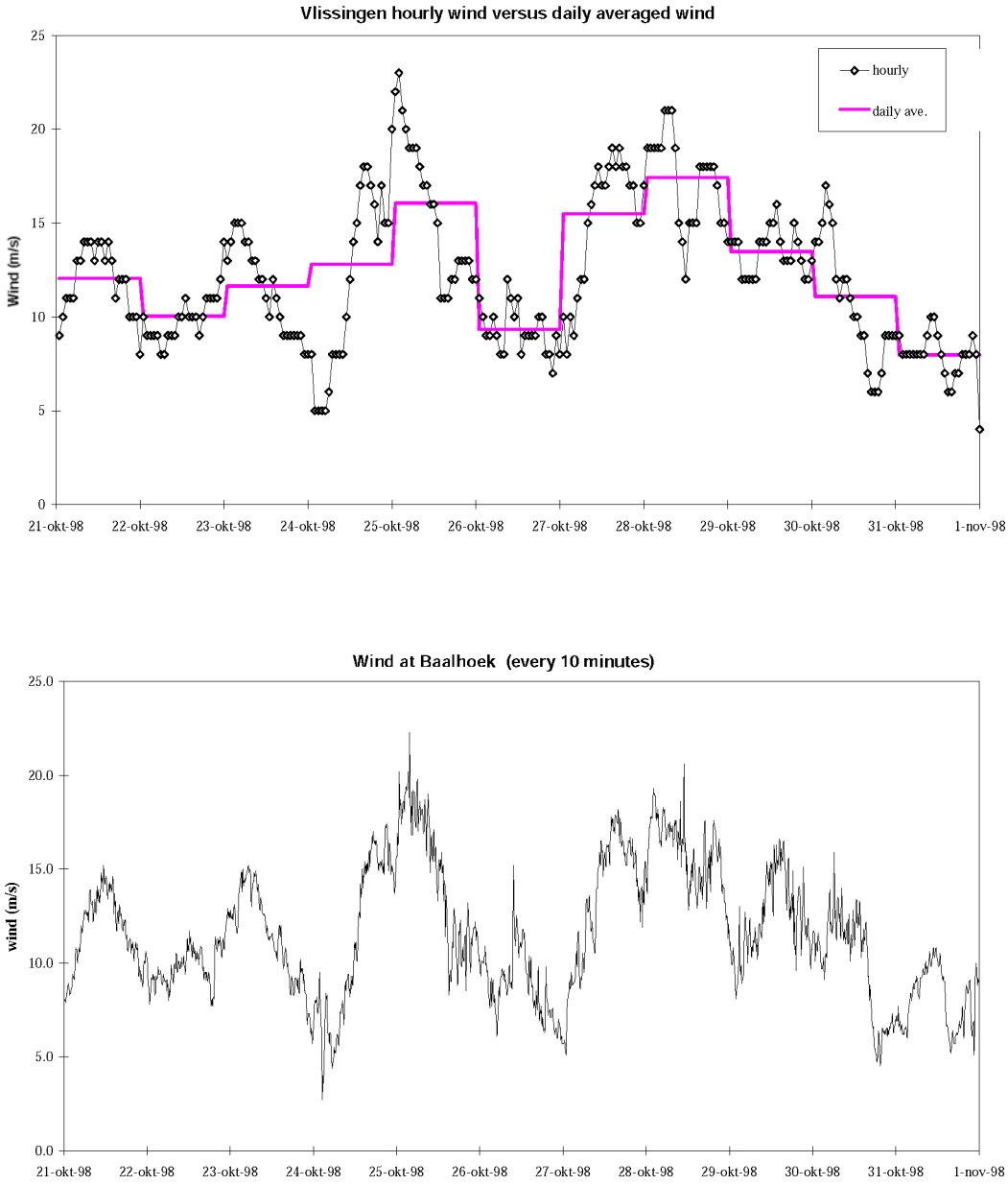

Figure 2.11 Wind data at Vlissingen (daily average and hourly) and Baalhoek (10 minutes), 21-31 October, 1998

3 Remote Sensing

3.1 Selection of remote sensing data

A number of satellites/sensors are potentially available for assessment of water quality, specifically SPM: NOAA/AVHRR, SeaWifs, LandSat, and SPOT. It was decided to use remote sensing images from the SPOT satellite for a number of factors, including image resolution (pixel size), availability/frequency, and cost. NOAA and SeaWifs have a resolution of approximately 1 x 1 km, which is not detailed enough for analysis of water quality in the Western Scheldt. Previous RESTWAQ studies of the North Sea and Dutch coastal zone have used NOAA (Vos et al., 1995-1998), because for these regions the resolution was appropriate. Other limitations of NOAA are saturation of the signal at about 20 mg/l (Vos and Schuttelaar, 1995; van Raaphorst et. al. 1998).

Both LandSat and Spot have higher resolution, 30 x 30 m and 20 x 20 m, respectively. The single LandSat 5 Satellite has a return period of 17 days, which is insufficient to provide many clear images of the region. In contrast, there are several SPOT satellites, and images are available nearly on a daily basis. The LandSat5 images are about 3 times cheaper than SPOT, but are of lower quality (Vos et al., RESTWAQ-2, PART II, 1998). Eventually, images were procured from 3 SPOT satellites (SPOT1, SPOT2 and SPOT4), and some separate processing for each satellite was necessary (see section 3.3).

Fourteen remote sensing images of the Western Scheldt estuary from the SPOT satellite were purchased, covering the period May 1996- November 1998 (Table 3.1). The images can be classified in categories of tidal water level:

- high water;
- mean water; or
- low water

and tidal phase:

- incoming water or 'flood';
- outgoing water or 'ebb';
- water that is at its minimum or maximum direction (reversing direction) or 'slack';

Additionally, images are given a quality ranking, based on the extent to which the image is cloud-free, and the sun elevation (sun angle). In general, the lower sun elevation, the poorer the remote sensing image, because less reflected light reaches the satellite sensor.

Table 3.1. SPOT RS images and their properties

Year	Month	Day	W (m/s)	Wdir	Tide	Direction flow	H(m)	Side	Sun elev.	Quality
1996	may	7	?	?	low	slack	-2.3	E	52.9	++
1997	august	12	?	?	mean	?	-0.5	E	53.2	++
1998	january	11	8	180	high	incoming	0.75	W	15.6	++
1998	april	2	4		low	slack	-2.1	W	42.2	0
1998	may	10	5	90	mean	incoming	-0.3	W	55.3	++
1998	may	10	5	90	mean	incoming	0.4	E	53.6	++
1998	june	1	4	240	low	outgoing	-1	W	58.3	+
1998	july	20	1	240	high	slack	2	E+0.8W	58.7	++
1998	august	6	9	260	high	incoming	1.1	W	53.3	++
1998	august	8	4	260	mean	incoming	-0.5	W+0.5E	52.1	++
1998	august	10	5	100	low	incoming	-0.9	W	53.6	++
1998	oktober	1	1	40	high	outgoing	1	E+0.5W	34.5	0
1998	november	17	5	250	high	incoming	0.7	W+E	18.9	+
1998	november	20	5	120	low	incoming	-0.8	W+E	18.2	0
H was determined at Terneuzen using tidal analysis program										

Of the 14 available images, a selection of 9 images was made for processing based on image characteristics. Images were selected for processing (Table 3.2) based primarily on the quality (++ Quality = Category I), as well as their spatial coverage of the region, and the time when the image was made. The images were selected so that they covered different seasons in the year, as well as different periods within a tidal cycle. Two images were selected in Category II because the provided additional information, not present in Category I:

- the image of May 1996 is of high quality and contains information on the area where effects of dumpings might be found in the future;
- the image of October 1998 contains information on a tidal phase of outgoing flow. In the first category the type 'outgoing flow' is unfortunately not present.

Table 3.2 Remote sensing images selected for processing

Category I										
Year	Month	Day	W (m/s)	Wind dir	Tide	Direction flow	H(m)	Side	Sun elev.	Quality
1998	january	11	8	180	high	incoming	0.75	W	15.6	++
1998	may	10	5	90	mean	incoming	-0.3	W	55.3	++
1998	may	10	5	90	mean	incoming	0.4	E	53.6	++
1998	july	20	1	240	high	slack	2	E+0.8W	58.7	++
1998	august	6	9	260	high	incoming	1.1	W	53.3	++
1998	august	8	4	260	mean	incoming	-0.5	W+0.5E	52.1	++
1998	august	10	5	100	low	incoming	-0.9	W	53.6	++
Category II										
Year	Month	Day	W (m/s)	Wdir	Tide	Direction flow	H(m)	Side	Sun elev.	Quality
1996	may	7	?	?	low	slack	-2.3	E	52.9	++
1998	october	1	1	40	high	outgoing	1	E+0.5W	34.5	0

In addition to SPOT images, a few NOAA/AVHRR images procured from the KNMI. These remote sensing images were also processed to test their usefulness for analysis of SPM patterns at the sea side of the Western Scheldt.

A total of 16 NOAA/AVHRR images was selected and calibrated using the results from a simple SPM model according to the RESTWAQ non-linear extrapolation method (Vos et al., RESTWAQ-2, PART I, 1998). The images were analysed on SPM patterns, and a comparison was made for the image of 14 February 1998 with that of SPOT from the Dali-catalogue of SPOT-Toulouse (this image was not purchased for the project because of some cloud cover).

3.2 Description of remote sensing images

3.2.1 General Description of SPOT RS images

Remote Sensing false colour composites were analysed on their general characteristics. The general conclusions of this inspection was as follows:

1. There is a clear correlation between the observed SPM patterns in the images and depth (at relatively low depth often higher reflections are observed in the images[3]). A map of average water depth for the estuary (for the model) is given in Figure 4.2.
2. There is a correlation between the observed SPM patterns and the tidal phase. At slack water (e.g. 20 July) the SPM patterns are absent indicating low SPM concentrations. For incoming and outgoing water, (some) erosion at tidal flats can be observed and concentrations are probably higher than for slack.
3. In winter, there is a clear triangle of relatively high SPM at the Vlakte van Raan, at the mouth of the Western Scheldt. This feature can be seen on 11 January, and 10 and 14 February from Dali Catalogue. A reprint of the false colour composite of 14 February[4] from the Dali Catalogue is given in Figure 3.3). This region of higher concentrations might be related to SPM that is washed out from the bottom from dumpings during the winter period (de Bie and Benijts, 1994). Until now, this the water quality of this area has hardly been sampled. However, so much silt was not expected since the bottom sediment in this area is mostly sand (1-10% silt). An example is shown in section 3.3, Figure 3.3.
4. The outflow of silt from the Belgium part of the Scheldt into the Dutch part is clearly recognisable, and can in some cases be related to the tidal phase. Reflections in the eastern part of the Scheldt are higher than for the Western part of the Scheldt indicating higher SPM concentrations. An example is given in the false colour composite, Figure 3.1.

[3] *A high reflectance corresponds with a higher SPM concentration for cloud-free, atmospherically corrected images, and assuming the absence of bottom reflection. Bottom reflectance occurs in the Western Scheldt estuary only near or at tidal flats (depth < 1-2 m).*

[4] *This image was not purchased because of extensive cloud cover and haziness in the estuary. The image is however, excellent for the North sea.*

5. The area below *Plaat van Baarland* is turbid in all images (this location is not sampled by the local authorities, co-ordinates are roughly (3°54', 51°22')). This was not expected since this area has a bottom with only a few-% sand (Van Essen and Hartholt, 1999), except for one small spot where the silt fraction is high (25%-50%). A detailed map of this area shows a complex bottom topography with various small flats (Hydrografische kaart, 1997).
6. At Breskens the water column is more turbid than at Vlissingen.

Figure 3.1 False colour composite of SPOT for 10 May 1998 (incoming water, rising tide). The influx of SPM form the Belgium part of the Scheldt can be seen.

The false color images were analyzed for patterns and features of SPM. A general description, and an overview of some important features for each image is given in Table 3.3.

Table 3.3. Description of SPM patterns in SPOT RS images

Year	Month / day	Remarks
1996	May 7	1. Silt follows river gully, river curves are clean. 2. River silt goes beyond Saefthinge 3. Interesting structures at tidal flats. At Doel the 'Leidam' is visible.
1997	August 12	1 River gully is relatively clean but silt is observed at curves of gully because of erosion. 2 Silt erodes from tidal flats, high concentration below Plaat van Baarland. 3 Also estuary gully is clean. There is remarkably no silt visible at 'Lage and Hoge Springer' whereas this area is known to be turbid, and has a bottom with a high silt content.
1998	January 11	This image corresponds very nicely with the depth contours of the Western Scheldt area since at relatively shallow areas the turbidity is higher: 1. Honte is deep and relatively clear; 2. Schaar van Spijker is shallow and relatively turbid; 3. Lage and Hoge Springer is shallow and bottom has high silt content: area is relatively turbid 4. High reflectance at Hooge Platen and Middelplaat with erosion at west side since water flows into the estuary; 5. Vlakte van Raan is relatively turbid. However, a gully ('insteek') below Kaloo with somewhat larger depth is visible as a somewhat less turbid area; 6. The Oostgat and Deurlo gullies can be discriminated as relatively clear water 7. Arera below Everingen is turbid. Bottom sediment maps shows only sand here? Origin of this silt may be: • This is a shallow area in general; • Silt erodes from Boeregat which has a very high silt content in the bottom; 8. The concentrations at MP2 (continuous OBS measurements) of the Kust2000 in-situ campaign are 1.5 times higher than those at MP1 (the OBS signals we not calibrated unfortunately). This is in agreement with Remote Sensing;
1998	April 2	1. A gradient left of Oostgat is again clearly present; 2. Silt at Schaar van Spijkerplaat increases; 3. A dumping of dry silt at Breskens of 0.4 kton (total in one day), is clearly visible; the ferry just passes this silt patch of dumped material. The ebb tide is retrieved correctly from the movement of the patch; 4. Silt at Lage Springer is clearly visible; 5. High silt below Everingen-Baarland.
1998	May 10 (West)	1. Silt erodes from Hoge platen, Schaar van Spijkerplaat is turbid, lot of silt below Plaat van Baarland; 2. Silt does not follow gully, gully is relatively clean. 3. There is at sea a remarkable green spot visible at Vlakte van Raan in the false colour composite. The image shows a lot of remarkable stripes probably smearing of material due to wind at the surface. According to RIKZ (L. Peperzak) there was a *Phaeocystis* bloom at this site during this period.
1998	May 10 (East)	1. The Scheldt river discharge seems to be high 2. Silt follows gully but also is in curves, river silt till Saefthinge 3. High silt below Baarland, silt at Middelplaat. 4. Middelgat area is clear. This area is known as a sedimentation area. 5. A minimum silt content near Hansweert is clearly visible. 6. Schaar van Waarde is turbid. 7. Above Plaat van Valkenisse the area is clear (sand area);

1998	June 1	1. High Silt below Hooge Platen, some silt North of Hooge Platen, erosion West of Middelplaat silt below Baarland again. Some silt west of Molenplaat. 2. Outgoing flow gives laminary type of silt structures
1998	July 20	1. No patterns or gradients in the image, probably clear waters, but river silt from Belgium Schedlt till Saefthinge very well visible 2. High water, small flow velocities give loss of silt gradients
1998	August 6	1. High silt at Hooge Platen and Middelplaat (high water, erosion, waves?) 2. High silt North of Hooge Platen and silt below Baarland 3. Stripe of silt North of Belgium coastline (from Paardenmarkt?), but relatively low silt in Scheur van Wielingen.
1998	August 8	1. High silt at Hooge Platen and Middelplaat (high water, erosion, waves?) 2. silt below Baarland, low silt in gullies except North of Hooge Platen 3. High silt at Sea 4. As usual at Breskens the water column is more than turbid than at Vlissingen.
1998	August 10	Like 8 August.
1998	Oktober 1	1. High water, outgoing tide. High concentrations visible at tidal flats (especially south of Molenplaat and Rug van Baarland). Water flows over these tidal flats and takes sediment with it. 2. Some details: Ships go out at such tides, this is clearly visible. Two ferries visible at Kruiningenpolder-Terneuzen (10h41m) that are close together according to their schedule. "Poineersbegroeing" at Plaat van Valkenisse is visible. Zimmermangeul north of Valkenisse is visible (close to the coast). Area is known to have peat.
1998	November 17	1. Belgium Scheldt is uniform till Saefthinge . There are no gradients in river, possibly due to low sun angle? 2. Colour differences between west and east side of the image.
1998	November 20	1. Not much gradients in estuary due to low sun angle. 2. Almost completely green estuary? Sea silt is still blue.

3.2.2 Description of NOAA/AVHRR images

The following NOAA/AVHRR daily images were processed:

Reference	Date	Time	Tide	Water Level
N0214134	*14-2-'98*	*13:49*	*incoming water*	*-0.50m*
N0319124	19-3-'98	12:47	incoming water	-1.1m
N0429065	29-4-'98	6:56	?	?
N0512125	12-5-'98	12:54	incoming water	+0.7m
N0514141	14-5-'98	14:13	incoming water	+0.7m
N0517065	17-5-'98	6:59	high water	+2.5m
N0517133	17-5-'98	13:59	low water	-2.0m
N0517164	17-5-'98	16:47	outgoing water	-0.2m
N0610141	1-6-'98	14:15		
N0610063	10-6-'98	6:31		
N0726061	26-7-'98	6:18		
N0802165	2-8-'98	16:51	high water	+2.0m
N0808063	*8-8-'98*	*6:31*	*incoming water*	*-1.1m*
N0830163	30-8-'98	16:34	high water	+2.3m
N0923131	23-9-'98	13:19	incoming water	-0.8m
N1110142	24-9-'98	8:21	outgoing water	-0.8m

The images on 14-2-98 and 8-8-98 (italic) coincide with images for which SPOT images are available (on 14-2 only a Dali print is available). For images up to 14-5-'98, Kust2000 OBS data (continuous) are also available.

The non-linear scaling procedure of Vos (RESTWAQ-2, 1998; page A1-A3) was applied in order to partially overcome the problem of saturation. Non-linear scaling was done on basis of a preliminary model run with sea boundary conditions for SPM of about 50 mg/l for February 1998. After some trial and error, scaling parameters C* =30.0 mg/l (crossing point of linear and non-linear curves), and δ=50.0 mg/l (half-saturation value) were applied. For summer images this does not lead to different results.

SPM patterns

The most prominent feature in the NOAA/AVHRR images is the concentration gradient along the (sea) model boundary. This gradient shows a decreasing concentration from Belgium to Walcheren, most often with a steep decrease in SPM at Oostgat. This information might be useful for set up of model boundaries. An example is given in Figure 3.2. Also a second gradient from the Belgium coast across the Scheur van Wielingen is seen. This leads to an image with a triangle of higher SPM concentrations at Vlakte van Raan. SPOT images also show this pattern (see Figure 3.3).

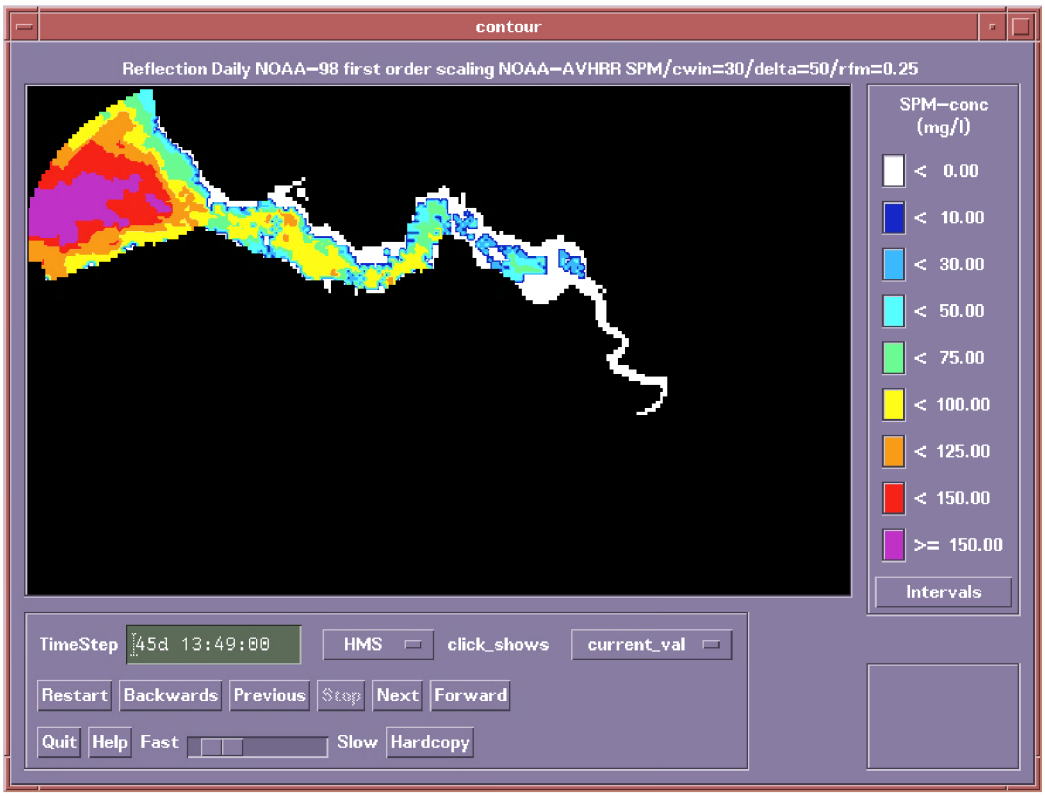

Figure 3.2 NOAA image of 14 February 1998, 13:49 (incoming water -0.50m), rescaled with model result and non-linear extrapolation method to overcome saturation effect.

Figure 3.3 SPOT image of 14 February 1998 from Dali Catalogue (~ 11.00 hours; low water). A triangle of high SPM concentration, typical for all winter images is visible at Vlakte van Raan at the mouth of the Western Scheldt.

In some of the NOAA/AVHRR images (not shown here) the tide could be recognised:

- High water reveals relatively low concentrations in the estuary, and relatively high concentrations outside the estuary ;
- Outgoing water reveals relatively high concentrations flowing out of the estuary along Scheur van Wielingen and the Belgium coast;
- Incoming water is in general rather unclear in patterns, but the at Oostgat is always recognised;
- However, for most of the images these tidal characteristics could not be confirmed neither be falsified.

In two images, SPM spots were clearly visible that *might* indicate dumping of SPM from the Belgium harbours at the dumpings sites R4 (Raan, image of 30-8-'98) and Paardemarkt (image of 17-5-'98).

Conclusions and recommendations for use of NOAA/AVHRR images

Atmospheric correction procedures that do not suffer from saturation are required for sue of NOAA/AVHRR images. Saturation of SPM with the current KNMI atmospheric correction procedure (Vos et al., 1998, RESTWAQ-2, Part I, Appendix A3) occurs and this prevents a detailed analysis of SPM patterns. With this respect, the current SeaWiFS sensor might offer more possibilities since it does not saturate at the sensor. Also use of the SeaWIFS atmospheric correction algorithms for NOAA/AVHRR sensors might offer possibilities for enlarging the amount of RS information for the sea entrance of the Western Scheldt estuary. This entrance is a site with intensive dumpings from the area of Zeebrugge (De Bie and Benijjts, 1994) and should therefore be monitored. A collection of SeaWiFS, NOAA/AVHRR and SPOT images might be very useful for monitoring this area.

3.3 Processing of remote sensing images

3.3.1 Processing of SPOT level 1 products to suspended matter maps

The selected remote sensing images were processed to SPM maps according to the methodology developed and outlined by Dekker et al., (1998) and RESTWAQ2 (Vos et al. 1998, Part II - Friesland). A full description of the processing is given in Peters et al., (1999). Essentially two steps (information flows) are required for the determination of SPM from remote sensing images, see Figure 3.4.

1) Algorithm development:
In the first step, a mathematical relationship between measured water concentrations and a satellite measured quantity is developed (bio-optical model). In this case, the relevant satellite parameter is the subsurface irradiance reflectance (R(0-)) in the SPOT band 2.

2) Processing satellite observations to apparent reflectances, R(0-) and finally to SPM.
This step involves calibration of the satellite observations, atmospheric correction and application of the (inverse) algorithm derived in step 1.

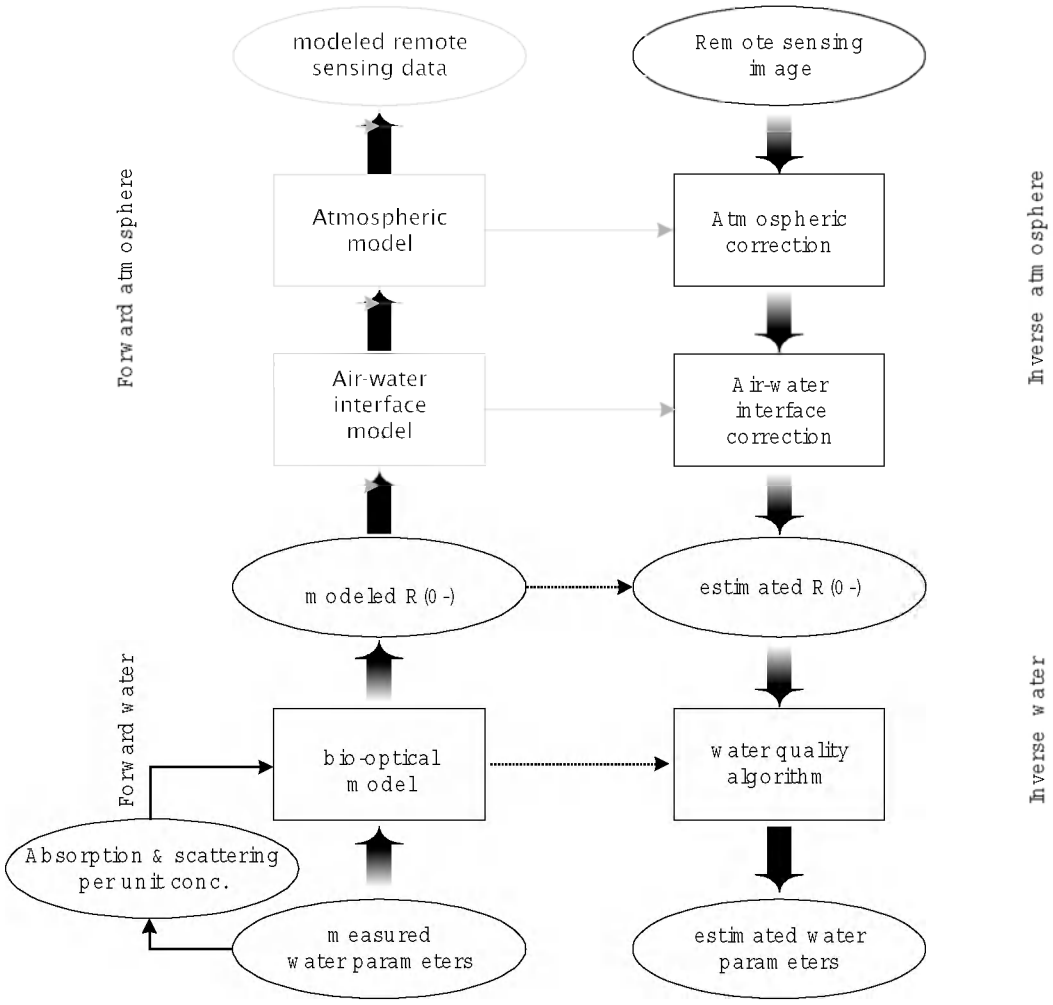

Figure 3.4 The forward and inverse model for remote sensing of water quality. To establish algorithms only the "forward water" and the "inverse water" sections are relevant; to carry out a sensitivity analysis of the operational method or in order to derive specifications for a dedicated remote sensing instrument, it is necessary to go through all the steps from "forward water" via "forward atmosphere" to "inverse atmosphere" to "inverse water". Once the method is operational it is only necessary to run through the modules "inverse atmosphere" and "inverse water"

The relationship between the water quality parameters and the radiance measured at the sensor is displayed in Figure 3.4 (after Hoogenboom et al., (1998)).

1) Algorithm development (forward modelling):

Because of the operational character of this project, use was made of the standard Gordon model for underwater light transport. In this model, the water quality parameters are linked to the R(0-) via the inherent optical properties (IOP) of the water. The inherent optical properties of the water are given by the total absorption (a) and backscattering (b_b) of the water, both depending on wavelength (λ) and expressed in (m^{-1}). The inherent optical

properties are physically related to the subsurface irradiance reflectance R(0-) which is the key parameter linking the properties to the remotely sensed irradiance data (Equation 1).

$$R(0-) = r\frac{b_b}{a + b_b} \qquad \text{Equation 1}$$

Where:

$R(0-)$	is the irradiance reflectance just below the water surface, (dimensionless, i.e. the fraction of solar radiance per sterradial that is reflected by the water column, excluding the surface reflection) for a given wavelength;
r	is the coefficient depending on geographic latitude and longitude and the volume scattering function.

The use of this model implies knowledge of the IOP of the water. Here it is assumed that the IOP are the sum of the IOP of the distinctive components in the water (including pure water itself), see Equation 2.

$$a(\lambda) = \sum_i a_i(\lambda)$$
$$b_b(\lambda) = \sum_i b_{bi}(\lambda) \qquad \text{Equation 2}$$

Where:

a_i	is the absorption due to component i;
b_{bi}	is the backscattering due to component i.

Following the law of Lambert-Beer it is then assumed that the IOP of a certain component are a linear function of the concentration of that component. This introduces the *specific* inherent optical properties (SIOP) of a component, see Equation 3. To typographically distinguish the IOP from SIOP the latter is indicated by an asterisk (*).

$$a_i(\lambda) = a_i^*(\lambda) \cdot c_i$$
$$b_{bi}(\lambda) = b_{bi}^*(\lambda) \cdot c_i \qquad \text{Equation 3}$$

Where:

a_i^*	is the specific absorption of component i;
b_{bi}^*	is the specific backscattering of component i;
c_i	is the concentration of component i.

Combining Equations 1 to 3 will link the concentrations of all the components to the subsurface irradiance reflectance, provided r and the SIOP of all the components are known. Because, little is known about the SIOPs of the Western Scheldt system, a measurement campaign was conducted (10 March 1999) for in-situ measurement of R(0-) spectra and collection of five samples for laboratory analysis of SIOPs.

The parameterization of the Gordon model requires some estimations for parameters that cannot be measured with the current laboratory set-up, such as the ratio between

backscattered and forward scattered light (B) and the shape factor r. In this case, use was made of in situ-measured R(0-) spectra in order to estimate these two parameters.

Mean values found were B = 0.042 and r = 0.38; these values were use for the subsequent modelling. All estimated and measured parameters were entered into the bio-optical model which then was used to simulate a data set containing R(0-) values integrated over the SPOT spectral bands as a function of SPM concentrations. For these simulations it was assumed that:

- CHL = constant = 15 ug / l
- CDOM = constant = 1.73 (λ 440)
- SIOPs are the mean value of the 5 in-situ measurements.

A number of boundary conditions forced the use only band 2 of SPOT for SPM retrieval. One of them was that simulated and measured R(0-) values matched best in this wavelength range. Another is that this spectral band is less sensitive than band 1 to errors in the atmospheric correction and errors in e.g. the CDOM concentration. SPOT band 3 observations have proved to be unreliable at low R(0-) levels.

From the set of simulations, an algorithm for the relationship between $R(0-)_{band2}$ and SPM was derived for each type of SPOT sensor separately (SPOT1, 2 and 4, HRV1 and 2).

2) Processing satellite observations to apparent reflectances, R(0-) and finally to SPM
The (forward modelling) relationships developed (above) were inverted and used to retrieve SPM maps from $R(0-)_{band2}$ maps. The procedure to derive R(0-) maps is part of the 2nd information flow and is discussed below.

After selection of 9 SPOT images for processing, a number of preparatory steps were taken:

1. SPOT spectral sensitivity curves were collected (SPOT1,2 and 4; of all three systems HRV1 and HRV2) for use in the forward modelling step.
2. All images were geo-referenced using the topographical map 1:50.000 towards the "Rijksdriehoek" coordinate system: image resolution of 20 m was maintained.
3. Next all selected images were corrected for atmospheric influences. For this the atmospherical correction code 'MODTRAN 3' was used, run in LOWTRAN 16 streams mode. Use was made of the Toolkit software package (de Haan et al., 1998). For operational use a prototype "fast and more robust" shell was build for specific processing of SPOT images (relying on a number of underlying Toolkit executables).

For the multi-temporal atmospheric correction, first all images were scanned for reference targets. Specifically dark water bodies of which some knowledge of temporal variability exists were selected, such as "Veerse Meer" and parts of the "Oosterschelde". These targets are used to pinpoint the atmospheric correction by simulating R(0-) values (at estimated concentrations) and matching satellite observed R(0-) with simulated values. This procedure ensures also that no negative values for R(0-) occur.

Supportive to this calibration of the atmospheric correction, targets were sought for that were relatively bright and invariant in time. At two locations (an aluminum factory and a

industrial site) such targets were found. Further analysis showed that, probably due to shadowing effects, there was at some occasions still significant temporal variation.

The total procedure commenced with the selection of a "reference image" (8 August 1998) which was processed to an optimum result. Criteria for quality check were: match with simulated dark water body R(0-) values, realistic values for the atmospheric parameters (horizontal visibility, atmosphere and aerosol type), and realistic values for the retrieved R(0-) and SPM values.

Next all images were processed, using simulated R(0-) values for the dark water bodies as reference as well as the R_{app} values of the bright targets from the reference image. All results were quality checked using the above mentioned criteria except that in this stage SPM validation was done only in a very general sense.

As a last decisive quality check, the SPM maps were validated using all available in-situ data: both the 20 year monthly averaged values and the continuous monitoring data from stations Vlissingen, Terneuzen and Baalhoek. Some validation results are presented below in Figures 3.5 and 3.6. Full validation results are given in Peters et al., 1999. In all cases, the SPM maps agreed very well with the in-situ data and can be considered final products. SPM maps as originally processed in ENVI software were then translated to ARCVIEW files for final presentation and exchange purposes, examples of which is given in Figure 3.7 for 11 January 1998.

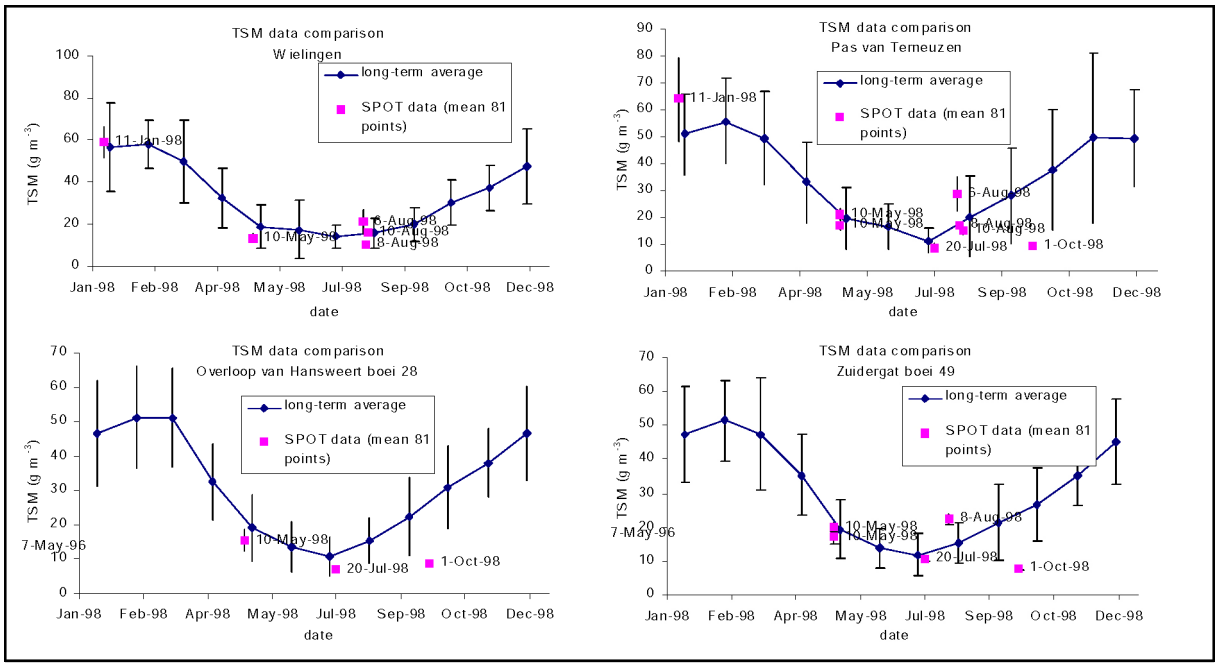

Figure 3.5 Comparison of retrieved TSM concentrations (pink squares) with long term averages (blue diamonds) for several locations in the Western Scheldt estuary. The retrieved concentration is averaged over a region of 180 x 180 m^2. and the standard deviation is indicated with error-bars. Complete validation results are given in Peters et al., 1999.

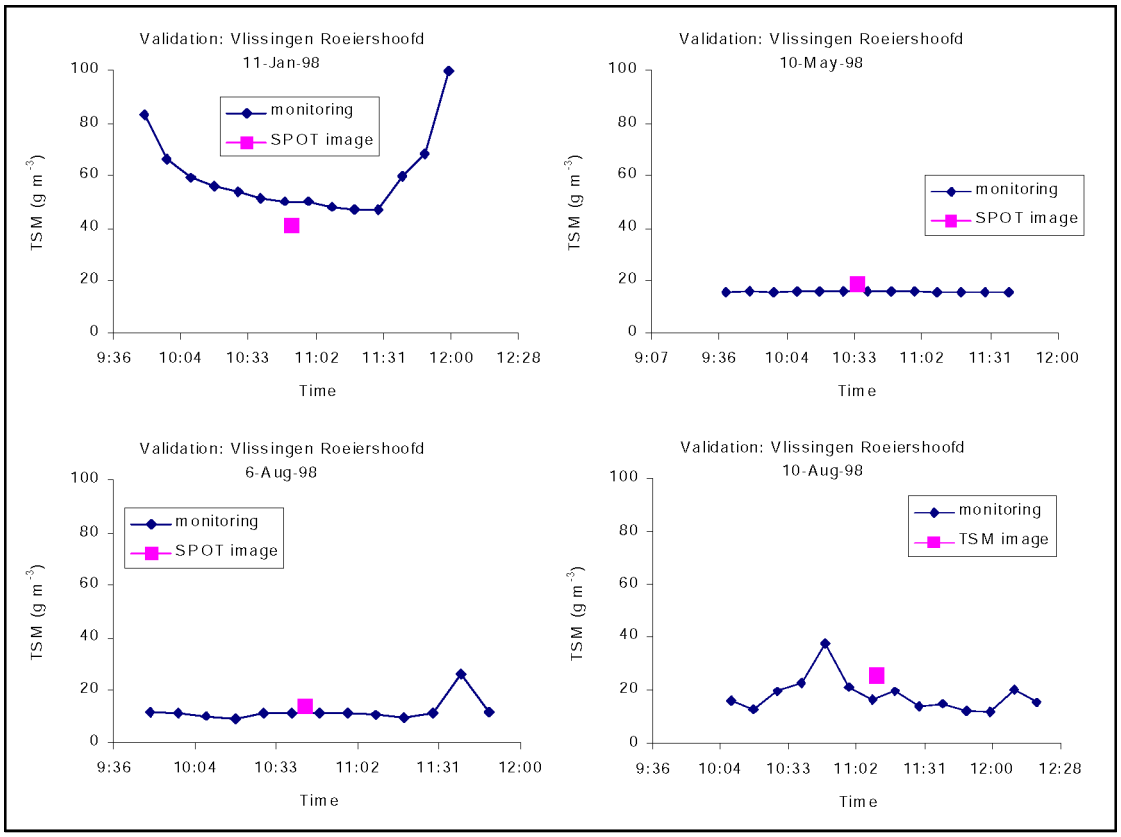

Figure 3.6 Comparison of some remote sensing results with continuous in-situ data at Vlissingen at the day and time of the satellite overpasses. Complete validation results are given in Peters et al., 1999.

3.3.2 Conversion of SPM maps from SPOT to SPM products at the SCALWEST model grid

The SPM maps prepared as described in section 3.3.1 are presented at a very fine rectangular grid of 20*20m (a raster). However, for direct comparison with model results, it is required that these SPM maps are also transformed to the curvilinear model grid of SCALWEST-fine, as given in Figure 4.1. Conversion of SPOT products (in ENVI binary format) to the aggregated curvilinear SCALWEST grid can be done in two ways:

1. Exact averaging of all SPOT pixel values over the SCALWEST curvilinear grid cells;
2. By selecting the SPOT pixel value at the middle of the SCALWEST grid cell;

Since the first procedure required more than 20 computation hours on a powerful (Silicon Graphics Origin 2000) workstation, the second procedure was selected. For purposes of comparing the remote sensing and modelling results and incorporating remote sensing in a final model calibration, this procedure is more than sufficient.

For 11 January 1998, an example is given in Figure 3.7 of the remote sensing SPM product (ArcView). In Figure 3.8, a representation of the same data as converted to the SCALWEST model grid is presented. In Figure 3.9, the same data is presented on an *aggregated* model grid, where 16 original grid cells (4 x 4) are aggregated to one aggregated grid. The aggregated SCALWEST model grid is relevant since this was the grid on which the model

results were obtained (see section 4). The remote sensing result as given in Figure 3.9 can be used for direct model comparison and model calibration only.

For presentation of the remote sensing result, the original SPOT maps presented in ArcView are preferred.

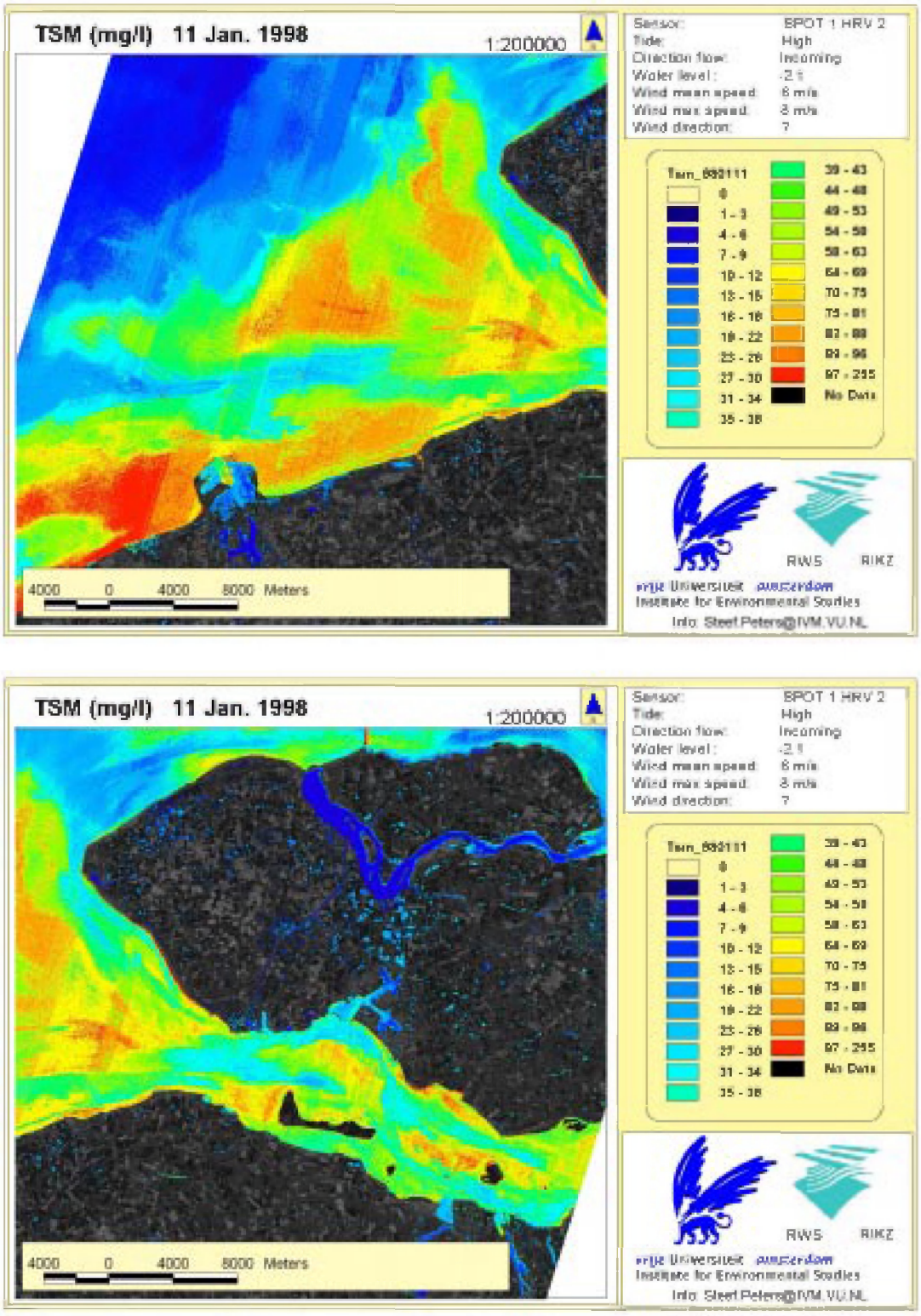

Figure 3.7 Maps of SPM (mg/l) for 11 January 1998 (presented in ARCVIEW)

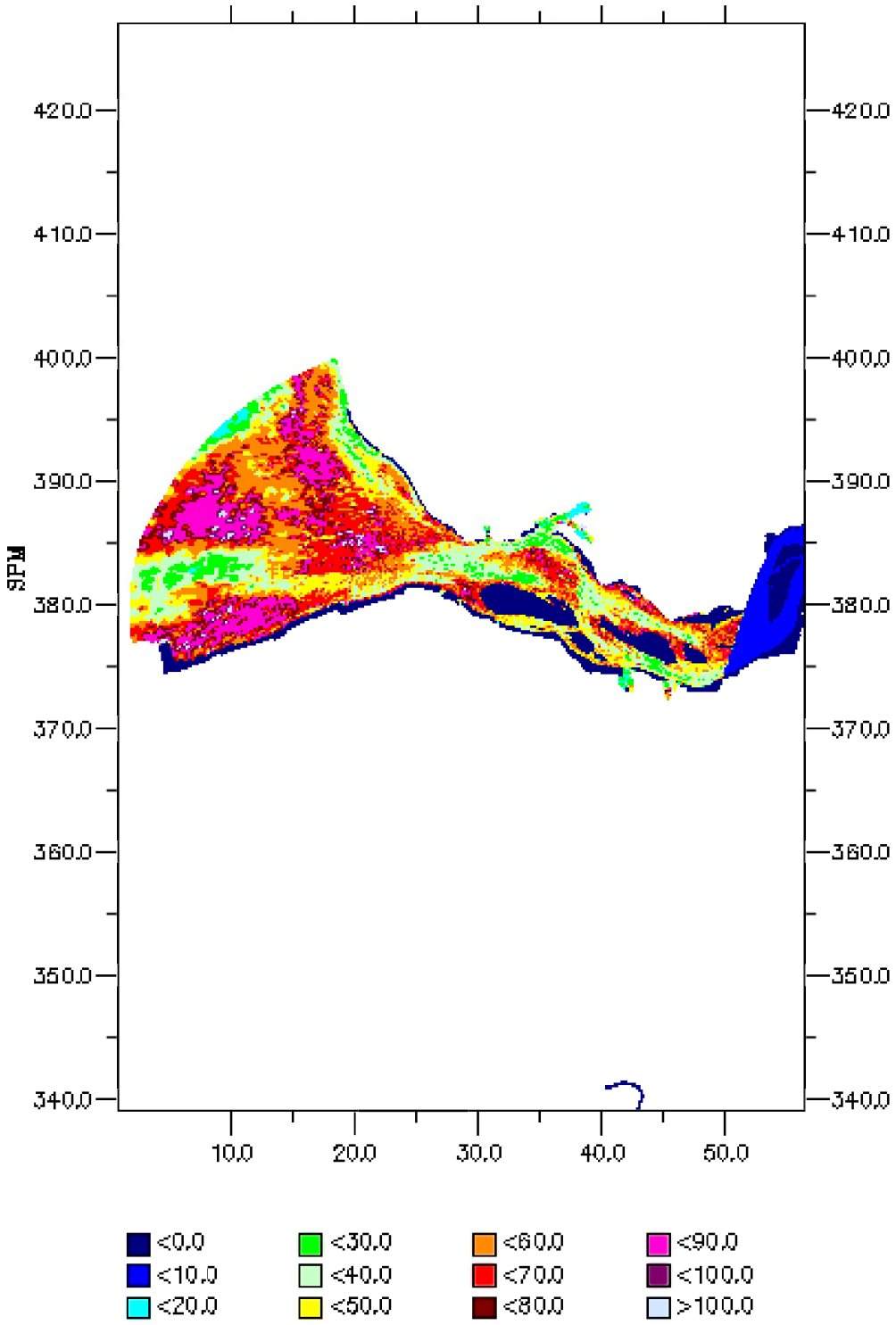

Figure 3.8 Remote Sensing SPM map (mg/l) for 11 January 1998 converted to the curvilinear SCALWEST model grid (no aggregation)

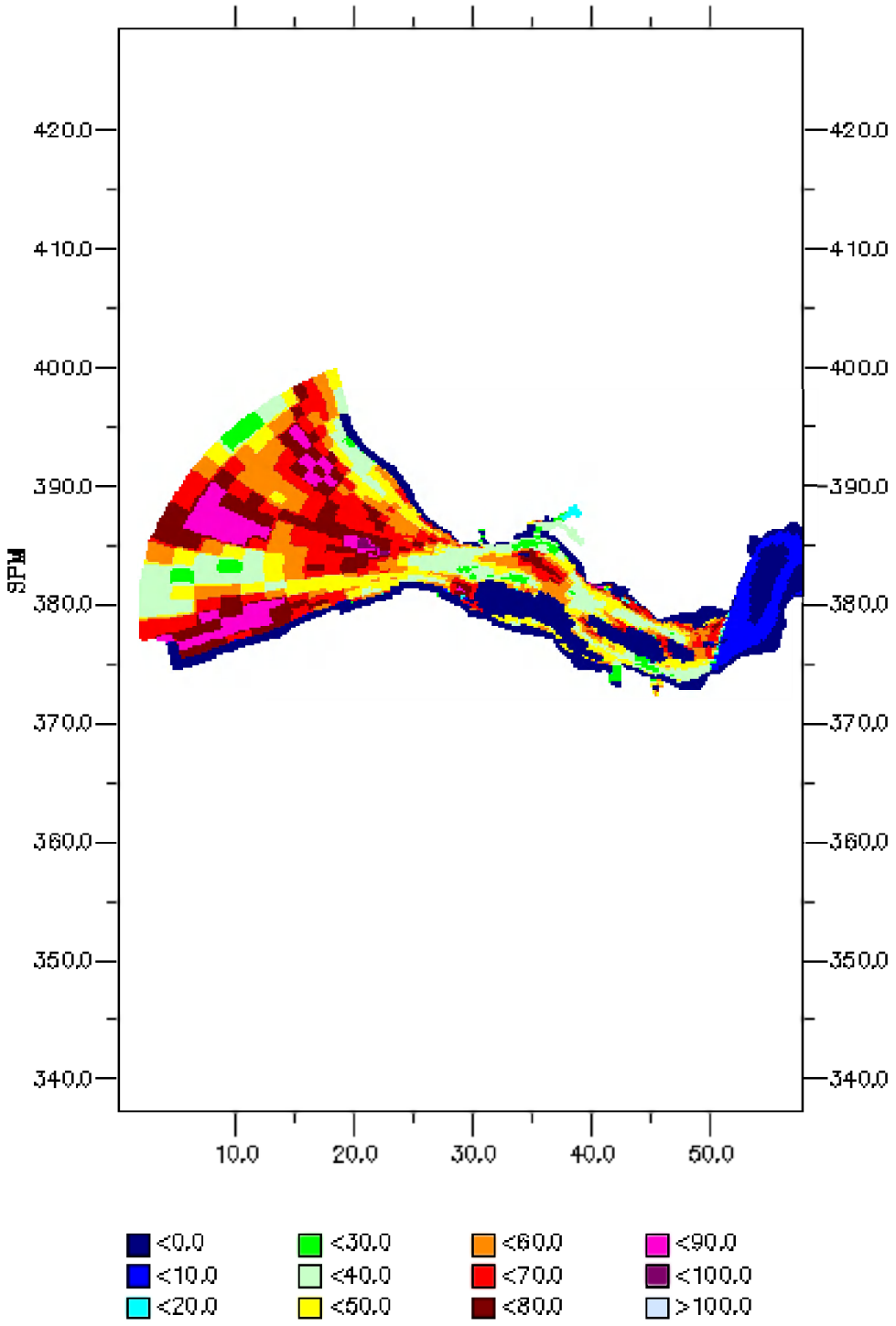

Figure 3.9 Remote Sensing SPM map (mg/l) for 11 January 1998 converted to the curvilinear aggregated SCALWEST model grid

4 Water Quality Model

4.1 Introduction

A 2-dimensional (vertically averaged) curvi-linear water quality model for suspended matter transport in the Western Scheldt estuary was set up, with the modelled region and the model grid as shown in Figure 4.1 (with RijksDriehoek co-ordinate grid). The model used is Delft3D-WAQ, run with only 1 layer in the vertical (also known as 'DELWAQ'). The model was run for the full year 1998.

An important input for this particular model is the bathymetry. The average water depth (a fingerprint of the bathymetry) is given in Figure 4.2. From this figure it follows that the area is characterised by relatively deep gullies connected to the sea, tidal flats and shallow areas at the side of the estuary (especially in some of the curves and at Saefthinge). The model used for this study includes the Western Scheldt up to the Scheldt river near the city of Antwerp.

The water quality model for suspended matter requires results from a hydrodynamic model for the water flows, which determines the advective transport of sediment. The model also needs input data for wind; wind creates water waves which in turn can 'stir up' sediment from the bottom.

Sediment enters the modelled area from the boundaries (boundary conditions at the open sea boundary and river boundary), where the concentrations are specified based on available monitoring data. The model also has an initial amount of sediment in the water column and on the bottom, which must be set at the beginning of a simulation (initial conditions). Sediment loads can be input to the model to simulate dumpings from dredging activities in harbours. Also, the water quality model includes processes such as sedimentation and resuspension that continually redistribute the sediment within the water column.

Due to morphologic dynamics and effects of dredging activities silt layers may get exposed and come in contact with the water column. The model does not consider these types of large scale changes in the bottom channels or tidal flats that also serve to redistribute sediment material in the estuary.

Dumpings data for harbour dredgings from 1997 (Tables 4.1-4.2) indicate that significant amounts of silt material are dumped and that this source of sediment should be included in the model. This will be further addressed in section 4.3.

Summarising, the calculated SPM concentrations in the model at any one time are a function of:

- input of sediment from boundaries, initial conditions, and loads (dumpings of harbour silt)
- advective transport based on the hydrodynamics (tidal water flow)
- dispersive transport (random, chaotic spreading of material)
- sedimentation and resuspension of material to/from the bottom, as affected by the tide induced water flow velocities and wind induced waves

The text box below summarises the inputs required for running the model.

What does the Water Quality model need as Input?

The Western Scheldt water quality model needs several types of information as input in order make a calculation:

- Results from a hydrodynamic model (water flow). This is provided by the 2-D (depth averaged) curvi-linear SCALWEST-fine model of RWS-RIKZ (WAQUA). The hydrodynamic model is run for a period of 14.5 days corresponding to approximately a spring-neap tidal period. The hydrodynamic results are used repeatedly to allow a water quality calculation of 1 year (see also section 4.2)
- Wind data for the whole year, as daily average wind speed: This is provided by the KNMI from measurement station Vlissingen (see also section 2.2.3).
- Boundary conditions of SPM concentration, for both the sea boundary, and the river boundary. The boundary conditions, which also have to be specified for the whole year, are extremely important in the model calculation and have a large influence on the calculated SPM concentrations. The boundary conditions used in the model are taken from the long-term monthly averaged concentrations (see also section 4.3.4).
- Initial conditions for SPM concentrations (in the water column) and bottom sediment thickness (see also section 4.3.5).
- Point source inputs of SPM: known point source inputs of sediment are specified as loads to the model, and must be defined with respect to the amount, the location and the date dumped. Dredged harbour sediment is an important input at the present (T0) situation (see also section 4.3.6). In the future (T1 situation), spreading of the tunnel boring material will be an important point source input.

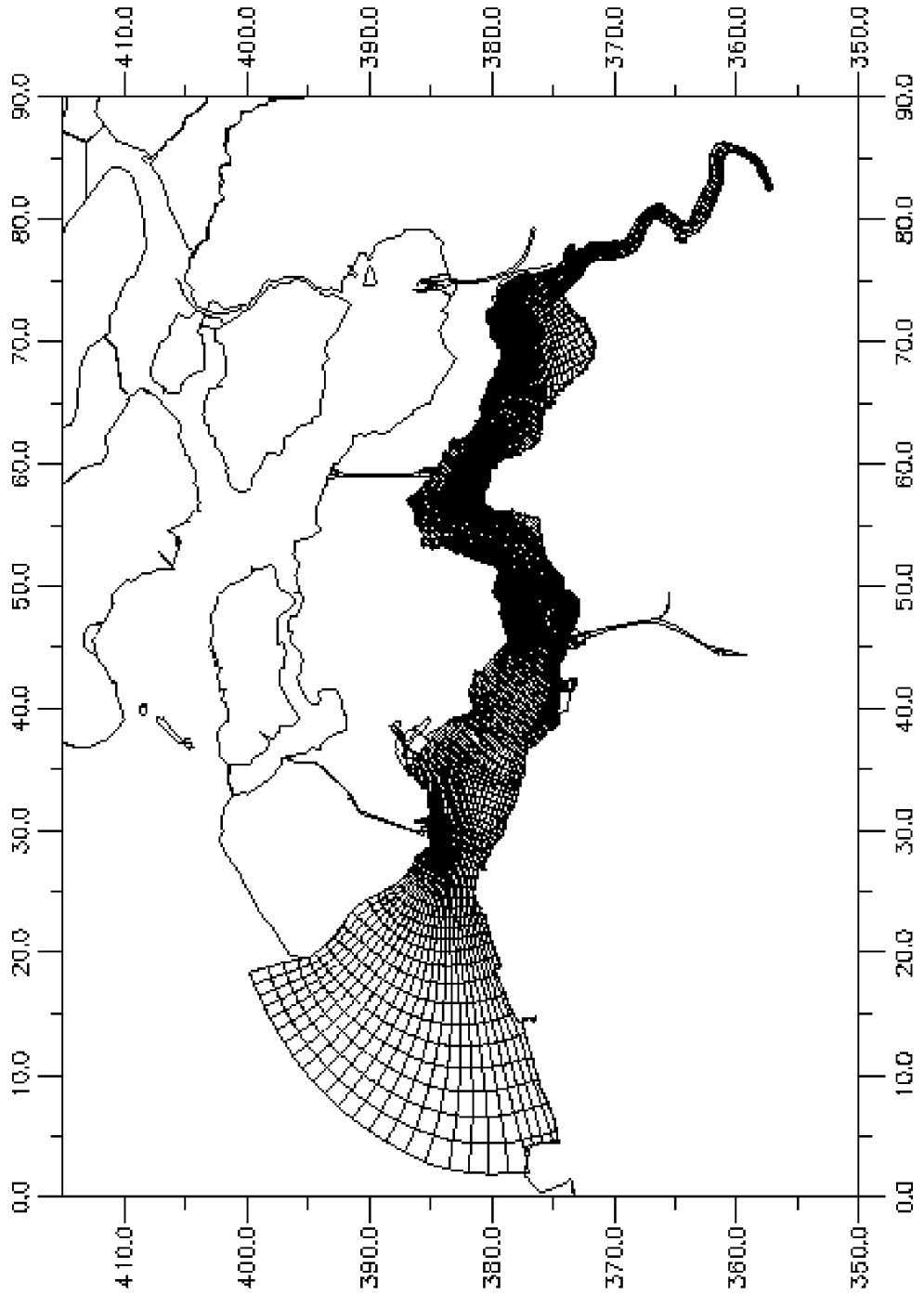

Figure 4.1 RESTWES model grid of the Western Scheldt (aggregated)

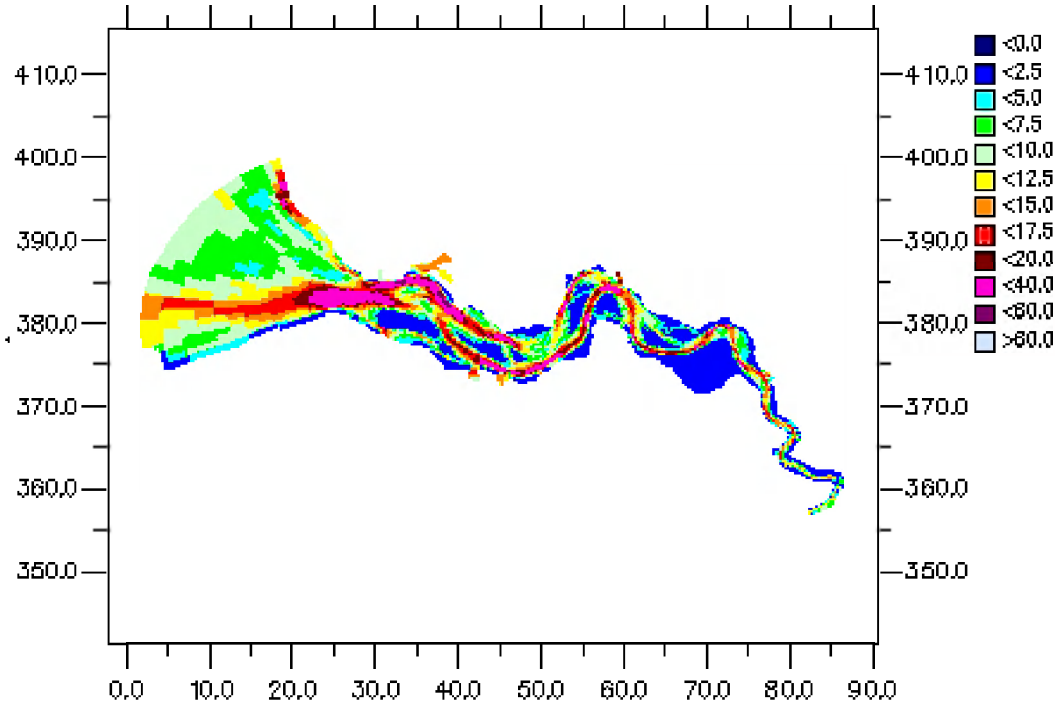

Figure 4.2 Average water depth of the SCALWEST fine model (total water depth averaged over 1 spring-neap cycle of 14.5 days).

Use of measurements for the modelling

In-situ data are used in the model for:
1. forcing function (e.g. boundary conditions);
2. model calibration and sensitivity analysis.

Sea boundary conditions were initialised with values inferred from twenty yearly monthly mean averages of SPM (van Maldegem, given in chapter 2). For the (final) model calibration the following data were used:

- Remote sensing images from SPOT processed to SPM values and converted to the model grid (9 images);
- Data from 3 continuous monitoring stations (Vlissingen, Terneuzen and Baalhoek);
- Twenty yearly monthly mean averages of SPM at 8 locations were used for the calibration.

The initial calibration of the model was based solely on the continuous in-site data from Terneuzen and Baalhoek. The model calibration is further described in sections 4.4 and in Appendix B.

This chapter further has the following sections:

4.2 Hydrodynamic modelling and coupling to water quality model
4.3 Set up of the water quality model;
4.4 Model calibration

4.2 Hydrodynamic modelling and coupling to water quality

The hydrodynamic modelling was conducted by RWS-RIKZ. The 2D curvilinear SCALWEST-fine model (2D-WAQUA) of RWS-RIKZ was run for 2 cases:

1. A 14 day period with calm winds. Boundary conditions for the Scheldt were forced with measured time series of water levels at the sea boundary for a spring-neap period with calm winds. The water level after 14.5 days is almost equal to that at the start of the simulation (i.e. a 'cyclic' simulation of water levels). The effect of the spring-neap variation is important for sediment modelling since it induces a variation of the bottom shear stress. This is shown in Figure 4.9.
2. A 1 day period with higher wind speed (8 m/s) from the West. Boundary conditions for the Scheldt were forced with measured time series of water levels at the sea boundary of the model for a period of 1 day for such winds. This period comprises an average tide for high winds from West. The water level after 1 day is almost equal to that at the start of the simulation (almost 'cyclic' simulation of water levels). The simulation was done for a period two days after spring tide.

The results from the hydrodynamic model were coupled to Delft3D-WAQ using a specialised coupling programme for SIMONA and Delft3D-WAQ. The conversion was confirmed to be mass conserving.
The first case was further used for the water quality model since:

1. It incorporates the spring-neap variation, and the second case does not do this;
2. It was found that the change in flow for the second case was not much. Changes were mainly induced for SPM due to the fact that solely a spring period is modelled (which is not realistic). Wind effects on salinity turned out to be small.

There remains one serious problem with the present hydrodynamics: a spring-neap cycle of 14.5 days is used in the model, but in reality it should be 14.75 days. This difference causes the model simulation to get out of phase with the continuous SPM in-situ measurements. This problem was partially solved for stations Baalhoek and Ternuezen by shifting the in-situ data over 8 days during comparison model results with in-situ data, since these time-series start end October and last only two months. For Vlissingen data this was not possible, and no shift was applied. There are also problems in comparing model results with remote sensing data: In order to compare model and remote sensing results at a specific moment in time, the model results had to be shifted, so that the correct day and time in the spring-neap cycle were found (e.g. 3 days after spring tide, 4 hours after high tide.). For comparison of the Remote Sensing data and the model data, the model result closest to the remote sensing data in time, and within one meter difference of water level at Terneuzen were selected This brings the results to a comparable tidal phase, however, the forcing functions in the model (e.g. wind) are then also shifted, so the comparison is not ideal.

For any future modelling simulations (e.g. for operational monitoring during the T1 phase) it is recommended re-run the hydrodynamic calculation and use a 29.5 days spring-neap period ('synodal' period) with nearly exactly 28 'lunar' days (24 hours 50 minutes).

4.3 Water Quality Model: Set-up and processes

4.3.1 Introduction

This section describes the set-up of the water quality model, covering the main points of:
1. Model grid for water quality;
2. Substances modelled;
3. Boundary conditions;
4. Inputs from harbour dredgings;
5. Model processes

More details on model set-up and processes are given in Appendix A.

4.3.2 Water quality model grid

The computational grid for the hydrodynamic model (SCALWEST-fine) consists of 76036 segments. Because calculation of water quality for one year on this grid would cost an excessive amount of computer calculation time, an aggregation of the model grid was made. With an aggregation of 4*4 grid cells, the resulting grid for water quality calculations consists of 4341 segments. All model computations were conducted using this aggregated grid (Figure 4.1).

4.3.3 Substances modelled

The substance of interest in the study is Suspended Particulate Matter (SPM), which is the total amount of fine suspended material (< 63 μm). In the water quality model for the T0-scenarios (no dumped material from tunnel silt), SPM is composed of 3 different sediment fractions:
1. (IM1, mg/l); This fraction is for sea silt
2. (IM2, mg/l); This fraction is for river silt
3. (IM3, mg/l); This is a heavy silt fraction

In the model approach, these 3 fractions are summed to obtain SPM (i.e. SPM = IM1 + 1M2 + 1M3). All three fractions exist in both the water column and in the bottom sediment layers. The bottom sediment consists of two layers, S1 and S2. In the simulations, the organic fraction of SPM (phytoplankton and detritus) is not explicitly simulated, but is implicitly included in the above 3 fractions.

In the T1 scenario, the dumped tunnel material is modelled as an additional, but separate fraction, and thus can be analyzed separately from the background SPM conditions.

4.3.4 Boundary Conditions

Boundary conditions of SPM concentrations are one of the most important input data for the water quality model (see Text Box). The concentrations SPM must be specified at both the sea and the river boundary over the entire period of the model calculation. At the

boundaries, the concentrations have been defined using average values from Breskens/Vlissingen (sea-side) and from Saefthinge from the twenty yearly mean SPM values of Van Maldegem (1992), Figure 4.3. These values are spatially uniform (i.e. the same over the all the boundary grid cells) but time-varying per month. At each of the boundaries, a different sediment fraction is specified:

- sea silt (IM1) at the sea boundary
- river silt (IM2) at the river boundary

We note, that similar to the PROMISE modelling study (Brummelhuis et al.1999, Gerritsen et al. 1999) in this study the source terms of sediments (boundaries + dumpings) are of utmost importance for the accuracy of the calculated result.

The current definition of the model boundaries has certain limitations:

- The model boundaries are spatially uniform, and have a constant value over a whole month. In practice, concentrations at the sea-boundary are not spatially uniform, but shows strong correlation with depth, especially in winter periods (see remote sensing images for Figures 3.4-3.6), and over time.
- The boundary conditions with respect to both flow and concentrations are simplified at the river boundary. In the model (hydrodynamic) calculation, the Scheldt river discharge was constant at 100 m^3/s . In actuality, it varies between extremes of 20 m^3/s and 600 m^3/s with 100m^3/s being the average value. Also concentrations vary heavily in the river Scheldt (Fettweiss et al., 1997).

For the purpose of the present model (defining the main SPM conditions in 1998 and assessing the effect of dumping of tunnel material), these points are not expected to cause significant problems. Nevertheless, for possible future refinement of the model, the boundary conditions could be adjusted in the model later on.

4.3.5 Model initial conditions

The amount of silt in the model are at the beginning of the simulation (i.e. the *initial conditions)* has to be specified, for both the water column and the bottom sediment. Particularly the silt in the bottom sediment is important as this is a large reservoir of material that can be eroded (resuspended) into the water column (see section 4.3.7 - model processes). For the initial conditions, both the amount (thickness) of the bottom sediment, and the composition (relative amounts of the 3 sediment fractions) have to be specified.

In the model, there are two bottom sediment layers, S1 and S2. The upper layer (S1) is more easily eroded than the lower layer (S2). In the initial conditions, the upper layer S1 exists only on the tidal flats (depth < 2m) and consists of the river silt and sea silt fractions (see Figure 4.5).

The lower layer S2 exist over the whole model area. The initial composition of this bottom layer is an important model parameter and different variations were checked during the calibration phase (see also Table 4.3). For best results, the initial conditions for S2 are a composition consisting primarily of the heavier silt fraction (IM3) which is 95% of the total mass of the bottom S2 layer.

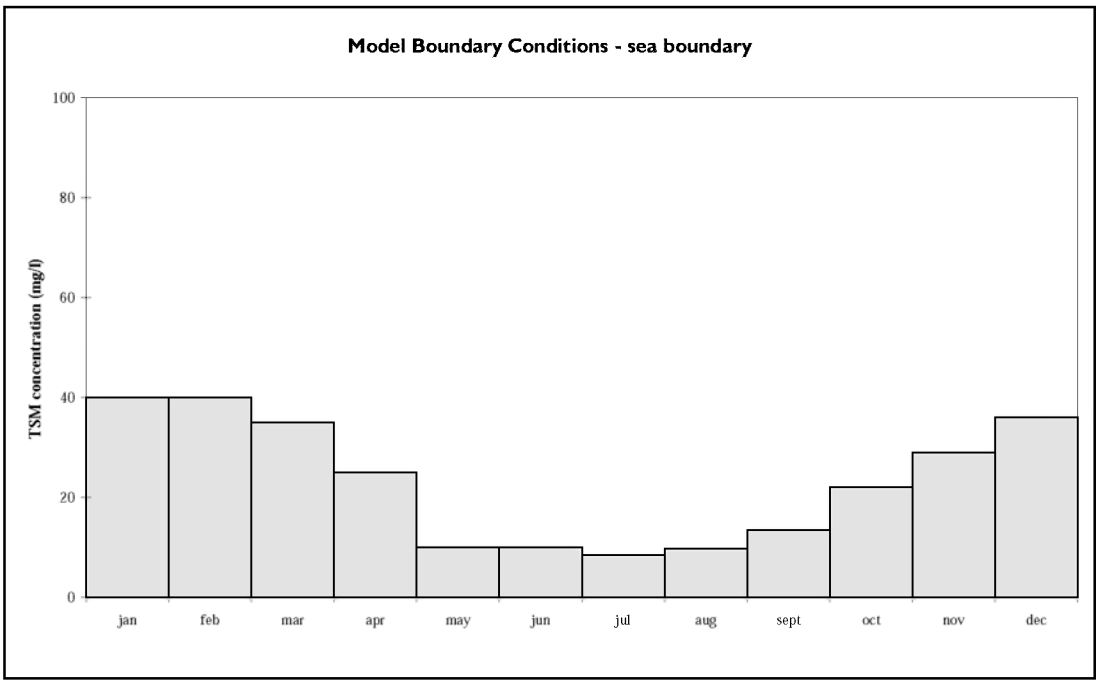

Figure 4.3a Monthly averaged concentrations of SPM inferred from twenty year monthly averages of van Maldegem used for model boundary conditions. Sea boundary: from stations Vlissingen and Scheur van Wielingen.

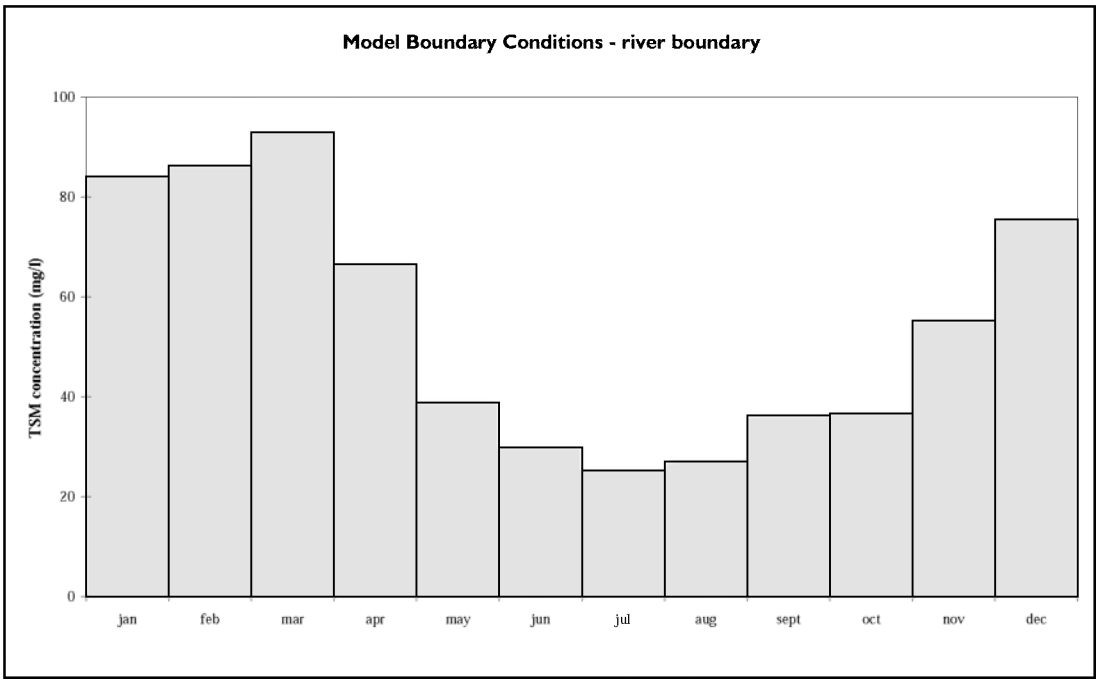

Figure 4.3b Monthly averaged concentrations of SPM inferred from twenty year monthly averages of van Maldegem used for model boundary conditions. River boundary: from station Saeftinge.

4.3.6 Inputs from harbour dredgings

Point source inputs of SPM are an important model input (Text Box). The main point source inputs of silt are from dumpings of dredged material, specifically from harbour dredging activities. Another possible source of silt is from morphological changes and dredging activities in which silt becomes resuspended in the water column. As stated in section 4.1, the model does not include these possible silt inputs.

In this section, the dumpings from dredging activities in Dutch and Belgium Harbours are discussed. The dumpings from dredging of Dutch harbours are within the modelled area and are included as model inputs. Most dumpings from dredging of Belgian harbours are just outside of the model area near the sea boundary, and these dumpings are not included explicitly as model inputs. The effect of the dumpings are included implicitly to a certain extent, as boundary concentrations.

Dutch harbours

Available data on loads from dumping of dredged harbour material indicates that these dumpings are quite significant. The main dumping locations are Terneuzen, Breskens, Vlissingen, Perkpolder and Walsoorden. Specific coordinates for these locations and model grid cell numbers are given in Appendix A. A summary of total amount (kilotons) of dumped dry silt for 1997 and 1998 are given in Table 4.1. All data has been obtained from RIKZ-Middelburg (van Maldegem).

Table 4.1 Dumped amounts of dry silt from dredging in Dutch harbours (ktons)

Dumping Location	1997	1998
Terneuzen	401	155
Breskens	197	109
Vlissingen	1140	80
Perkpolder	50	--
Walsoorden	9	--
Kruiningen	59	--
Baahoek	-	4
Total	1878 Ktons	385 Ktons

The 1998 data for the Dutch harbour dumpings became available at a final stage of the project. This data was provided as wet volume of dumped material, per dumping location and dredging location. A conversion of wet volume to the modelled parameter, i.e. SPM as mass dry silt was made (Appendix A). The details of 1998 dumpings are given in Table 4.2.

Table 4.2 Dumped amounts of dry silt for from dredging of Dutch harbours in 1998 (ktons)

Dump locations	Dry weight silt per location (Ktons)	dredge location	Start date	End date
Baalhoek	3.7	PerkPolder	8-apr-98	9-apr-98
Breskens	9.0	Handels/jachthaven	1-dec-98	4-dec-98
	57.6	Handels/jachthaven	2-feb-98	1-apr-98
	5.4	Handels/jachthaven	23-sep-98	29-sep-98
	4.4	Handels/jachthaven	8-jun-98	17-jun-98
	6.8	westbuitenhaven	13-jan-98	14-jan-98
	5.6	westbuitenhaven	3-apr-98	7-apr-98
	8.7	westbuitenhaven	4-jun-98	15-jun-98
	11.7	westbuitenhaven	15-sep-98	17-sep-98
Terneuzen	11.9	Oostbuitenhaven	8-sep-98	15-sep-98
	72.1	Oostbuitenhaven	5-jan-98	22-jan-98
	1.7	Westbuitenhaven	9-apr-98	10-apr-98
	3.0	Westbuitenhaven	17-aug-98	3-sep-98
	53.2	Westbuitenhaven	2-okt-98	15-okt-98
	13.5	Westbuitenhaven	23-dec-98	24-dec-98
Vlissingen- total	80.2	various locations	5-dec-98	24-dec-98
TOTAL	348.5			

Data for 1998 were added to the model as loads of dry silt (fraction IM2). Loads are assumed to be mixed very rapidly into the water column, and therefore are added to the water phase, not the bottom sediment layer.

It is notable that the 1998 data show amounts of silt 6 times less than those of 1997. Since the procedures followed for converting the 1997 data could not be checked, there is at the moment more confidence in the 1998 data. Nevertheless, the large difference between the two years indicate that procedures for data processing, including conversion of wet weight volumes to dry weight silt must be clearly documented, and the general procedures for the data processing need to be further operationalized. The data were very difficult to obtain in a digitized manner, and additionally needed significant processing to obtain the aggregated data as presented in Table 4.1 and 4.2. Furthermore, there were some discrepancies between the data obtained for all of 1998 and those previously made available for 4th quarter 1998 by van Maldegem.

Belgium harbours

Data on dumping of dredged material from Belgium harbours (MUMM, 1998) show that these amounts may be significant. Probably these are the largest dumpings from dredging activities around Europe (Gerritsen et al., 1999). For 1-4-1997 till 31-3-1998 an amount of 14.9 Mton dry matter was dumped (MUMM, 1998) at a few locations near the mouth of the Western Scheldt (near the model boundary). Given average silt-fractions for the Belgium dumpings documented by De Bie and Benijts (1994) (~50%) this might roughly be 7 Mton silt, although uncertainties are significant in this number since the actual silt fractions are not known.

From the Belgium dumpings only the dumping at Paardemarkt ('ZB_O') is within the model grid. It amounts roughly 4 Mton, but is treated in the present model, like for all Belgium dumpings, as part of the silt at the model boundary.

4.3.7 Model processes

The model includes a set of processes that are considered to be important for the SPM content of the Western Scheldt estuary. Specifically, four processes are responsible for the distribution and fate of SPM which enters the Western Scheldt from the boundaries, from dumpings, or from the initial conditions:

1. Setting of sediments;
2. Erosion from tidal flats by flow and wind induced waves;
3. Erosion from gullies by tidal flow;
4. Erosion from gullies by wind induced waves

The processes as relevant to the Western Scheldt are described generally below and further details are given in Appendix A. Complete formulations are given in the DELWAQ Technical Reference Manual (WL|Delft Hydraulics, 1997).

Process 1: Settling of sediments

Settling of silt from the water column to the bed sediment is one of the important model processes. Sedimentation can occur when the water flow velocities (represented as shear stress, tau) are below a critical value (tau-critical for sedimentation). The model includes three fractions of sediment, each having different value of tau-critical.

The sedimentation rate (flux) is a function of the settling velocities, and each of the three silt fractions has a different settling velocity. Settling velocities for the sea fraction and river fraction are concentration dependent, while the third silt fraction is modelled with a constant settling velocity of 100 m/day, and a high critical shear stress for sedimentation of 4.0Pa. Both these values were varied somewhat during the model set up, but it was concluded that the amplitude for spring-neap variation at Terneuzen was best represented with the values given here. This gives a spring-neap cycle variation of SPM.

Process 2: Erosion from tidal flats by flow and wind induced waves

In the model, there are two bottom sediment layers, S1 and S2. The upper layer (S1) is more easily eroded than the lower layer (S2). The erosion of each layer is controlled by the model parameter for critical shear stress of erosion (tau-critical for erosion), see Figure 4.4:
Tau-critical erosion (S1) = 0.6 - 1.5 Pa (seasonally variable)
Tau-critical erosion (S2) = 4.0 - 5.0 Pa (seasonally variable)

If the shear stress is greater than the critical values, material in the sediment layer will come into resuspension. Material from the lower sediment layer (S2) will only be eroded if all the material in the upper layer (S1) is gone. The shear stress is caused by a combination of water flow (velocity) and wind induced waves.

On the tidal flats, the upper sediment layer (S1) is present throughout the whole year. The model parameters for erosion have been set so that the upper sediment layer (S1) is stable on the tidal flats under conditions of no wind (no waves). The resulting bottom thickness for the top layer was used as initial condition for all later runs and is given in Figure 4.5. Here the tidal flats can clearly be seen. On the tidal flats, the upper layer (S1) is never fully eroded during the winter seasons, so the second layer (S2) is never exposed (and never eroded). The seasonably variable value of critical shear stress for erosion in S1 is chosen to simulate the effect of stabilisation of the tidal flats by biological influences (diatoms) during the spring-summer period.

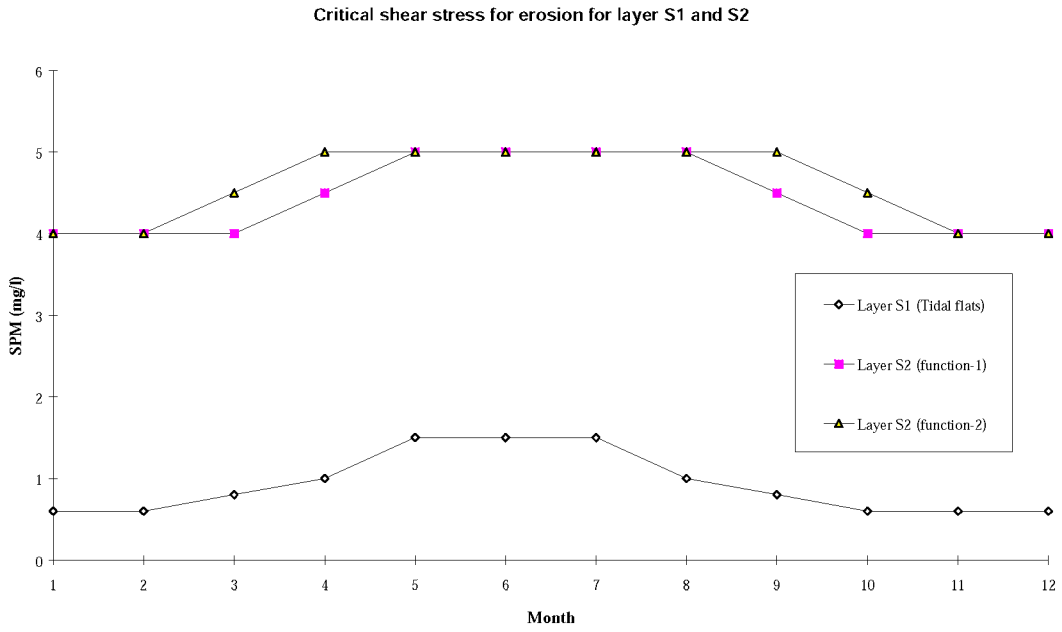

Figure 4.4 Critical shear stress for erosion in sediment layers S1 and S2

In the areas outside the tidal flats, a second bottom layer (S2) with much higher critical shear stresses for erosion was used. This upper sediment layer (S1) has no sediment outside the tidal flats.

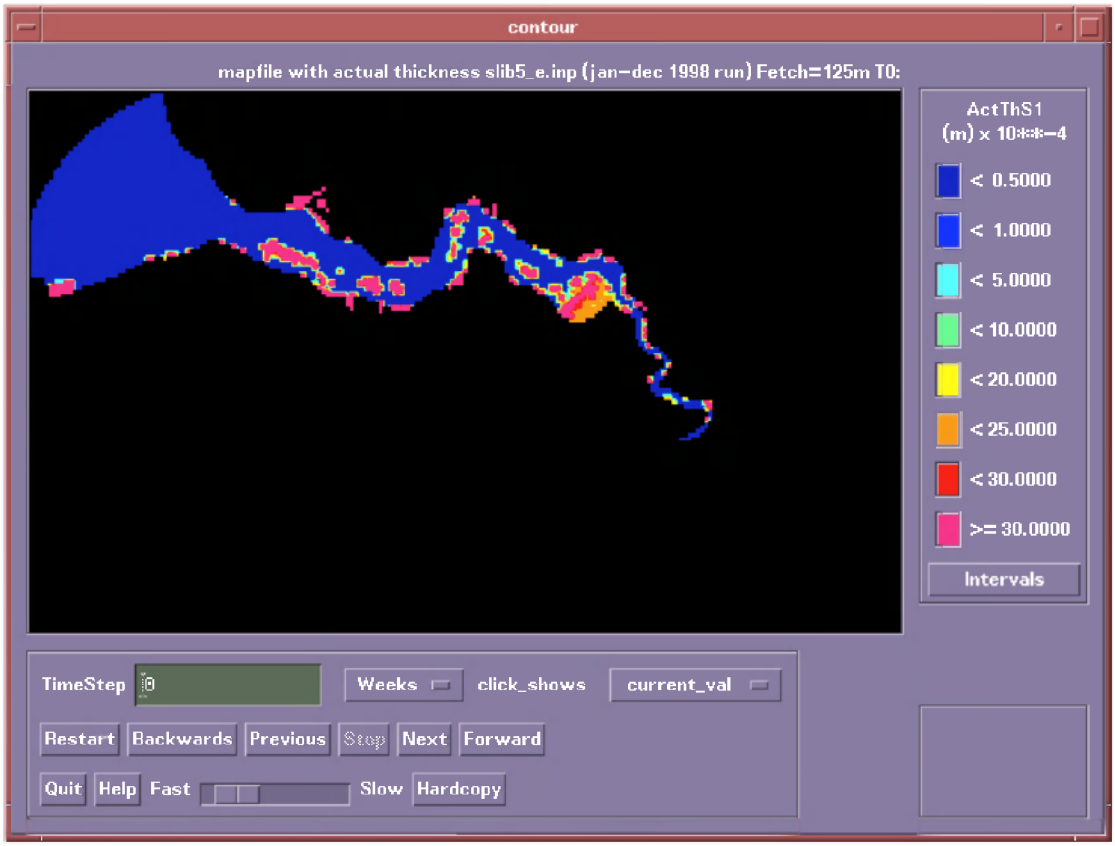

Figure 4.5 Initial thickness of the bottom sediment layer (thickness of two sediment fractions) used for 1-1-1998. The tidal flats can clearly be seen here.

The shear stress created by wind is calculated according to Bijker (in DELWAQ Technical Reference Manual, WL|Delft Hydraulics, 1997), and is a function of the wind speed, water depth and fetch (length of open water in the direction of the wind), see Appendix A. On tidal flats (i.e. shallow water depths), capillary waves (T < 1 sec) can be important in causing resuspension of sediment. Fetch on tidal flats (where average water depth is < 2.0 m) is set to 125 m. With this parameterization, capillary waves are generated (T~0.5 sec, H~45 cm) which can cause erosion during storm periods with wind speeds greater than 10 m/s.

Process 3: Erosion from gullies by tidal flow

Gullies may release some sediment at high shear stresses caused by tidal flow. This process is modelled primarily with the second sediment layer (S2) which has a high critical shear stress for erosion. The critical shear stress for erosion of S2 was set at 4.0-5.0 Pa (seasonal variation). With this value, erosion from the second sediment layer occurs only during spring tide, when highest flow velocities are present. As a result, a distinct difference in SPM concentration is found between spring and neap tides (which have much different shear stress due to flow). The difference in bed shear stress between a spring and neap period is shown in Figures 4.6a and 4.6b for the tidally averaged neap and spring tide respectively .

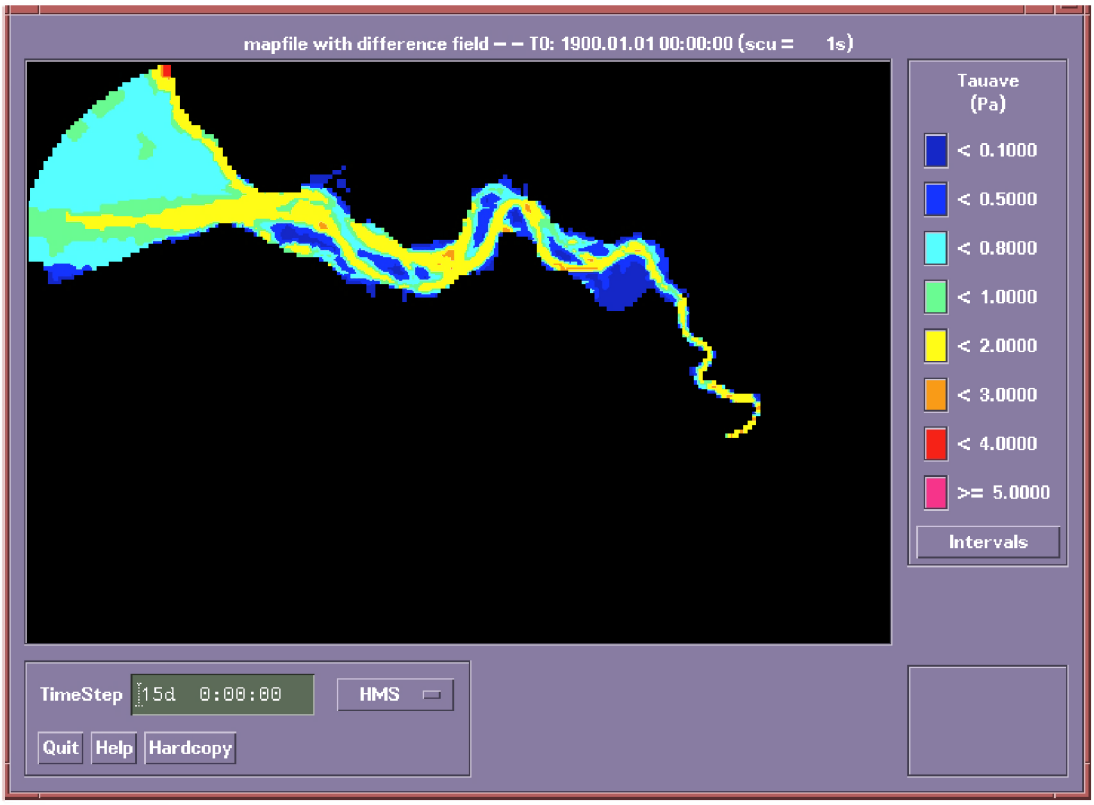

Figure 4.6a The *average* bed shear stress over 7 model days without wind for the *neap period*

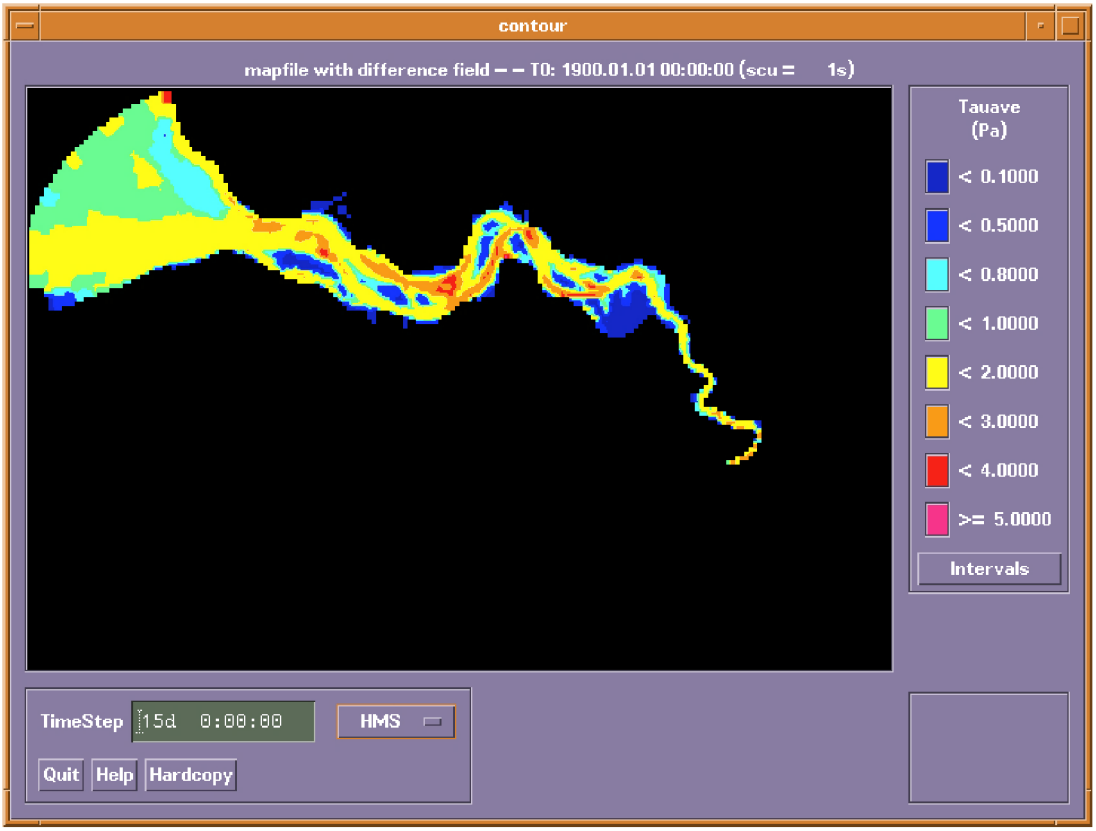

Figure 4.6b The average bed shear stress over 4 model days without wind for the *spring period*

Process 4: Erosion from gullies by wind induced waves

In contrast with the tidal flats, capillary waves do not contribute to erosion in the gullies. In the gullies, waves with longer periods (T~ 2.5s, H~ 1m) are important for erosion. Waves with a long fetch (~5-10km) can very well erode the shallow sides of the gullies (depth<2.5m) at high wind speeds.

In the model, the fetch is set at 6 km for computational segments with a (tidally averaged) water depth greater than 2.0 m in order to generate erosion effects in the gullies. This results in extra erosion during periods of high wind, e.g. January, begin March, and end October. For segments with an (average) water depth less than 2.0 m (i.e. all tidal flats), a fetch of 125m is retained.

Model limitations

The model set-up as described above includes the main inputs and processes which are considered important on the spatial and temporal scale at which the Western Scheldt is being studied, i.e. the entire Western Scheldt for a period of 1 year. At different (smaller) spatial and temporal scales of concern, some of the following processes could also be important:

1. *Stratification:* Both the hydrodynamic and the water quality model are depth averaged, and stratification was not modelled. Stratification may have an important effect on bed shear stresses and settling of sediment (Gerritsen et al., 1999). However, stratification is only expected to affect the Belgium part of the Scheldt. It may also affect the turbidity maximum in that area, though Buchard and Baumert (1998) suggest that the main mechanism for the turbidity maximum is the tidal asymmetry, which is included in the 2D model. Analysis of the continuous in-situ data from Terneuzen show that concentrations are similar at different depths, thus the use of a depth averaged model seems to be appropriate.
2. *Fluid Mud Layers:* Fluid mud or 'luthocline' or is a suspension of silt with a very high concentrations of more than 10 grams per liter. This process is not included in the current model. It may play an important role at tidal flats, were water can be stagnant, and/or be at very high concentrations. Fluid mud layers may also be formed when large amounts of silt are dumped, either from harbour dredging or from the tunnel. If fluid mud layers are formed on the tidal flats, silt may flow off the tidal flats as fluffy layers on the bed.
3. *Secondary flow:* secondary flow (included in 3 D models) might generate additional erosion by flow in curves like 'Schor van Baalhoek'. It is not modelled, but might be an additional explanation for the 12 hour frequency observed in the Baalhoek data (Chapter 2).
4. *Wave induced currents at tidal flats:* breaking waves at the sides of tidal flats can induce local currents. This process is not modelled.

One factor which could be important for providing more detailed spatial results is:
Detailed variations in flow and SPM concentrations for boundaries: model boundaries have a constant influx of water as specified in the hydrodynamic model. The constant influx of water is combined with constant monthly averaged concentrations (from 20 yearly means)

of SPM data. For the Scheldt river, the flow is yearly averaged (100 m^3/s). For the sea boundary, the boundary concentrations are spatially averaged (although monthly varying), and must partially also include the effect of silt dumpings from Belgium harbours on the Western Scheldt. Due to these simplifications in defining the model boundaries, the calculated SPM concentrations can never have large changes in time near the model boundaries. By the sea boundary, the calculated SPM calculations will also be spatially homogeneous as compared to remote sensing data.

4.4 Model calibration

4.4.1 Introduction

In section 4.3 the set-up of the water quality model is described. The model was set up by initialisation of some of the model parameters in test models. The results of these test models were often derived from *qualitative comparison with a single data set (either the Terneuzen set or the Baalhoek set of continuous data).* Remote sensing data were not used, and no validation was done for the spring and summer period.

After the first model set-up, a proper calibration for SPM was conducted, using *all available data simultaneously.* These calibration data are:

1. Continuous in-situ data for SPM (mg/l) at Baalhoek, Terneuzen and Vlissingen (described in Chapter 2).
2. Twenty year monthly mean averages for SPM for 8 locations (described in Chapter 2).
3. 9 processed images from remote sensing, transformed to the aggregated SCALWEST model grid (see section 3.3.2).

A proper and objective calibration for such large amounts of data is hardly possible by visual inspection, thus quantitative methods for model calibration, such as a cost function, are preferred. Various cost functions were developed and tested successfully by Vos and ten Brummelhuis (1997) and Ten Brummelhuis et al. (1999) in the PROMISE project for the North Sea, and in the RESTWAQ-2 project (1998, PART I) for the Dutch coastal zone. The formal methodology is described in Vos and Ten Brummelhuis (1997). A simplified version of this methodology was applied in this study as described generally below, and in more detail in Appendix B.

4.4.2 Cost functions for data-model integration

A cost function (or Goodness-of-Fit criteria) calculates the difference between model results and measurements ('observables'), while taking into account the uncertainty in the measurements. If the model result is within the uncertainty range of the measured data, data and model are said to be in agreement and no difference is counted. The greater the difference between model and data, the larger the resulting value of the cost function.

Three separate cost function were used to compare the model with the available data sets and calculate the differences between model and data. The three cost functions were developed to compare the model with the key features of the different data sets.

In a final step, a total cost function value was calculated as the sum of the three individual cost function results (normalized sum).

When a cost function is calculated for several different model simulations (calibration runs), the simulation with the lowest cost function value is the best one (i.e. is the simulation which best matches all the data). Equations for the cost functions are given in Appendix B.

Use of remote sensing data in a cost function

To compare model result with remote sensing data, the model result ideally has to be at the exact date and time of the remote sensing image. For comparison of the Remote Sensing data and the model data, the model result closest to the remote sensing data in time, and within one meter difference of water level at Terneuzen were selected and compared to the remote sensing data. The absolute date of model results could not be used because the model hydrodynamics are slightly out of phase. Thus a time 'shift' in the model results are needed in order to make a comparison with a specific time (see also Section 4.2).

The cost function for the model and remote sensing data, focuses on the gradient in SPM concentrations from West to East in the Western Scheldt. To quantify this gradient along the axis of the estuary, the region is divided into 9 zones (Figure 4.7). For the cost function, both the model data and remote sensing data are aggregated for the 9 zones. Only averaged concentrations per zone are compared. The uncertainty in the remote sensing data is taken to be 10% of the SPM concentration, This estimate was estimated from the accuracy of processing of the level 1 SPOT images (section 3.3.1).

Use of in-situ data in a cost function

Two different cost functions were defined for use with the monthly averaged data and the continuous in-situ data.

The model concentrations of SPM and in-situ data were monthly averaged before the difference between the model and the data was calculated. For the continuous in-situ data, this leads to reduction of much of the information in the cost function. However, it was found that use of daily averages did not give very different results. Nevertheless, the cost function is not sensitive for a difference in the oscillations of spring-neap tide and lunar tide. Such cost-functions still need to be developed in the future. This can be done by explicitly using the amplitude and phase of these oscillations in the cost functions (beside the SPM concentrations), obtained from a fourier analysis of modelled and observed time-series of SPM.

The calculation of the cost function requires a value for the uncertainty (S) in the in-situ data. For the twenty year monthly averaged data, the uncertainties were set equal to the monthly standard deviations. For the continuous in-situ data, the uncertainties were taken to be 20% of the observed averages.

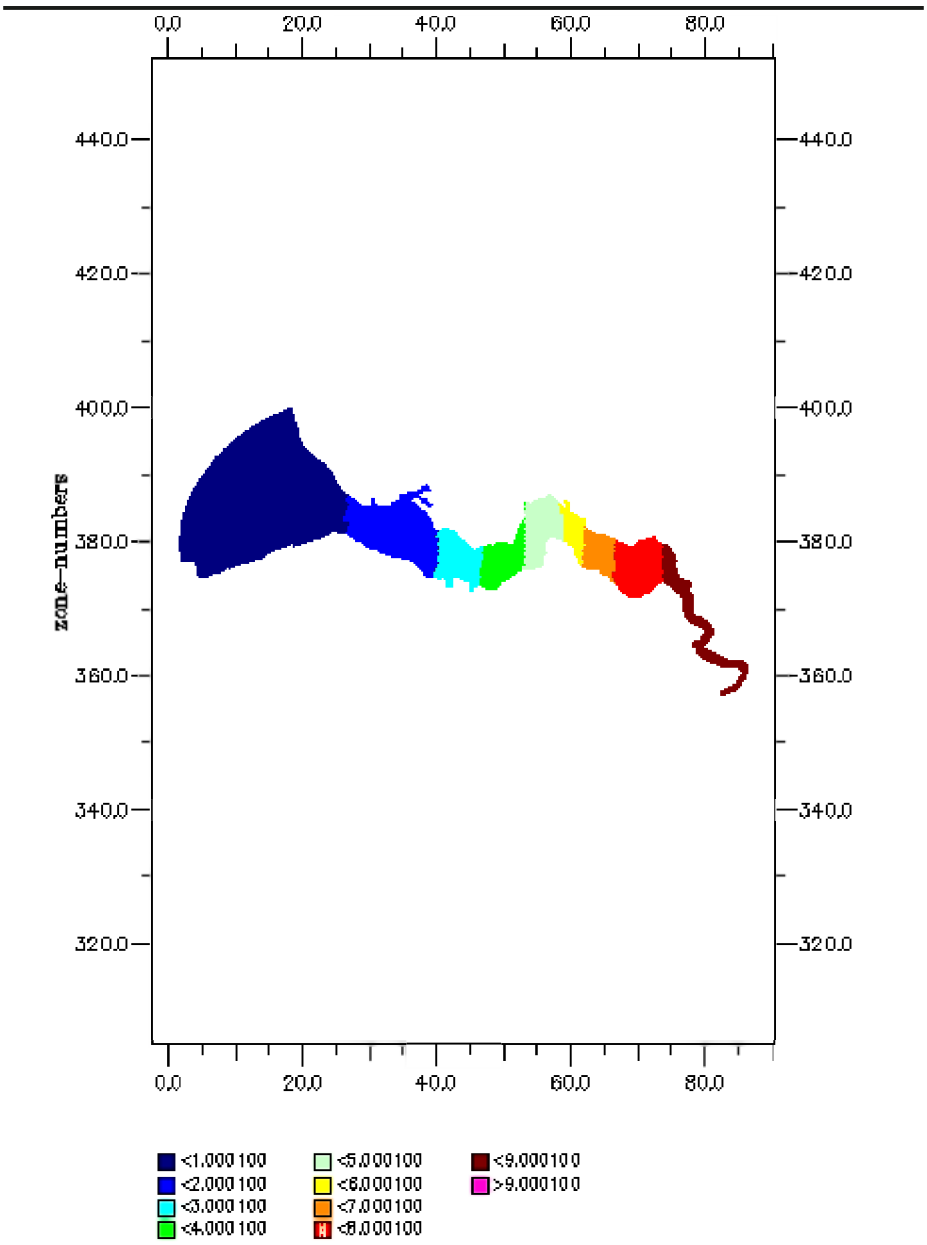

Figure 4.7 Definition of zones used in the remote sensing cost function for comparison of Remote Sensing SPM data with model results. Only averaged concentrations per zone are compared. (<1.000100 = zone 1; < 2.000100 = zone 2; etc.)

Total Cost function

Each cost function results in a cost function value which is indicative of how well the model compares with a particular data set (the lower the cost function value, the better the comparison). Furthermore, a total cost function was calculated as the sum of the 3 individual cost functions (these were first normalized, since they are not of the same order of magnitude). The total cost function was used to determine the best model calibration.

4.4.3 Calibration parameters

The main model processes and process parameters have been described in section 4.3 and Appendix A. An overview of process parameters and their final settings is given in Table 4.3. After the model set-up, 11 calibration simulations were done with variations of the parameters. Parameters that were optimised during the model calibration are shown in *italic*. For other parameters, the parameter values were determined during model set-up and remained fixed.

A description of the different calibration simulations and an analysis of results using the cost function is described in Appendix B. The best model calibration run was selected on basis of the cost function, i.e. the simulation with the lowest cost function result.

Table 4.3 Final values for model parameters and inputs. The parameters which were varied during the model calibration tests are given in italic. Other values were determined during the model set-up and remained fixed through the calibration.

Parameter	Description	Unit	Final value
ZResDM	*Erosion rate for layers 1 and 2*	*g/m2/s*	*17280*
TauCRS1DM	Critical shear stress layer 1	Pa	Function, Fig A.3
TauCRS2DM	*Critical shear stress layer 2*	*Pa*	*Function 2, Fig A.8*
Fetch for H< 2m	Fetch for waves for depth < 2m	m	125
Fetch for H> 2m	Fetch for waves for depth > 2m	m	6000
TauCSIM1	Critical shear stress sedimentation IM1	Pa	0.1
TauCSIM2	Critical shear stress sedimentation IM2	Pa	0.1
TauCSIM3	Critical shear stress sedimentation IM3	Pa	4
Manning	Manning coefficient for Chezy form.	-	0.026
VSedIM1	Settling velocity IM1	m/day	Function, Fig A.1
VSedIM2	*Settling velocity IM2*	*m/day*	*Function, Fig A.1*
VSedIM3	Settling velocity IM3	m/day	100
Bottom-comp.S1	Initial bottom for layer S1 at start	-	Figure 4.5
Bottom-comp.S2	*Ratio of (IM3/DM) in layer 2 at start*	*%*	*95*
Sea Boundary IM1	*Concentrations of IM1 at sea boundary*	*mg/l*	*Function, Figure 4.3a*
River Boundary IM2	Concentrations of IM2 at Antwerp	mg/l	Function, Figure 4.3b
Dumpings	*Amounts for Dutch harbour dumpings*	*Mton*	*1998 dumpings, Table 4.2*

Conclusions about model set-up and calibration

A dynamic water quality model for SPM has been set up for the Western Scheldt estuary. It was calibrated on in-situ data and remote sensing data simultaneously, taking into account estimates (a band width) for errors in the data. During the final model calibration 5 model parameters were varied, and the effect of adding dumpings of harbour silt was tested. The best model result will serve as a basis for a T1-scenario simulation (dumping of silt for 1999 from Tunnel boring).

The cost function is crucial for objectively analysing model results with respect to 3 different data sets of the Western Scheldt. The continuous measurements, the monthly averaged measurements and the remote sensing all provide a different 'truth' of the SPM

conditions in the Western Scheldt. It was observed during the calibration, that the model results which compared very well with one set of data (e.g. continuous SPM measurements at Terneuzen), did not compare well with the longterm monthly averaged concentrations, or the remote sensing. Pitfalls occur if the model calibration focuses on one local station only. *For the optimal model calibration, there is a need of various data sources, from various techniques and from various locations.*

The best model result therefore, is the one that *on the whole* has the best comparison with all the data. *The cost function is the only method for objectively making this assessment.* Because the model is optimized on different information sources, when the model result is compared to measurements at one specific location, or to a remote sensing image at one specific moment in time the results will never be perfect.

An additional difficulty in comparing model and remote sensing results at a specific time is due to the out-of-phase spring-neap cycle in the model (see section 4.2). In order to compare model and remote sensing results at a specific moment in time, the model results had to be shifted, so that the correct day and time in the spring-neap cycle were found (e.g. 3 days after spring tide, 4 hours after high tide.). This brings the results to the same tidal phase, however, the forcing functions in the model (e.g. wind) are then also shifted, so the comparison is not ideal.

The model and data analysis suggests that the continuous monitoring station Terneuzen is situated at a position where the total SPM might be dominated by a local source of SPM. This will need further investigation. Note that the 12 hour frequency peaks in SPM observed at Baalhoek also indicate that at this station there is a large effect of local SPM fluctuations.

5 Model results and comparison with in-situ and remote sensing data

5.1 Introduction

In this chapter, several different model results are presented, and a comparison is made with the continuous in-situ data for 3 stations, the in-situ data from Van Maldegem (twenty year monthly mean averages for 8 stations), and remote sensing data.

In this chapter, only the results for 1998 are presented, representing the T0-situation (the present natural situation, including harbour dumpings but excluding the dumpings of tunnel silt). Results are discussed with respect to:

- the visual agreement between the results (how far was the model calibration successful with respect to the data?);
- the characteristic differences between modelled SPM and measurements?;
- recommendations for reducing observed differences?
- the relative value of the different sources of information for monitoring a T0 situation: in-situ, remote sensing and modelling?
- the effect of differences on any of the conclusions drawn from a T1-scenario (a scenario including tunnel silt).

5.2 Model results per location, comparison with continuous in-situ data

One method of presenting model results is to show a time line of calculated SPM concentrations at a particular location(s). In Figures 5.1-5.3, the results of the final calibrated model are presented for locations Terneuzen, Baalhoek and Vlissingen, with the continuous in-situ data for comparison. Model results are presented both with and without dumpings from dredged harbour silt for 1998.

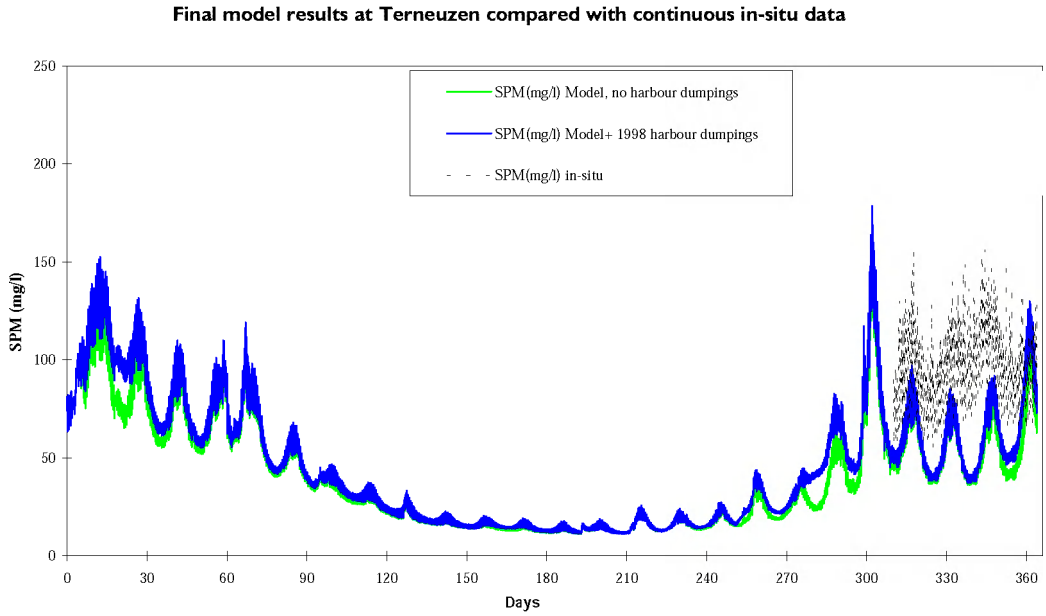

Figure 5.1a Model results for SPM concentration at Terneuzen, complete year 1998.

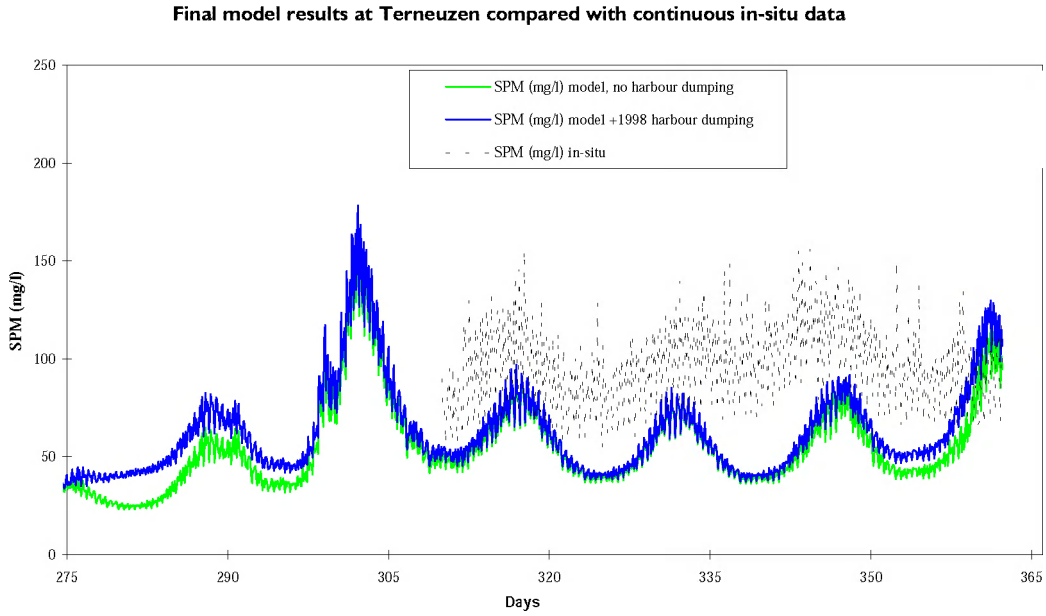

Figure 5.1b Model results for SPM concentration Terneuzen, October-December1998 (day 275 =2 October).

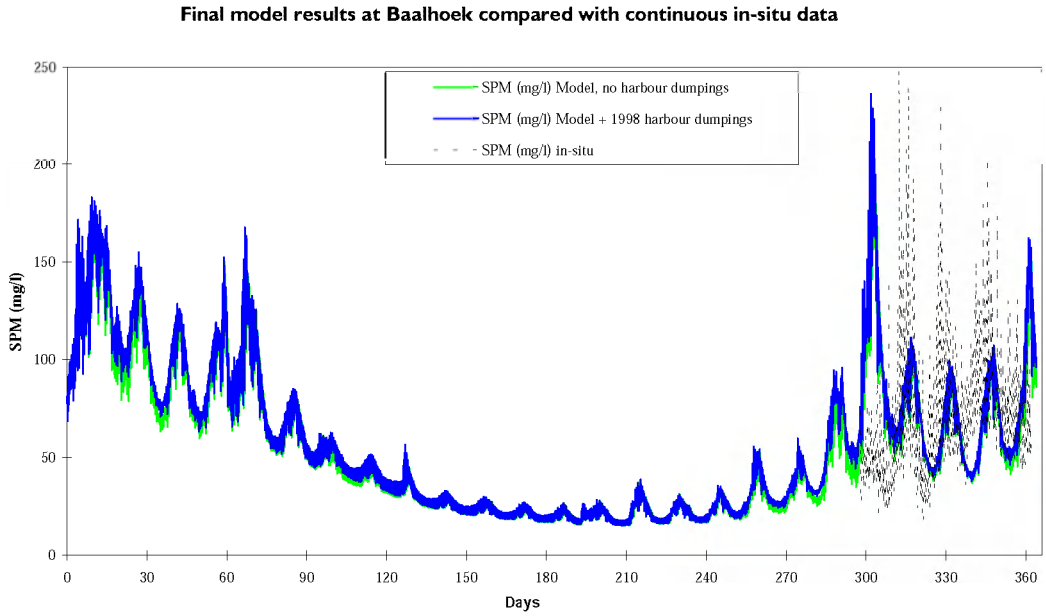

Figure 5.2a Final model results for SPM concentration at Baalhoek, with and without 1998 harbour dumpings.

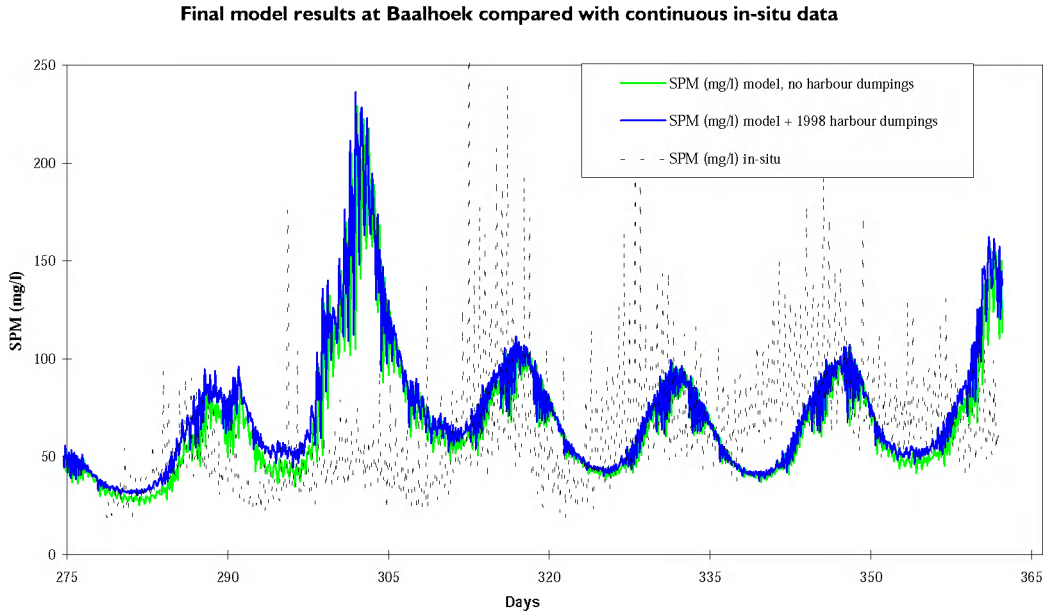

Figure 5.2b Model results for SPM concentration Baalhoek, October-December1998 (day 275 =2 October).

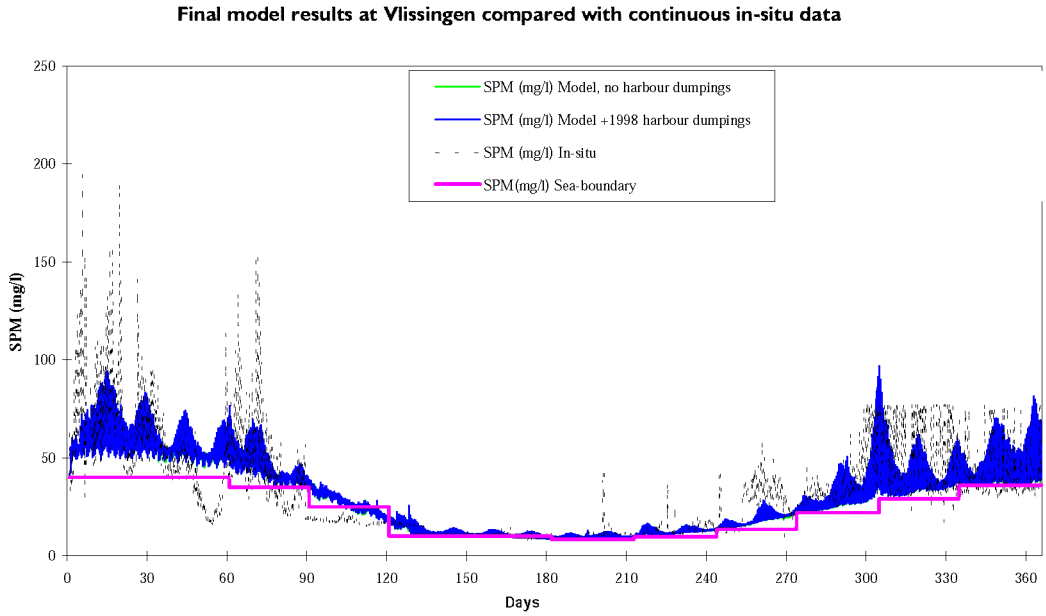

Figure 5.3 Final model results for SPM concentration at Vlissingen, with and without 1998 harbour dumpings.

Discussion

- The model can represent the seasonal variation of SPM, as seen at Vlissingen; at the other locations continuous in-situ data is only available in October - December;
- The model can represent the spring-neap variation of SPM well at all stations;
- For summer, both model and data for Vlissingen do not show a spring-neap variation;
- The model represents reasonably well the effect of wind speed on SPM at Vlissingen (for wind data see Chapter 2). However, the model can not explain the sudden drop in SPM for the beginning of February. It might follow from the wind direction which is not taken into account in this SPM model;
- The model does not predict correctly the 12 hour frequency peaks of SPM in November 1999 observed for Baalhoek;
- The SPM variations in the data for winter periods (Jan-March, Nov-Dec), are larger than for the model. SPM drops back to a low level at Vlissingen at the end of March, but the model reaches this lower SPM level one month later.

Conclusion

The optimised model can very well explain the spring-neap cycle in the data, and the general seasonal behaviour of SPM. However, all more chaotic behaviour in the continuous SPM data, especially those at the tidal time scale, can not be modelled at present.

There is a time-shift in the model which is due to an error in the synodal period (in the hydrodynamic model). This period was chosen to be 29 days in the model, whereas it must be 29.5 days. This time-shift required a relative shift of the data before they could be compared with each other.

5.3 Model results per location, comparison with monthly average data

In Figures 5.4a-h, the final calibrated model is compared to the monthly averaged in-situ data of Van Maldegem at 8 locations. Model results include dumpings from dredged harbour silt for 1998. At the selected locations, the model results have been averaged over each month, and thus are directly comparable to the van Maldegem data.

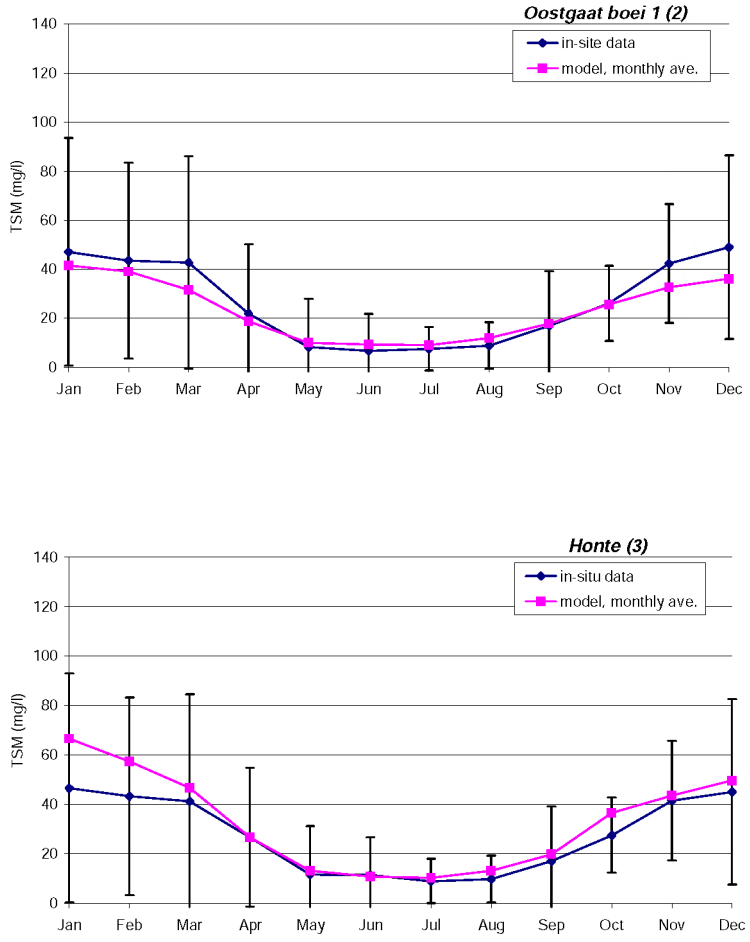

Figure 5.4(a-b) Monthly averaged model results for SPM concentration compared to stations of Van Maldegem

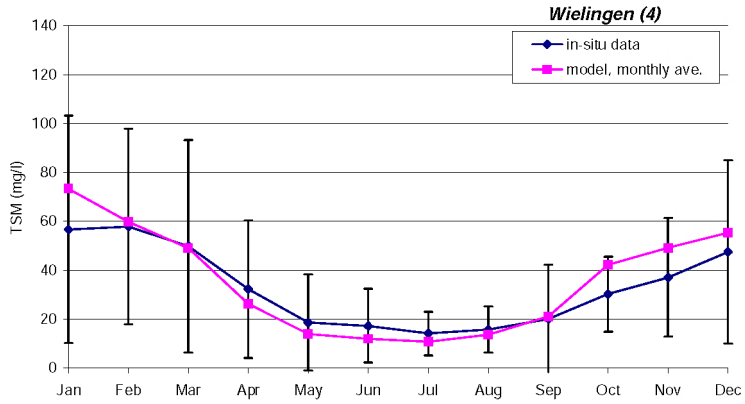

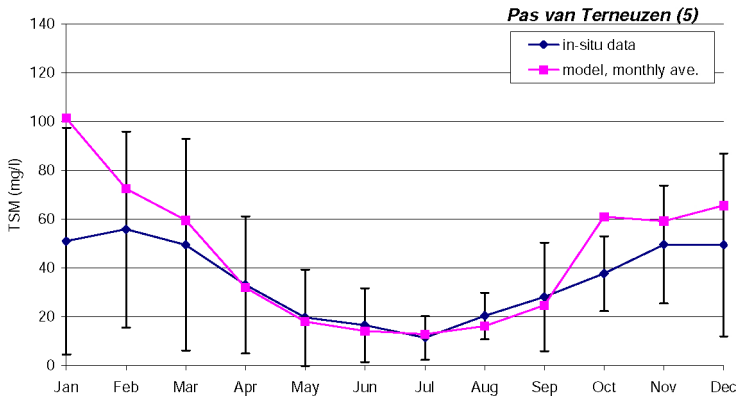

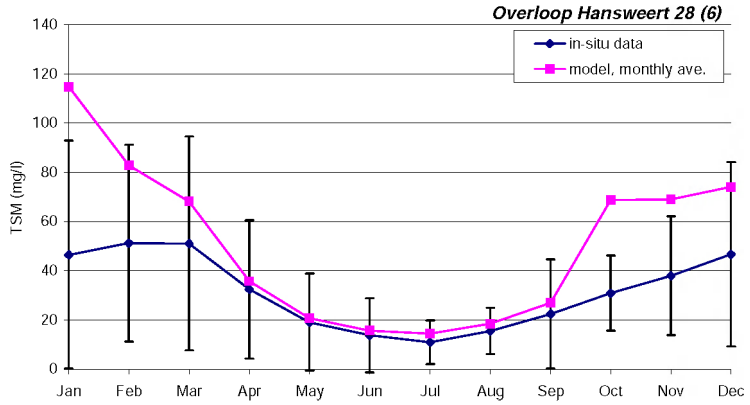

Figure 5.4(c-e) Monthly averaged model results for SPM concentration compared to stations of Van Maldegem

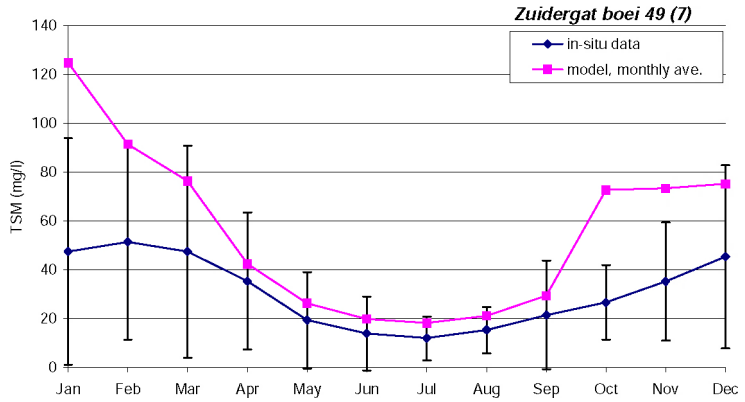

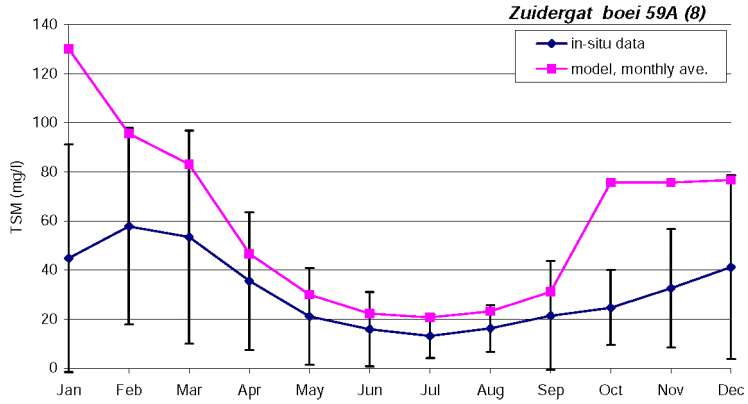

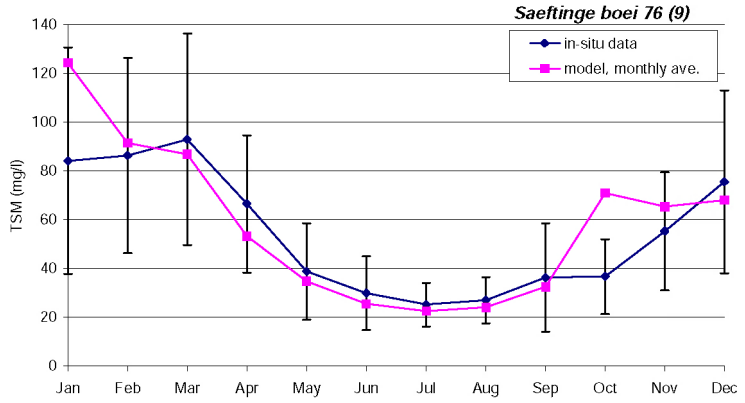

Figure 5.4(f-h) Monthly averaged model results for SPM concentration compared to stations of Van Maldegem

Discussion

On the whole, the model compares very well with the longterm monthly average SPM concentrations, and is within the standard deviation range for almost all months at all locations. The comparison is best in the months April - September, while in the winter and fall months there are some differences.

In January, the model has high concentrations compared to the measurements. The high model concentrations are due to the storm conditions (wind > 10 m/s) that prevail during much of January 1998. The continuous measurements at Vlissingen also show high concentrations during January, with occasional peaks of nearly 200 mg/l. Also in October and November, the model results are high at some stations. In this period, there are also storm conditions. In the model, the high wind causes resuspension of bottom sediment (from wind induced waves), resulting in the high calculated SPM concentrations.

During the months April - September, the modelled results are very close to the longterm monthly averaged SPM concentrations. Only at Zuidergat (stations 7 and 8), the modelled concentrations are a bit high, but still within the standard deviation. At Saeftinghe, (station 9), the modelled concentrations are slightly low, but within the standard deviation.

5.4 Synoptic model results through the year

Model results can also by shown synoptically, i.e. as a map of SPM concentrations for the whole area at a specific moment in time. In order to show the variation of SPM concentration throughout the year, model results are presented at 4 different times: February, May, July and October (Figures 5.5 and 5.6). Each result is during the spring period of the tidal cycle during rising water. The model results are given on the 4*4 aggregated model grid.

These model results show some of the important spatial features in SPM concentrations:

- In all maps there is a gradient of increasing SPM concentrations moving from west to east.
- There is a strong seasonal pattern in SPM concentrations. Concentrations are high (>50 mg/l) in most of the Western Scheldt in the winter (February) and fall (November), and concentrations in most of the estuary are low during the spring-summer period (as seen in May and August). This seasonal pattern is the same as seen in the in-situ data at Vlissingen (continuous) and the longterm monthly averaged data.

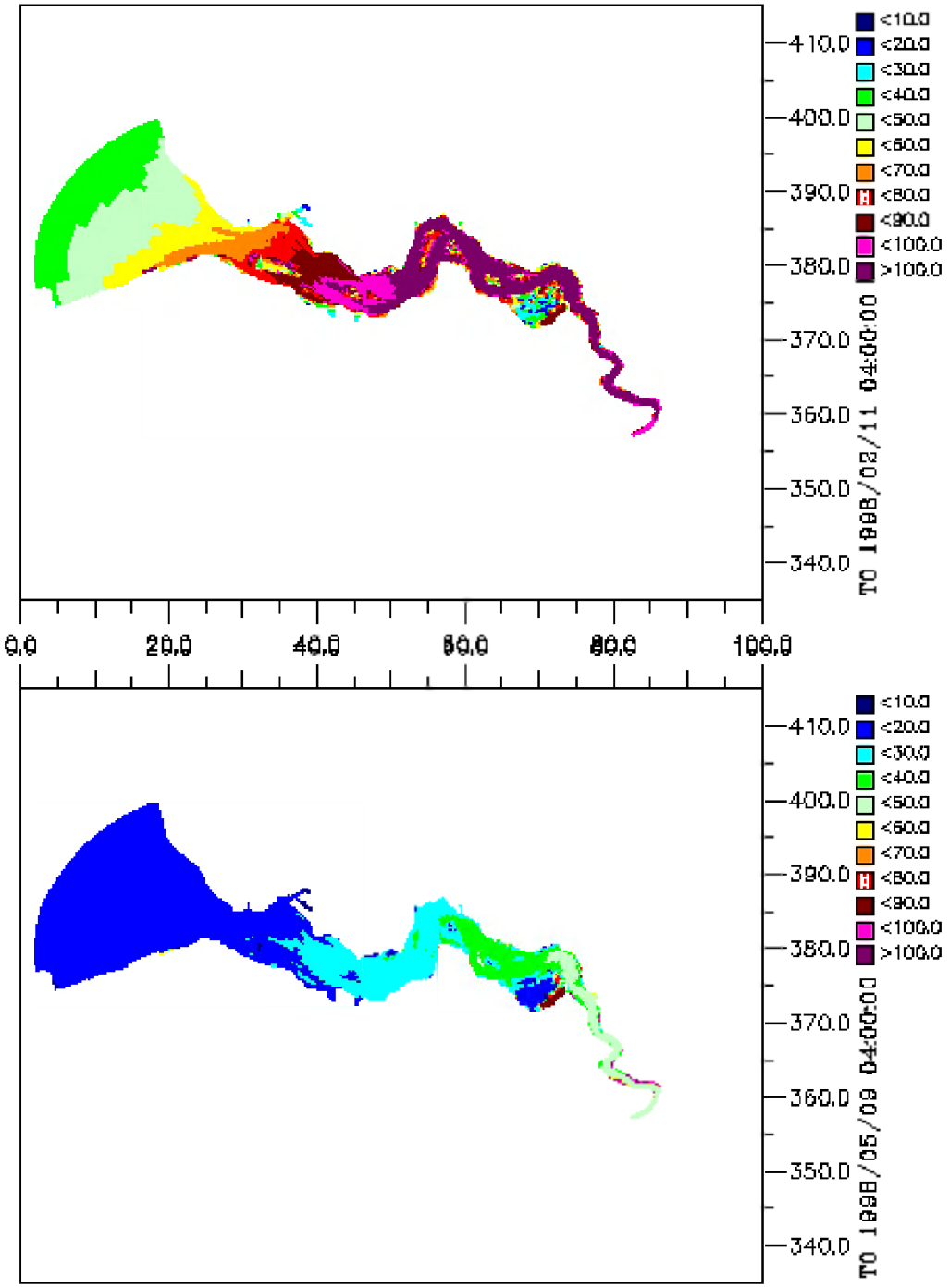

Figure 5.5 Model results for SPM on 11 February 1998 (top) and 9 May 1998 (bottom). Both times are during spring tide, high water

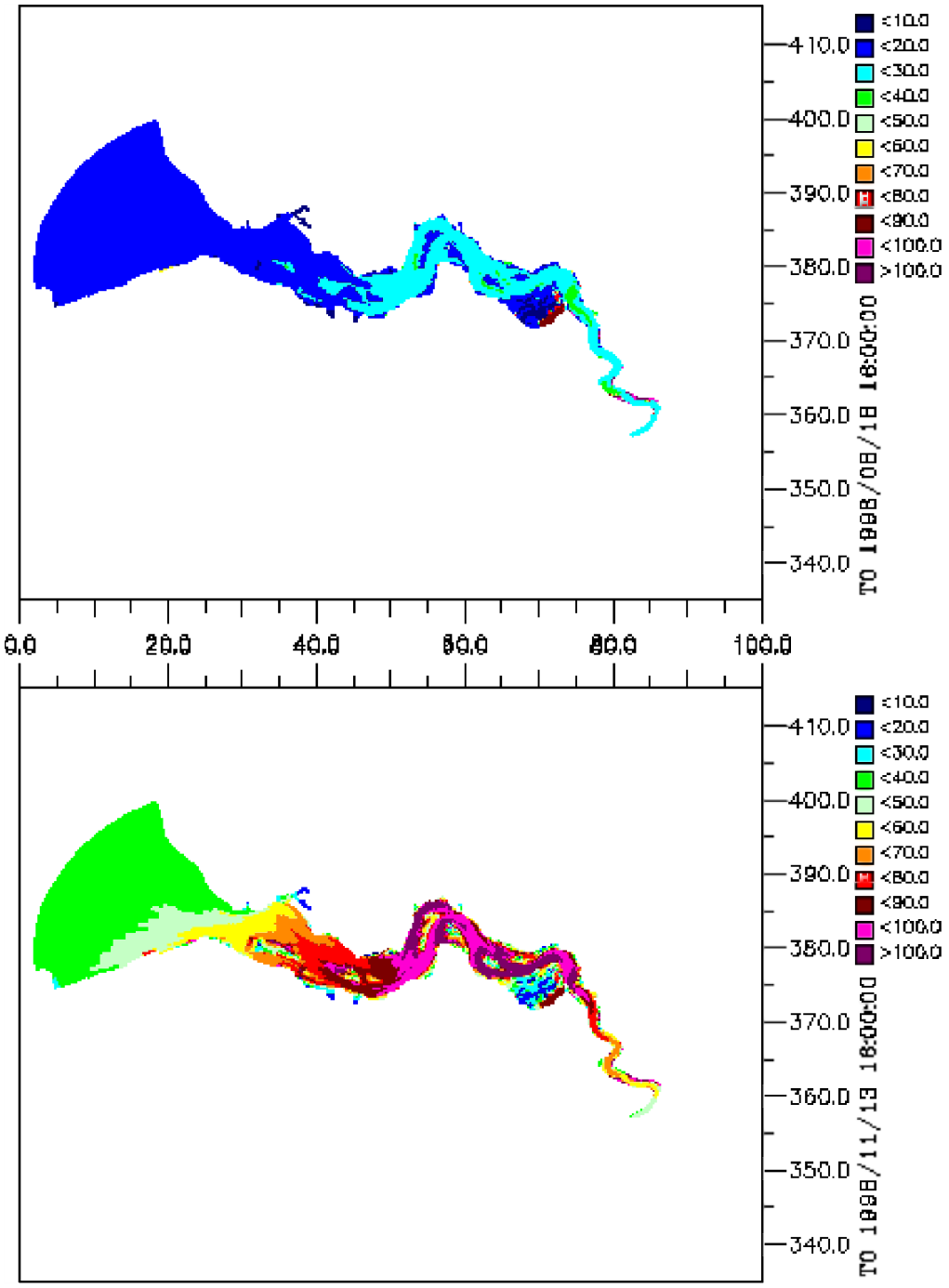

Figure 5.6 Model results for SPM on 18 August 1998 (top) and 13 November 1998 (bottom). Both times are during spring tide, high water.

5.5 Synoptic model results and comparison with remote sensing data

An integration of the remote sensing data with the model has been done during the calibration phase by using the cost function. In this section, the final model results are presented at the specific times corresponding with remote sensing images (Figures 5.7-5.14). Model results are presented together with the remote sensing data to allow a visual comparison. These remote sensing maps are presented on the full non-aggregated SCALWEST model grid. The model results are given on the 4*4 aggregated model grid.

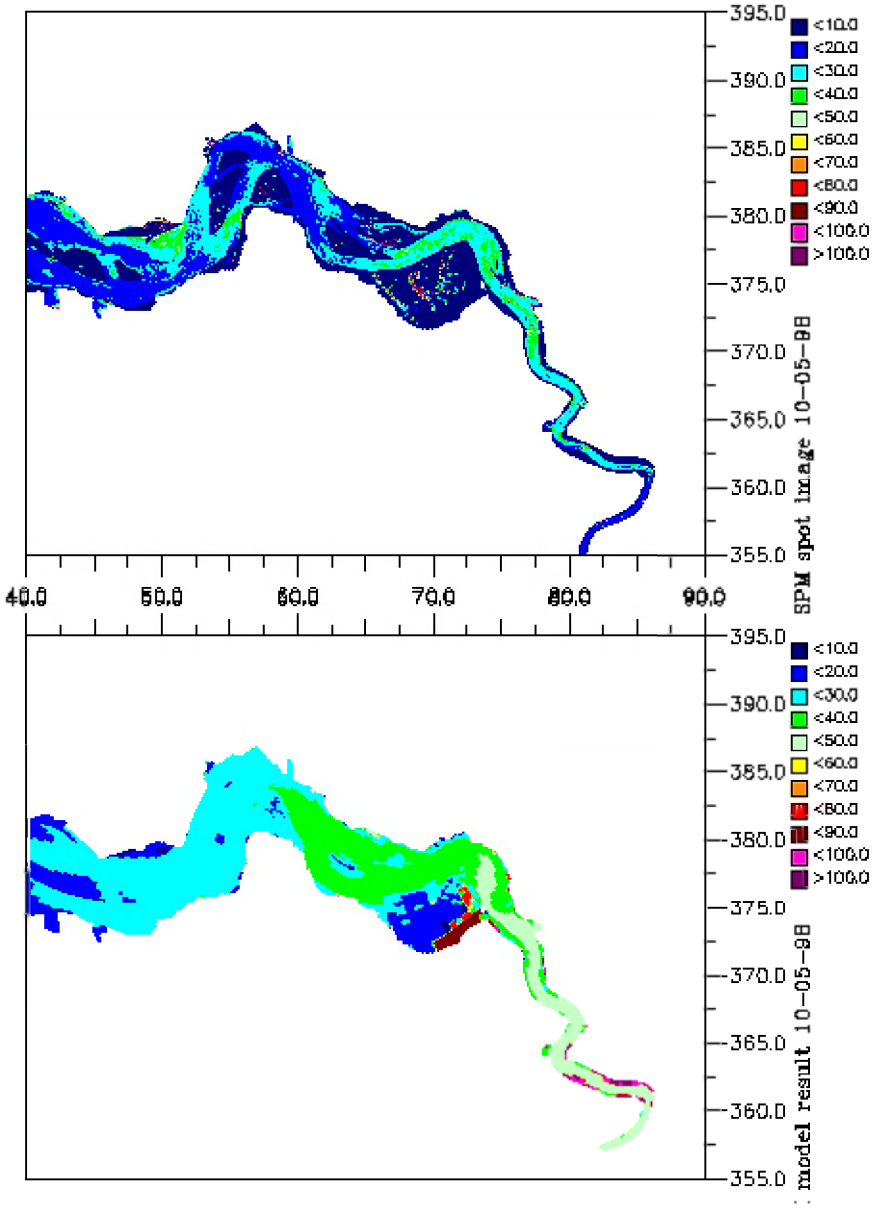

Figure 5.7 Comparison of remote sensing SPM maps with model results for 10 May 1998 (east side Western Scheldt, mean water, incoming tide).

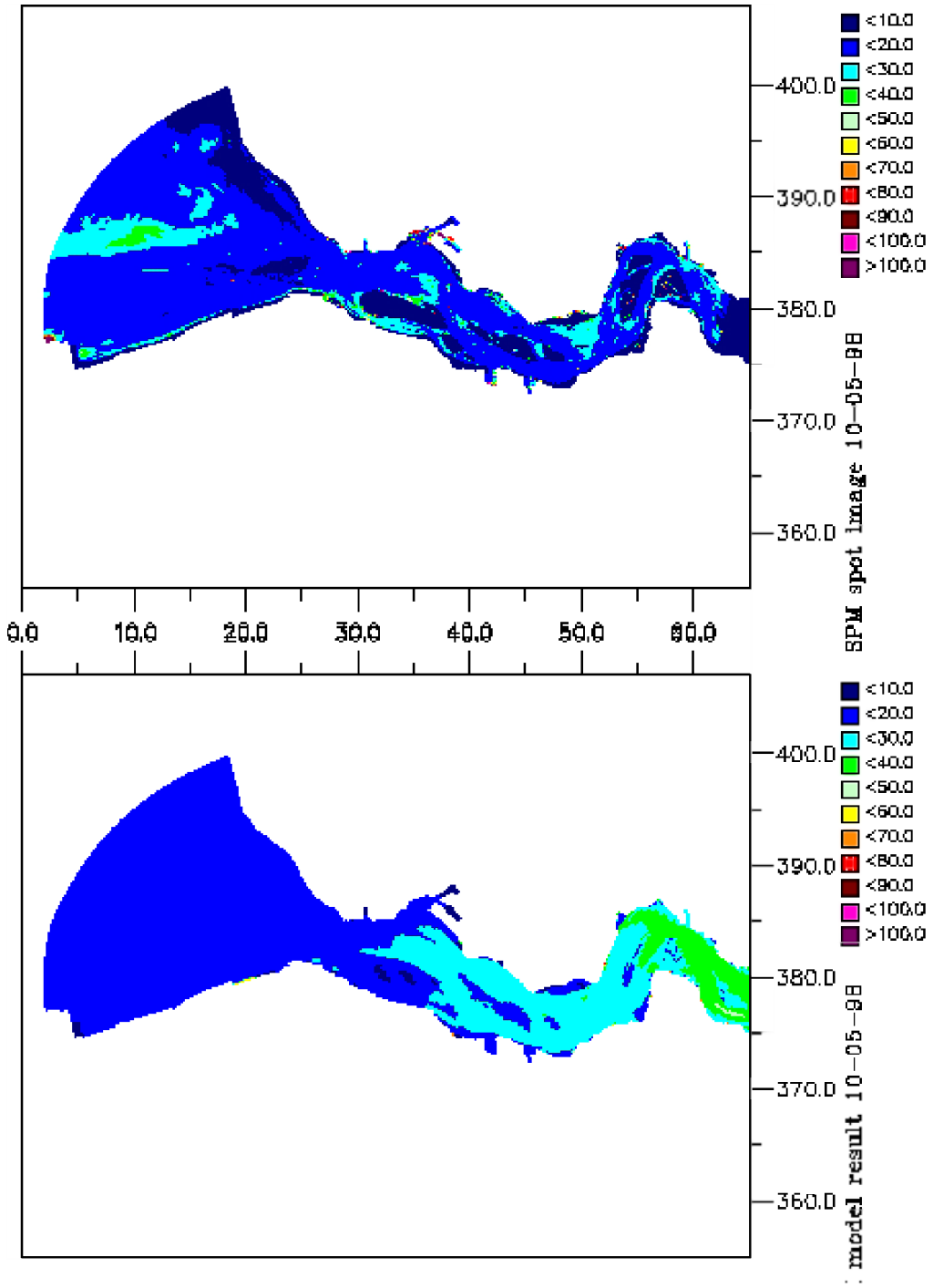

Figure 5.8 Comparison of remote sensing SPM maps with model results for 10 May 1998 (west side Western Scheldt, mean tide, incoming water).

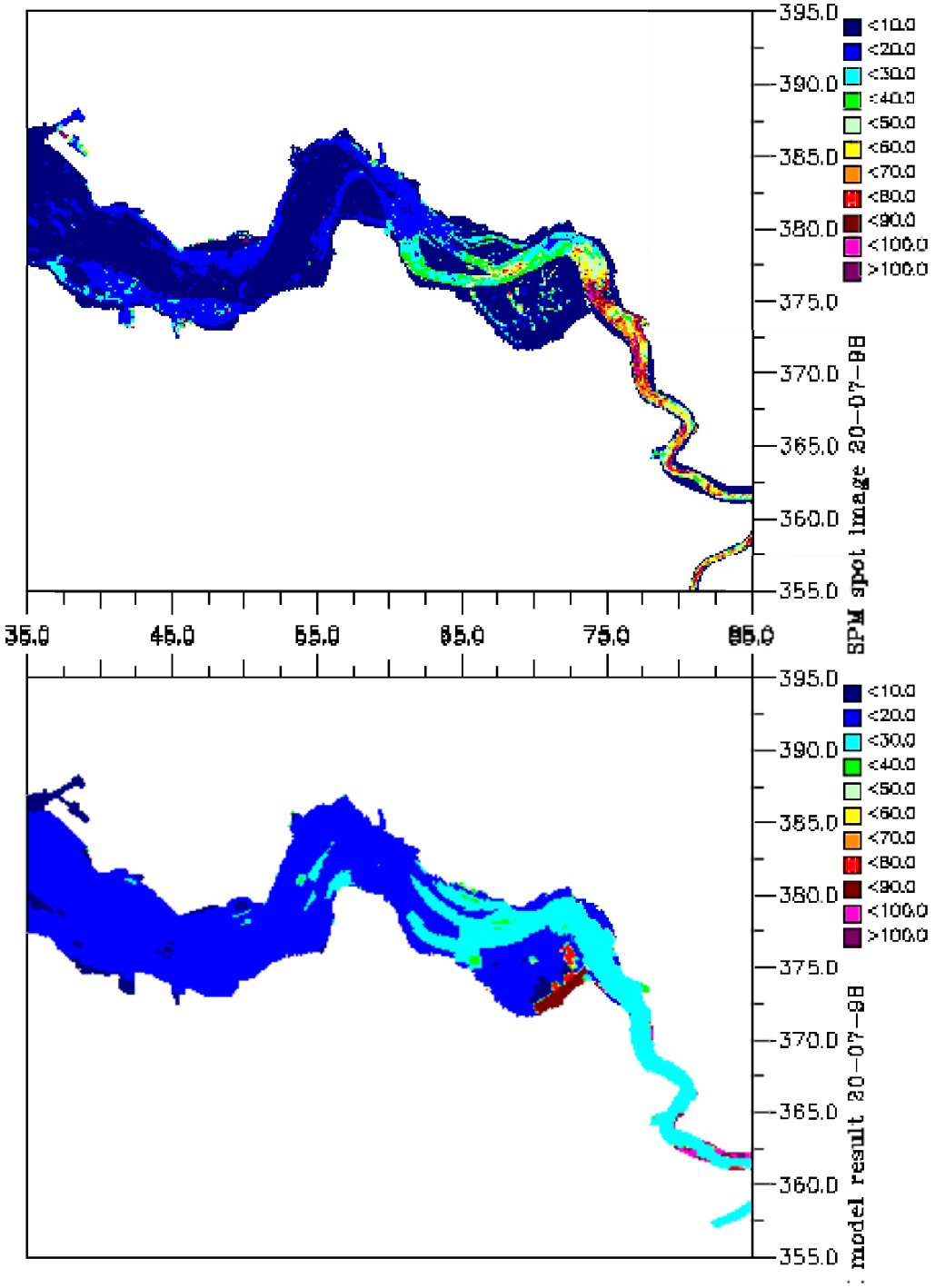

Figure 5.9 Comparison of remote sensing SPM maps with model results for 20 July 1998 (high tide, slack water).

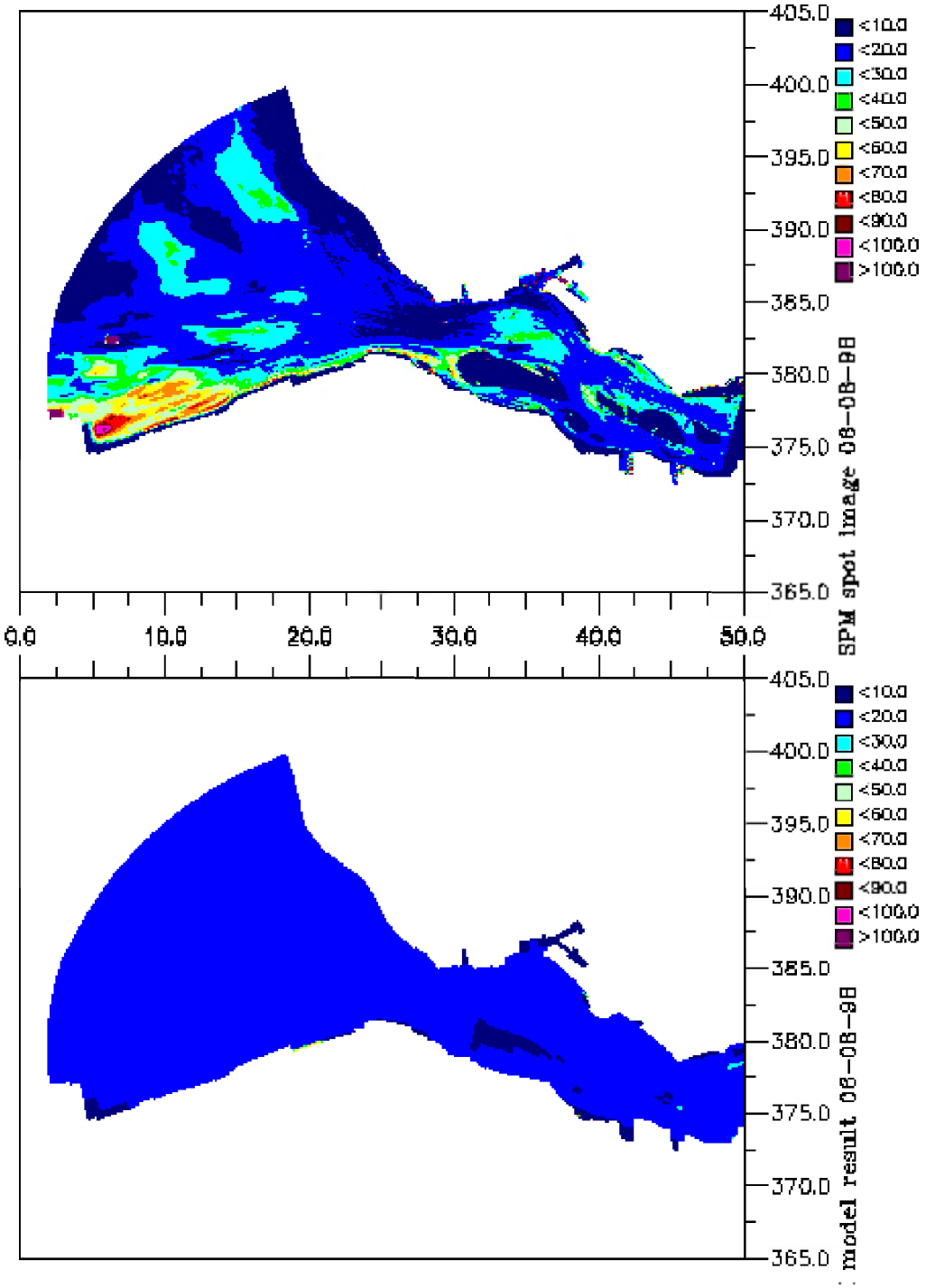

Figure 5.10 Comparison of remote sensing SPM maps with model results for 6 August 1998 (high tide, incoming water).

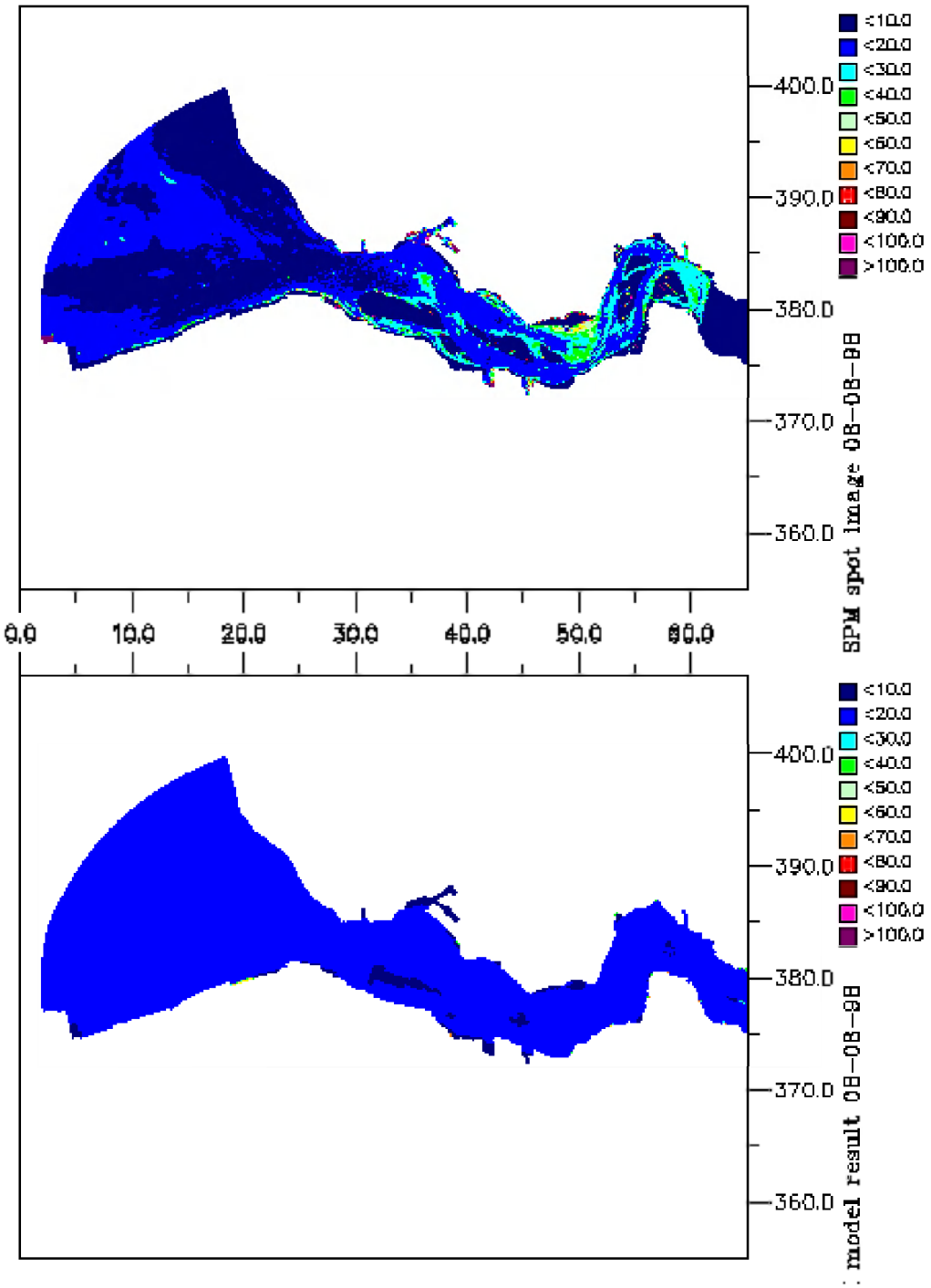

Figure 5.11 Comparison of remote sensing SPM maps with model results for 8 August 1998 (mid tide, incoming water).

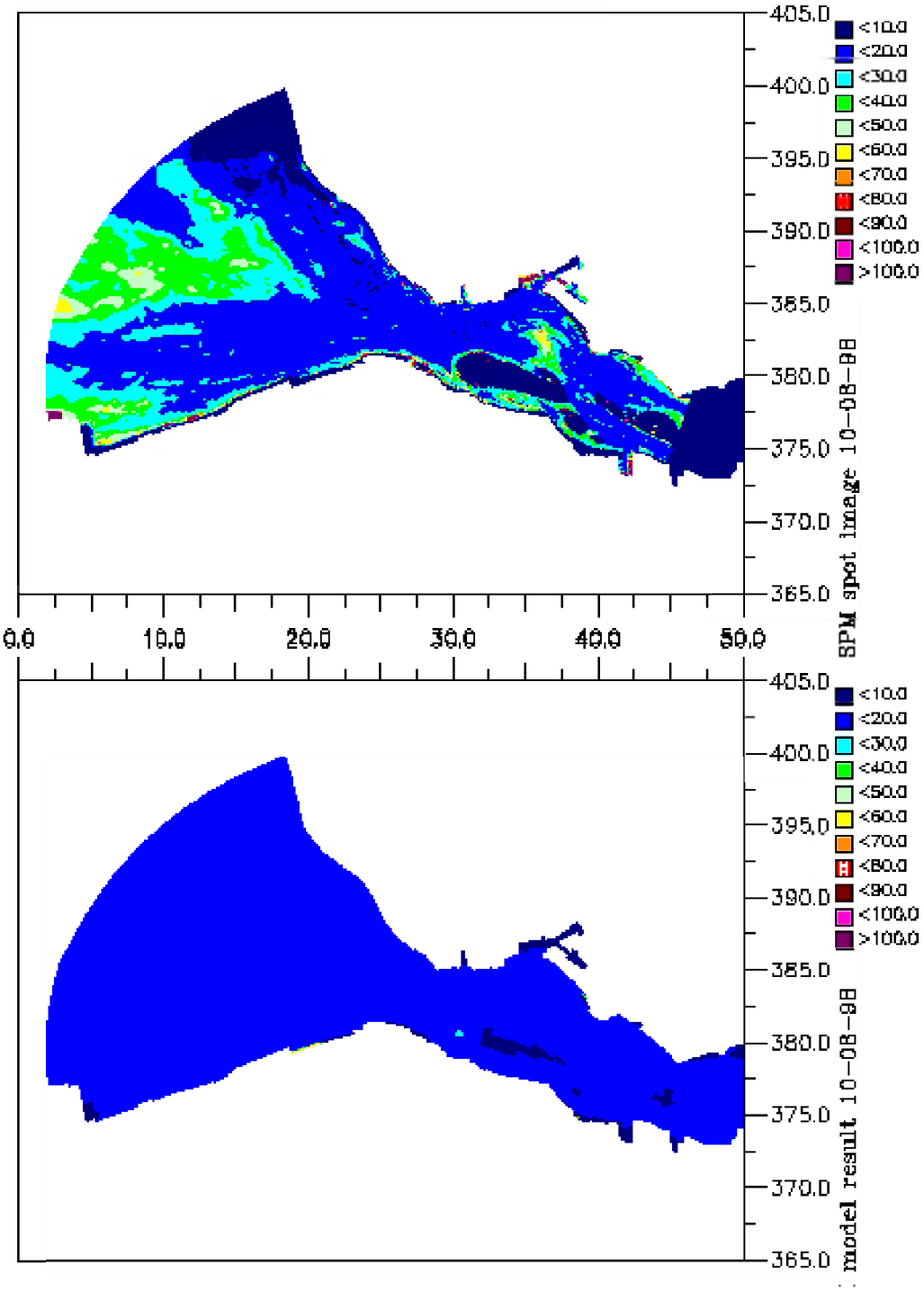

Figure 5.12 Comparison of remote sensing SPM maps with model results for 10 August 1998 (low tide, incoming water).

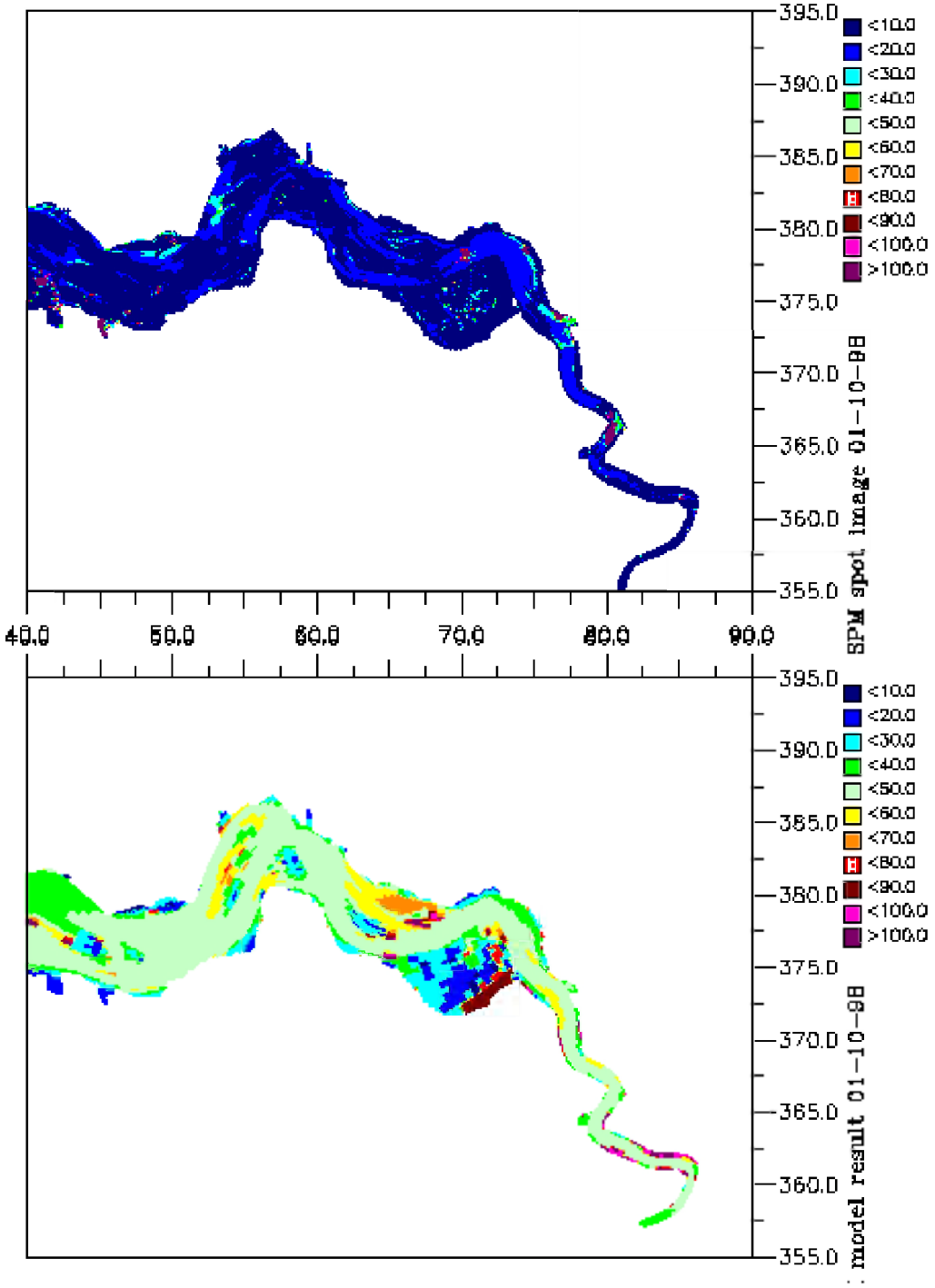

Figure 5.13 Comparison of remote sensing SPM maps with model results for 1 October 1998 (high tide, outgoing water).

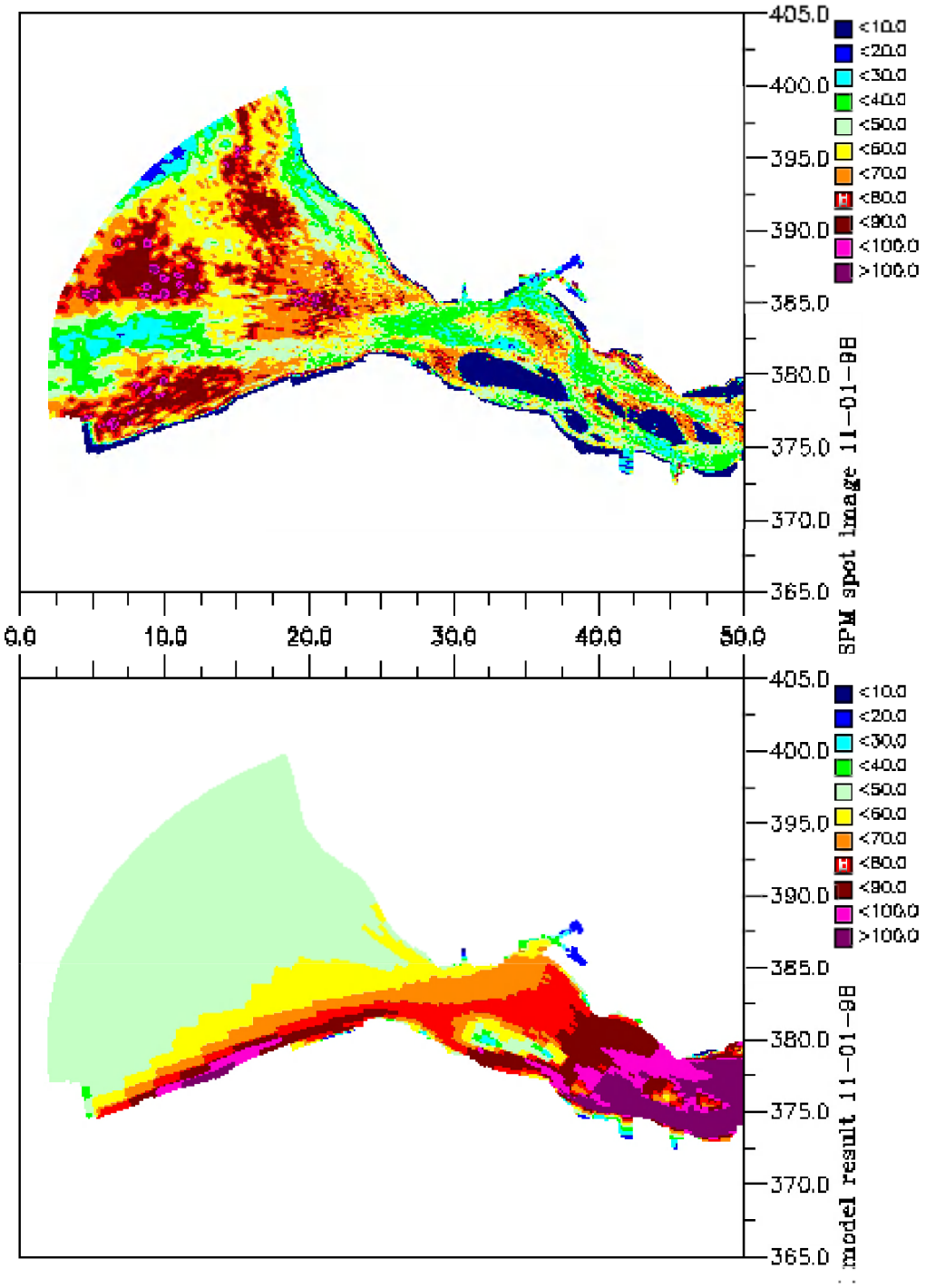

Figure 5.14 Comparison of remote sensing SPM maps with model results for 11 January 1998 (high tide, incoming water).

Comments on model and remote sensing results

For comparison of the Remote Sensing data and the model data, the model result closest to the remote sensing data in time, and within one meter difference of water level at Terneuzen were selected and compared to the remote sensing data. The absolute date of model results could not be used because the model hydrodynamics are slightly out of phase. Thus a time 'shift' in the model results are needed in order to make a comparison with a specific time (see also Section 4.2). The shift brings the model and remote sensing results to a comparable tidal phase, but the model forcing functions (e.g. wind) are then also shifted, so the comparison is not ideal. Comments for comparisons follow:

1. *10 May, 1998, east & west:* For the eastern part of the Scheldt (see Figure 5.7), the modelled SPM is too high at this time; For the western part of the Scheld the average concentration is good, but the detail seen in the remote sensing image are not shown by the model results (Figure 5.8).
2. *20 July 1998:* For the eastern part of the Western Scheldt (see Figure 5.9) the SPM concentrations in the Belgium Scheldt in the Remote Sensing image are much higher than for the model, indicating that for this moment an SPM influx from Belgium takes place that is not modelled. This might indicate the actual need for proper SPM data from the local Belgium authorities from their continuous monitoring stations at Prosperpolder (examples are given by Fettweiss et al., 1998). However, the remote sensing shows a very steep concentration gradient moving downstream, and within the estuary the remote sensing concentration is lower than the modelled concentration. This high concentration gradient seen in remote sensing is less pronounced in the model results.
3. *August, 1998 (6, 8, & 10):* On these 3 dates, the comparison between model results and remote sensing data is reasonably good, but the model shows very little spatial variation in calculated concentration (Figure 5.10-5.12). Almost all of the model area is between 10-15 mg/l. In contrast, the remote sensing shows several interesting patterns in SPM concentration. On 8 and 10 August, elevated SPM concentration are clearly seen at the Vlakte van Raan at the mouth of the estuary. On 8 and 10 August, high SPM concentrations are seen along the Belgian coast, possibly from localized dumpings. For these dates, the agreement between model and remote sensing is generally good, even though the model does not generate the complex patterns observed in the images.
4. *1 October, 1998:* The Remote Sensing image of 1 October 1998 (Figure 5.13) gives much lower SPM concentrations (5-20 mg/l) as compared to the model (40-75 mg/l).
5. *11 January 1998:* This is a (unique) winter remote sensing image (see Figure 5.14). Due to the simplified boundary conditions in the model, the complex gradients in the remote sensing image are not shown in the model results. This concerns especially the gradients in Scheur van Wielingen. In addition, the model simulated high SPM values in the inner Scheldt estuary due to erosion by wind. The remote sensing image indicates that this erision seems tobe over estimated.

In general, Remote Sensing images show much more detail of SPM patterns and gradients than the model results. The modelled concentrations are based on a number of processes, assumptions of boundary conditions and dumping of dredging material which are simpler

than reality. Localized and temporal processes causing detailed SPM patterns and gradients are therefore not shown in the model results.

In the comparison of model results with remote sensing images, the uncertainty in the remote sensing results should also be considered. For example, validation of remote sensing with in-situ data (see Peters et al., 1999) show that the image of 1 October has low concentrations when compared with longterm monthly averaged data at stations Pas van Terneuzen, Hansweert, Zuidergat and Saeftinghe (stations 5, 6, 7 and 9 respectively). The model results had high concentration in October at these same stations (see Figure 5.4).
Thus in a comparison of remote sensing and model results for 1 October, the remote sensing results are significantly lower than the model results. The 'true' concentration are most likely between the two.

5.6 Conclusions about T0 conditions for SPM in the Western Scheldt, 1998

Conclusions about the T0 conditions for SPM in the Western Scheldt can be drawn from the analysis of the different data sources:

- in-situ data (long term monthly averages and continuous measurements)
- remote sensing
- dynamic water quality model

Each data source provides different information about SPM concentrations. The best description of the T0 conditions is based on a combination of all 3 sources, taking into account the strengths and weaknesses of each.

In-situ data

In-situ data is collected at a number of fixed locations over time. The data is thus ideal for analyzing variations in SPM concentrations over time at the selected locations, including comparison of the locations

The long-term monthly averaged in-situ data clearly shows the seasonal trend in SPM concentrations over a year and the natural variation in concentrations (based on the standard deviation) in the Western Scheldt. This is the only data source that shows this trend. From this data set it can be seen that all locations in the Scheldt have relatively high concentrations with large natural variation in winter and fall, and low concentrations with low natural variation during the summer months.

Typical winter concentrations are 40-60 ± 40 mg/l. The concentrations are lowest at the sea side, due to influx of North Sea water with relatively low SPM concentrations. Highest concentrations are measured at Saaftinghe, where the average monthly concentrations for January - March are 80-90 ± 40 mg/l.

Typical summer concentrations at all locations in the Western Scheldt are 10-20 ± 10 mg/l. Again, concentrations are lowest at the sea side, and highest near the Belgian border (e.g. Saaftinghe) where summer concentrations are slightly higher than 20 mg/l.

The continuous in-situ data are important in showing short time scale details in concentrations that are not present in the monthly average data. This is the only data set that shows concentrations changes correlated to the daily tidal cycle, the spring-neap tidal cycle as well as the seasonal cycle (from Vlissingen only). This high-temporal data shows that large changes in SPM concentration can occur over very short time periods, perhaps due to wind conditions or localized erosion from bottom sediments.

Continuous data at Terneuzen for October -December 1998 show concentrations between 60-150 mg/l, varying regularly over the spring-neap cycle. Continuous data at Baalhoek over the same period show a much larger concentration range (25-250 mg/l), with much more extreme concentration variations over short time periods. The difference in these signals may be due to very localized effects.

Remote Sensing data

The strength of remote sensing is that it provides details about SPM concentrations and patterns at any one moment in time (snapshot) that are not available from any other data source. One example is the elevated SPM concentrations seen at the Vlakte van Raan, or along the Belgian coast at the south side of the mouth of the Western Scheldt. Information about these SPM features is not available from in-situ data or the model. With sufficient remote sensing images, detailed SPM concentrations and patterns can be seen over time. However, due to variations in SPM over tidal and spring-neap cycles (as seen in the continuous in-situ data), the validity of a remote sensing image is restricted to one moment in the tidal cycle and is therefore not representative for longer periods.

Due to large fluctuations in SPM concentration within a tidal cycle and a spring-neap cycle, making composites of remote sensing images is not recommended (either daily, weekly or monthly). This is in contrast to previous RESTWAQ studies, specifically southern North Sea and Dutch coastal zone, where such composites were very valuable remote sensing products. In the North Sea and Dutch coastal zone, SPM variation over time scales of days-week (tidal cycle and spring - neap cycle) were not significant compared to variation over months. Also for purposes of the previous RESTWAQ studies, i.e. large scale SPM transport over a year, the weekly and monthly composites provided sufficient detail.

Dynamic water quality model

The dynamic water quality model combines the high temporal scale of the (continuous) in-situ data with the large spatial scale of remote sensing data. The model is the only information source which can give information on SPM at all times at all locations in the Western Scheldt. Through the process of data model integration as used in the cost function, the available information from both in-situ and remote sensing data are incorporated as best as possible into the model. The model is thus optimized on in-situ and remote sensing data.

The model results clearly show the seasonal pattern as well as the spring-neap variation of SPM concentrations in the Western Scheldt. Also the model shows generally increasing SPM concentrations moving from west to east. The model is limited in its ability to

simulate detailed patterns in SPM concentration as seen in the remote sensing, and very short term variations in SPM concentrations as seen in the continuous in-situ data. It can be concluded that these are effects caused by localized conditions and effects which are not included in the general model processes.

6 T1 scenario for dumping of tunnel material at Terneuzen

6.1 Introduction

With the calibrated water quality model for 1998 it is possible to make predictions for the T1 phase by simulating tunnel material dumping scenarios. The T1 situation is the situation during the dumping of silt from the tunnel boring. In this chapter, results are presented for one hypothetical dumping scenario. The dumping considers 'Boomse Klei' to be dumped with a pipeline near Terneuzen Dow Chemicals (Figure 6.1).

In the modelled T1 scenario, 1 Mton (dry weight) tunnel material was discharged at a constant rate into the Western Scheldt over a period of 1 year (1 January - 31 December). This amount is based on predictions of a total of 1.5 million m^3 'Boomse Klei' being excavated and dumped over a period of 1.5 years. The Boomse Klei consists primarily of very fine silt (<63 μ) (RWS, 1998). As a rough estimate, a conversion factor of 1ton per m^3 is assumed. It is recognized that the amount of the dumped material is a very rough estimate, and a new scenario can be calculated when more precise information on the dumping amounts are known. The chosen scenario provides an indication of the expected increases in SPM concentration, as well as the spreading patterns and the transport of the dumped material.

For the T1 prediction, the 1998 model simulation is run again, with the addition of the tunnel material. The tunnel material is modelled as a separate (additional) sediment fraction, having the same characteristics as the river silt. The dumped material is added to one model segment, in the water column. All other model inputs are the same as in the 1998 model simulation (i.e. wind conditions, boundary conditions, initial conditions, and dumping from harbour dredging), and all parameter settings are the same.

6.2 Predictions for the T1 scenario

6.2.1 Results per location

Model predictions are presented for specific locations, where previous model results have been shown (in Chapter 5). Figures 6.2a-c show predicted T1 concentrations for 1 year at locations Vlissingen, Terneuzen and Baalhoek, with the 1998 concentrations as reference.

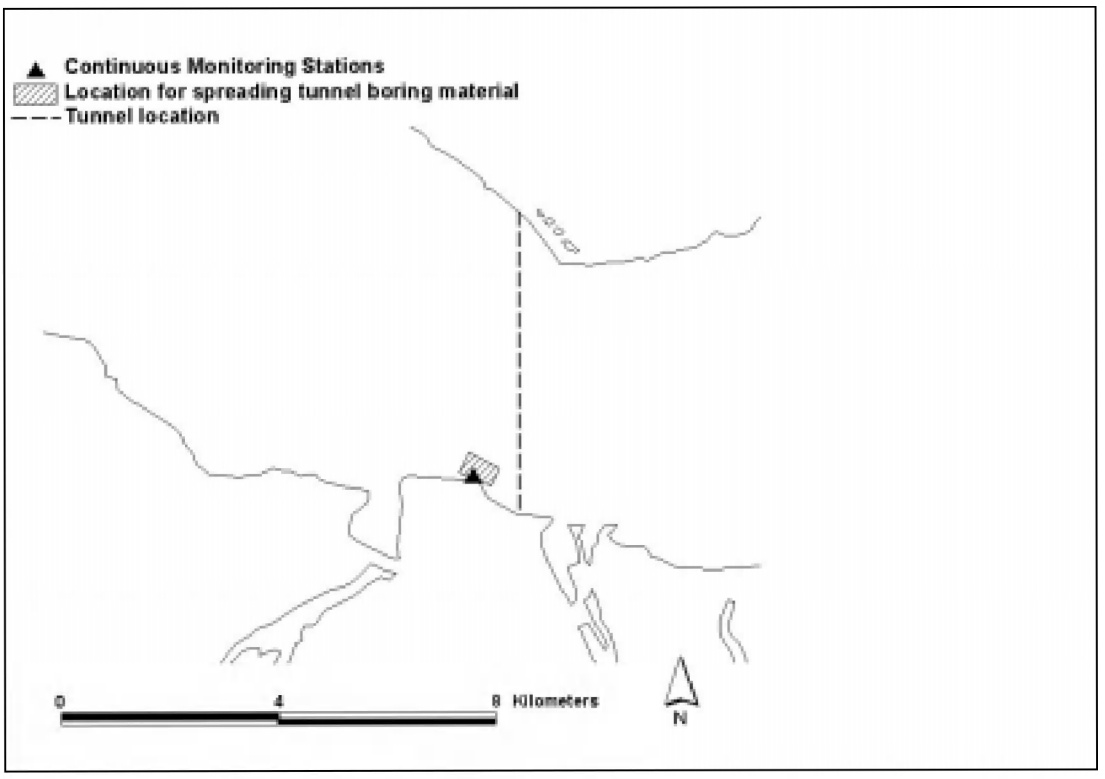

Figure 6.1 Location of dumping location for tunnel boring material Boomse Klei

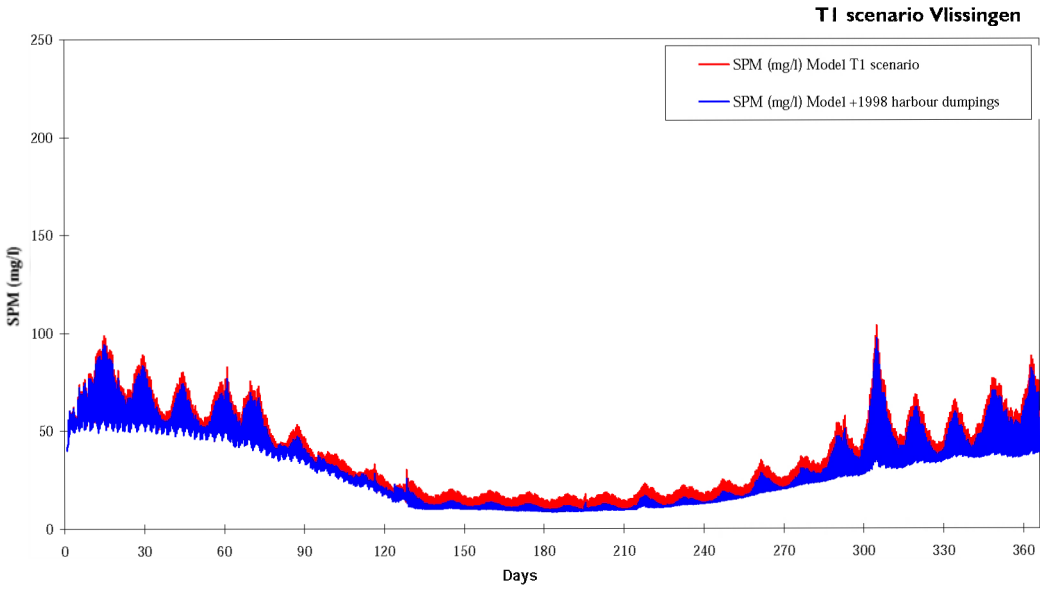

Figure 6.2a Predicted T1 concentration of SPM at Vlissingen due to continuous dumping of 1Mton tunnel boring material. 1998 concentrations are shown as reference.

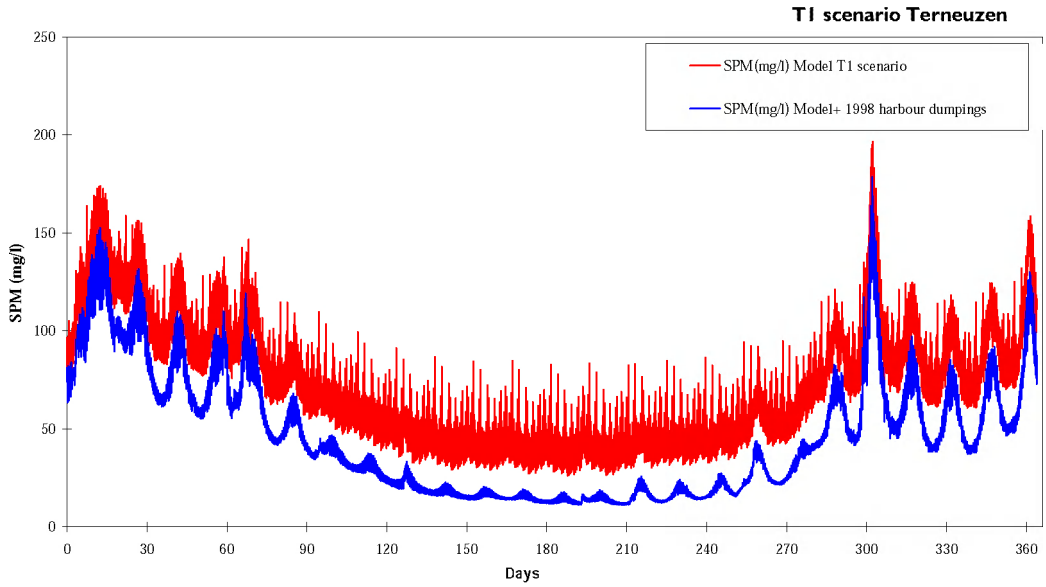

Figure 6.2b Predicted T1 concentration of SPM at Terneuzen due to continuous dumping of 1Mton tunnel boring material. 1998 concentrations are shown as reference.

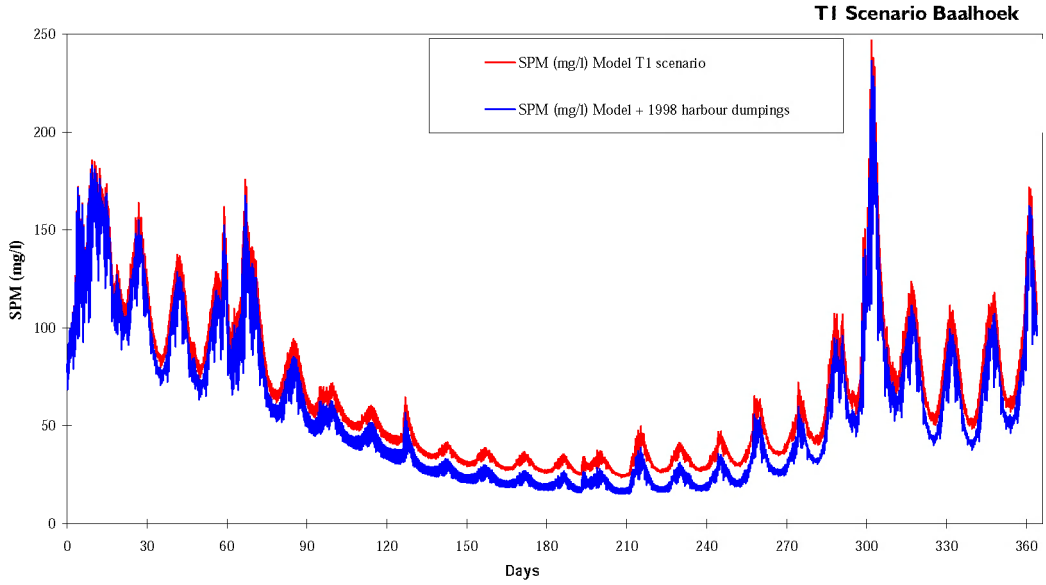

Figure 6.2c Predicted T1 concentration of SPM at Baalhoek due to continuous dumping of 1Mton tunnel boring material. 1998 concentrations are shown as reference.

Additionally, T1 predictions can be presented as monthly averaged concentrations. Figure 6.3a-h shows expected increases in monthly averaged SPM concentration at 8 locations. The 1998 model predictions and in-situ data with standard deviation (Van Maldegem, 1992) for the same locations are shown as reference. The in-situ data are important since they indicate the normal background levels, and the natural variability. This gives an indication of whether the increase of SPM is significant in comparison to the natural situation.

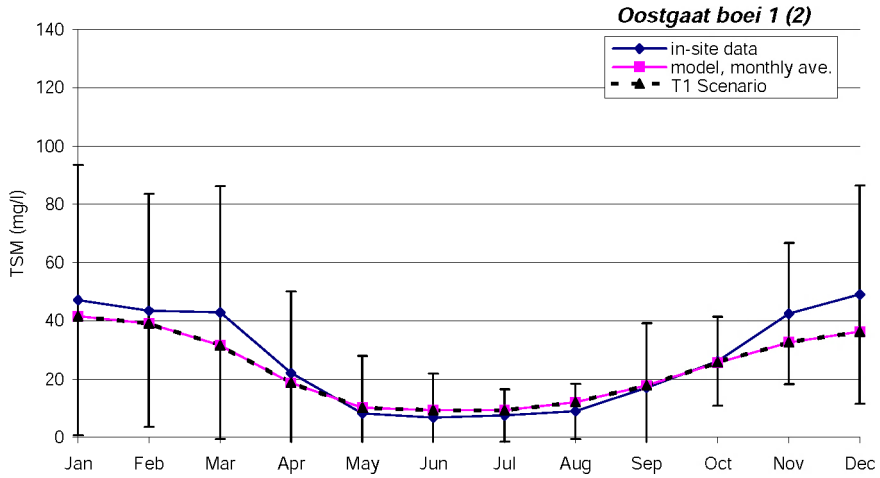

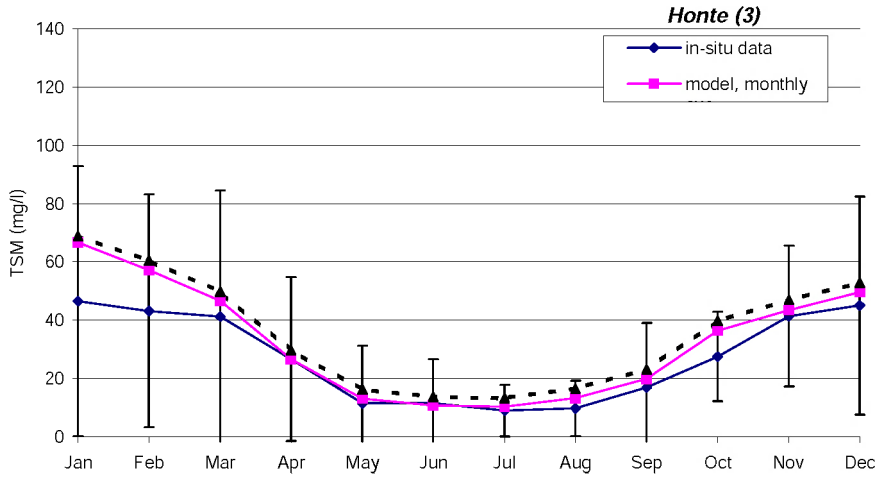

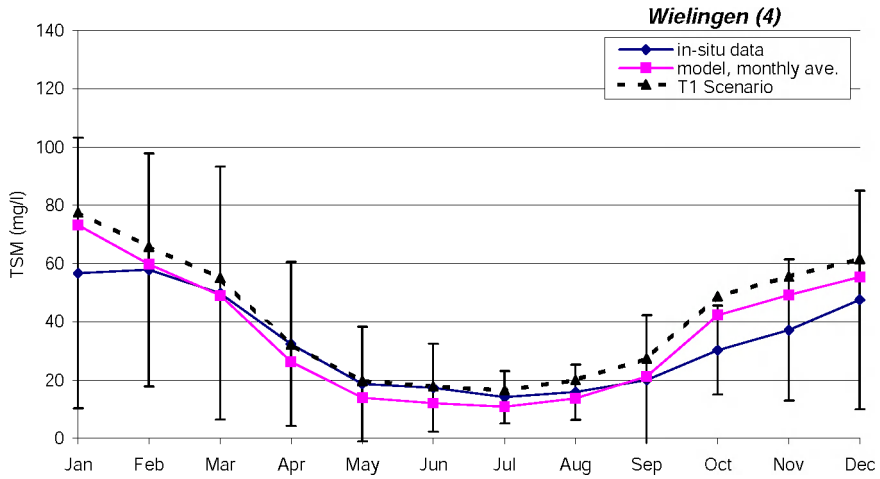

Figure 6.3a-c Predicted T1 monthly average SPM concentrations at Oostgaat, Honte and Wielengen

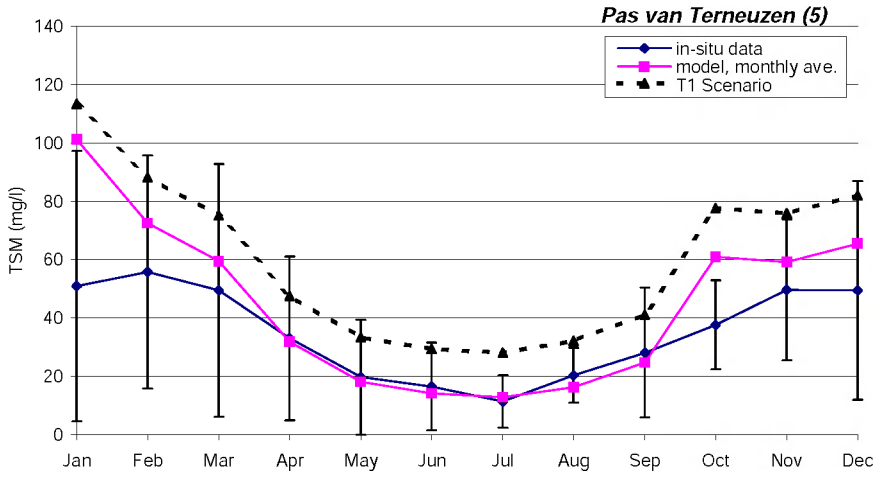

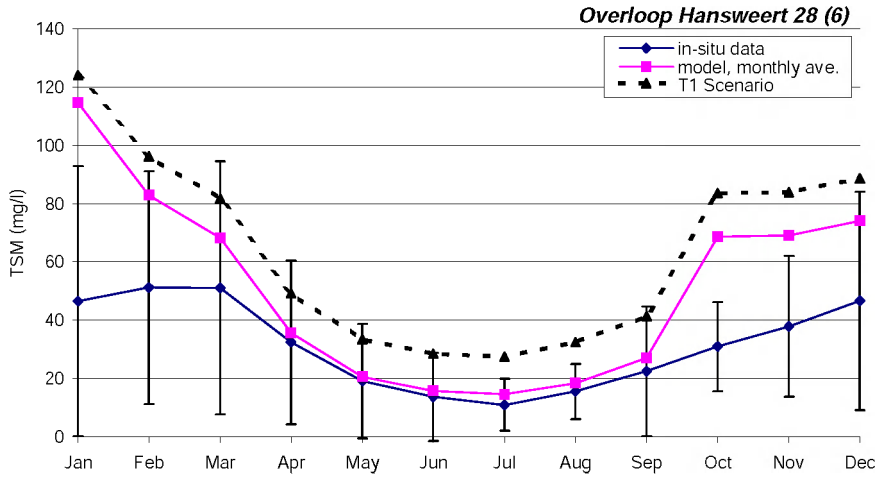

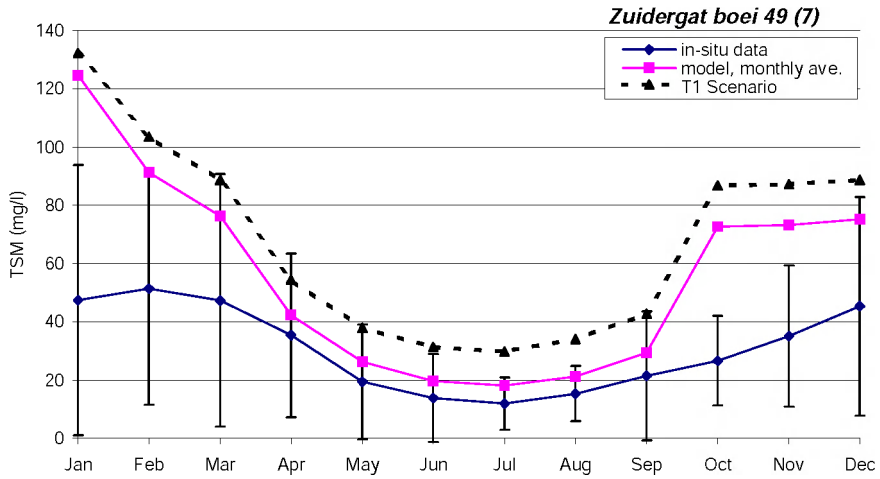

Figure 6.3d-f Predicted T1 monthly average SPM concentrations at Terneuzen, Hansweert and Zuidergat

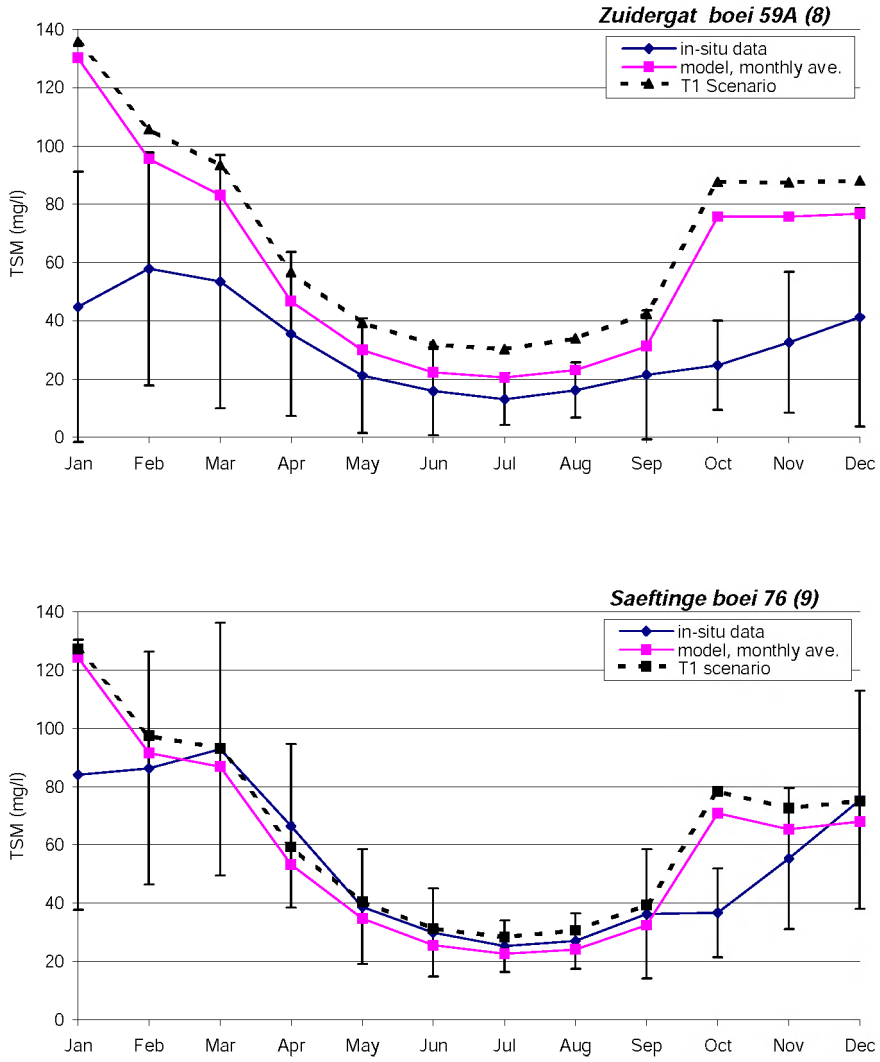

Figure 6.3h Predicted T1 monthly average SPM concentrations at Zuidergat and Saeftinghe

The model results show:

- Close to the dumping location, an increase in SPM concentration of ~30-40 mg/l can be expected. This can be seen in Figure 6.2b, for predicted results at continuous monitoring station Terneuzen.
- Further away from the dumping location, an increase in SPM concentration of 5-20 mg/l can be expected, depending on the exact location. This can be seen at Vlissingen (Figures 6.2a) where the increase is <5 mg/l. At Baalhoek (Figure 6.2c) the increase is ~10mg/l.
- Looking at the Van Maldegem monitoring stations, at monthly averaged results (Figure 6.3) the highest increase is noted at Pas van Terneuzen (~20 mg/l). Other stations show smaller concentration increases.
- at Terneuzen, the increase of SPM during the summer due to the dumping of tunnel silt is much larger than the fluctuations due to tide and wind in the background signal for SPM ('natural' SPM) (Figures 6.2 b). Here, the largest impact of the dumping can be

seen, which can be expected since the monitoring location is directly next to the dumping location.

- At Baalhoek and Vlissingen, the increase in SPM during summer is relatively small, but probably can still be observed. At Baalhoek the increase is in the order of the tidal fluctuations for summer. At Vlissingen the increase is somewhat larger than the tidal fluctuations;
- Figures 6.2 a-c show that the increase of SPM during winter due to the dumping of tunnel silt is much smaller than the fluctuations due to tide and wind in the background signal for SPM ('natural' SPM) for all 3 stations;
- From the monthly averaged results, it can be seen that at most stations in the Western Scheldt, the predicted concentrations during the summer are higher than the natural range of SPM concentrations. In the winter months, the predicted concentrations are usually within the natural range of SPM concentrations.

Thus, the effect of the dumping of tunnel material will be most prominent during the summer months, when the natural background concentrations of SPM are lowest. During the winter months, the increased SPM concentration will likely be within the range of natural fluctuations.

6.2.2 Synoptic Results

The model can also show predicted concentrations for the T1 phase synoptically for a selected moment in time (snapshot). Results of the T1 scenario simulations for 4 moments during the year: February, May, August and November (Figures 6.4 - Figure 6.7), corresponding to results previously shown for the T0 situation (Figure 5.5-5.6). The concentration for the tunnel material is shown in the lower frame, while the total SPM concentration for the T1 situation are shown in the upper frame.

Synoptic results have also been processed into a computer animation, which shows how the dumped tunnel material moves through the Western Scheldt with the tidal motion.

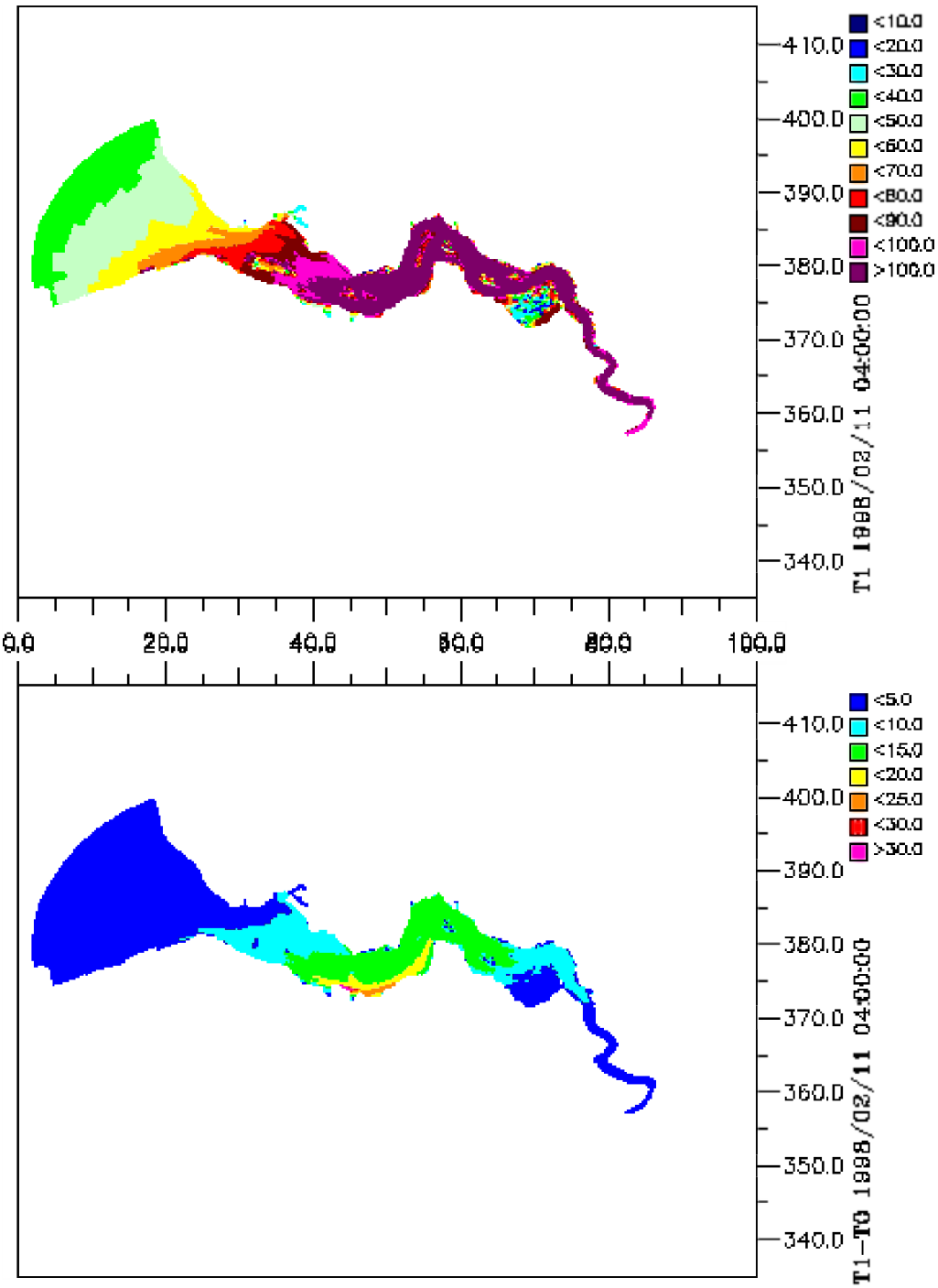

Figure 6.4 Results for concentration of tunnel material (bottom) and the total SPM concentration, including tunnel material (top), as derived from the model for 11 February. All concentrations in mg/l. The T0 concentrations for the same date are shown in Figure 5.6.

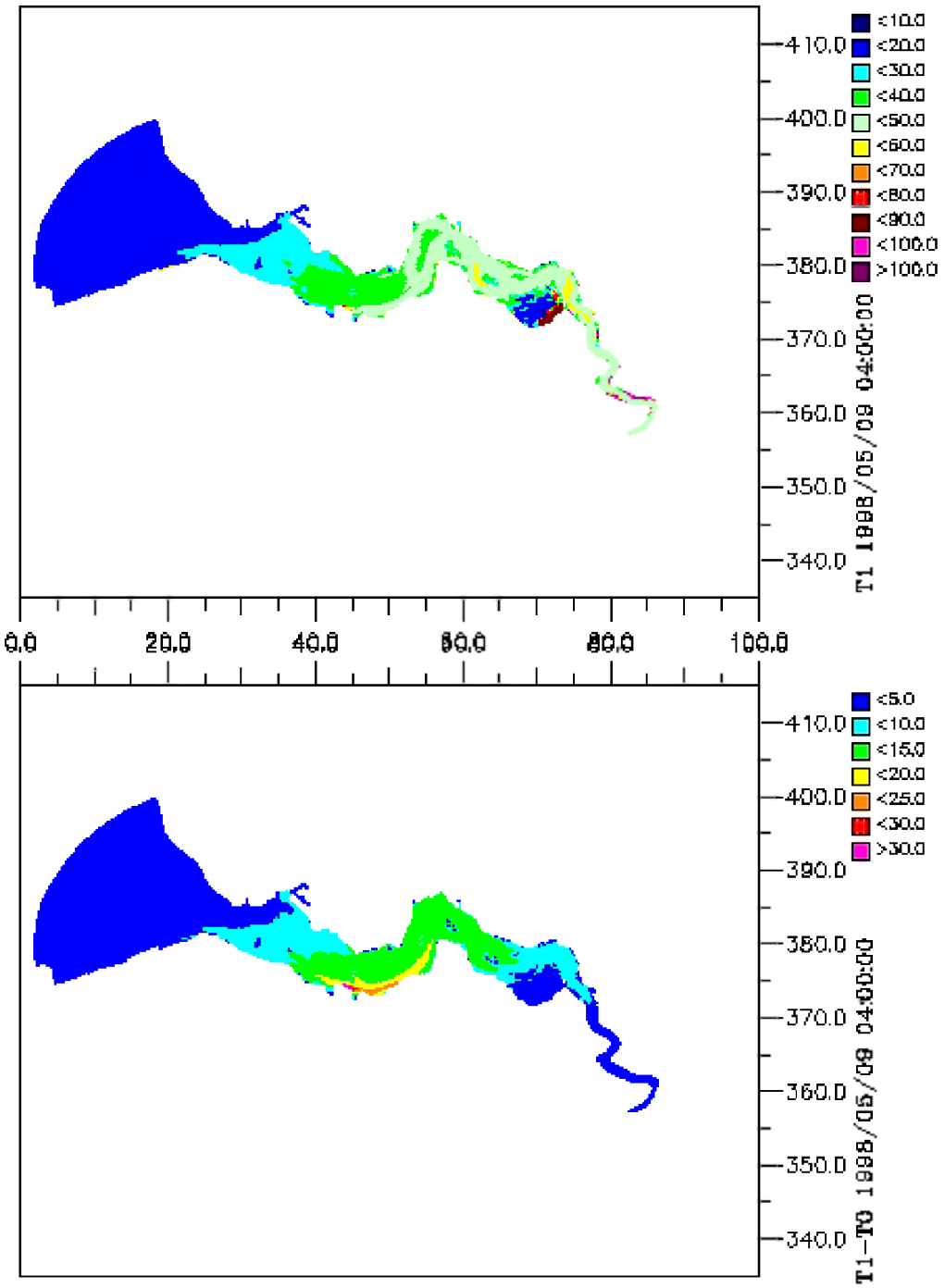

Figure 6.5 Results for concentration of tunnel material (bottom) and the total SPM concentration, including tunnel material (top), as derived from the model for 9 May. All concentrations in mg/l. The T0 concentrations for the same date are shown in Figure 5.6.

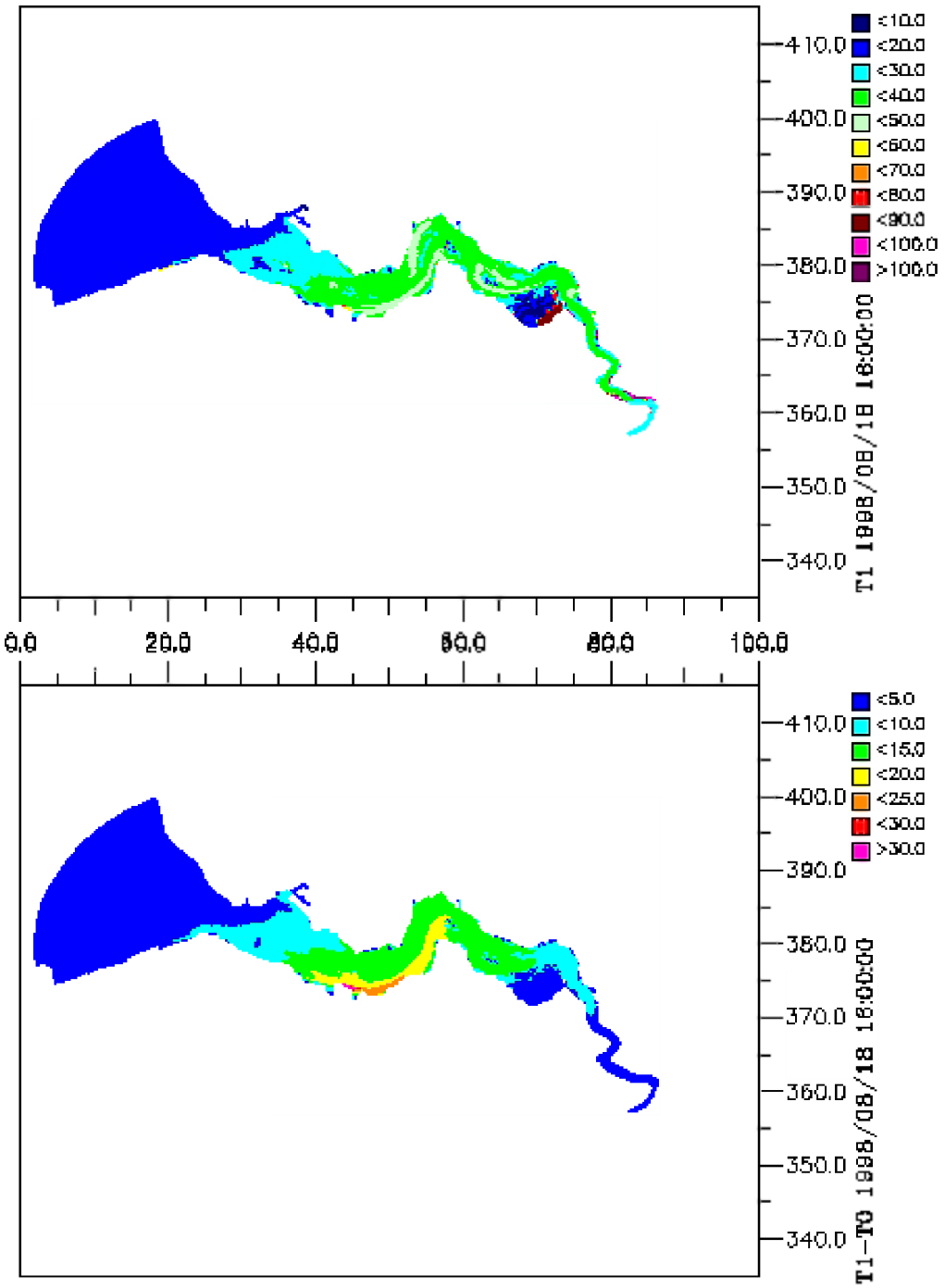

Figure 6.6 Results for concentration of tunnel material (bottom) and the total SPM concentration, including tunnel material (top), as derived from the model for 18 August. All concentrations in mg/l. The T0 concentrations for the same date are shown in Figure 5.7.

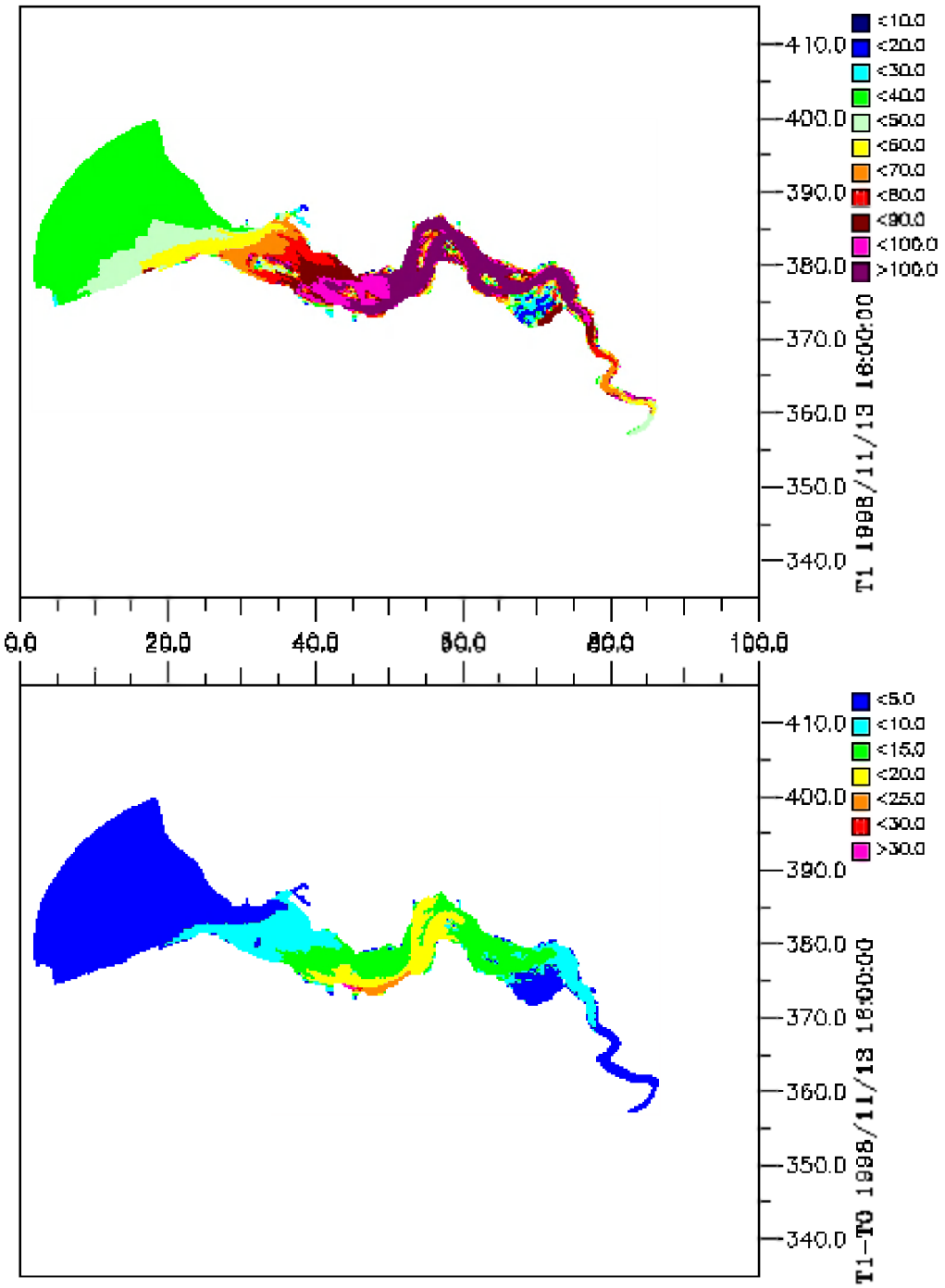

Figure 6.7 Results for concentration of tunnel material (bottom) and the total SPM concentration, including tunnel material (top), as derived from the model for 13 November. All concentrations in mg/l. The T0 concentrations for the same date are shown in Figure 5.7.

From these figures it follows that:

The dumping of tunnel sediment creates a 'plume' of increased concentration which fluctuates around the dumping location, moving upstream and downstream with the tide. The predictions show a maximum SPM concentration of about 30 mg/l in the immediate vicinity of the dumping location.

A concentration increase of 25 mg/l is seen in a limited area, which can extend a few kilometers from the dumping location. A concentration increase of 10-15 mg/l is seen in a large area, extending upstream to Baalhoek (~17 km). At Vlissingen, a concentration increase of, on average, 2mg/l is predicted.

Because a constant discharge of tunnel sediment has been assumed, the predicted *increase* in SPM concentration is constant over the year. Due to the natural seasonal variation in SPM, the concentration increase may not be 'visible' in the fall and winter months (when background concentrations and natural variability are high). The SPM concentration increase will most likely be 'visible' in the summer months, when background concentrations and natural variability are low.

6.2.3 Results for the bottom sediment

The water quality model can also make predictions for changes to the bottom sediment due to the dumping of tunnel material.

Results for the increase in bottom sediment thickness after approximately 6 months of continuous dumping (27 June 1998) are given in Figure 6.8. Results are shown for the sedimented thickness of tunnel silt (top). The thickness of the sedimented material was calculated assuming a sediment density of 2650 kg/m^3. The thickness of natural silt is shown in the bottom frame as a reference.

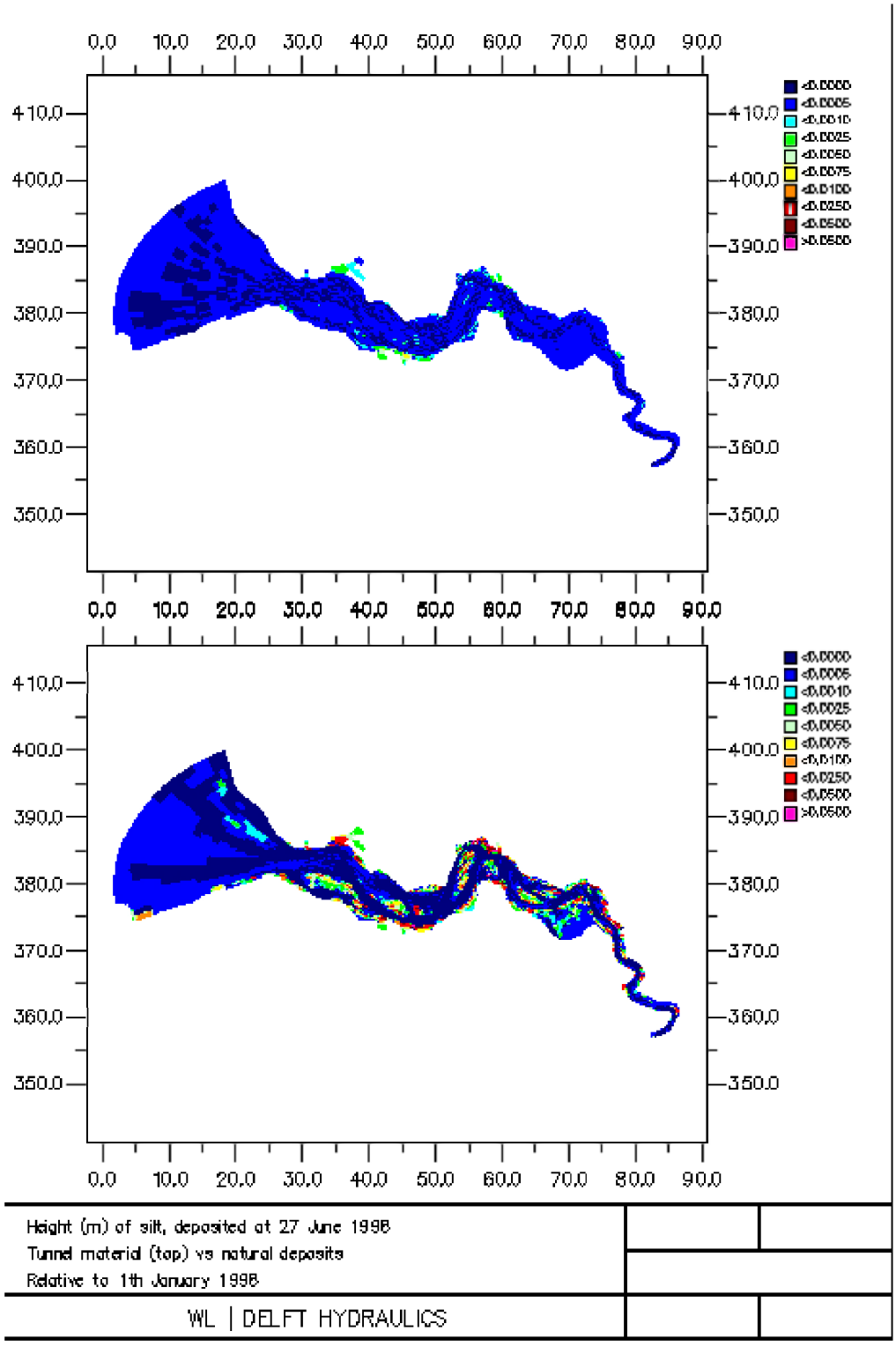

Figure 6.8 Results for bed height (in m) for 27 June. Top of figure is dumped tunnel silt, whereas bottom is natural deposit of silt. The natural deposits are obtained relative to 1 January 1998.

Figure 6.9 shows the time-history of bottom silt composition for two locations on the Molenplaat. Dumping of tunnel silt is continuing at a constant rate over the time period.

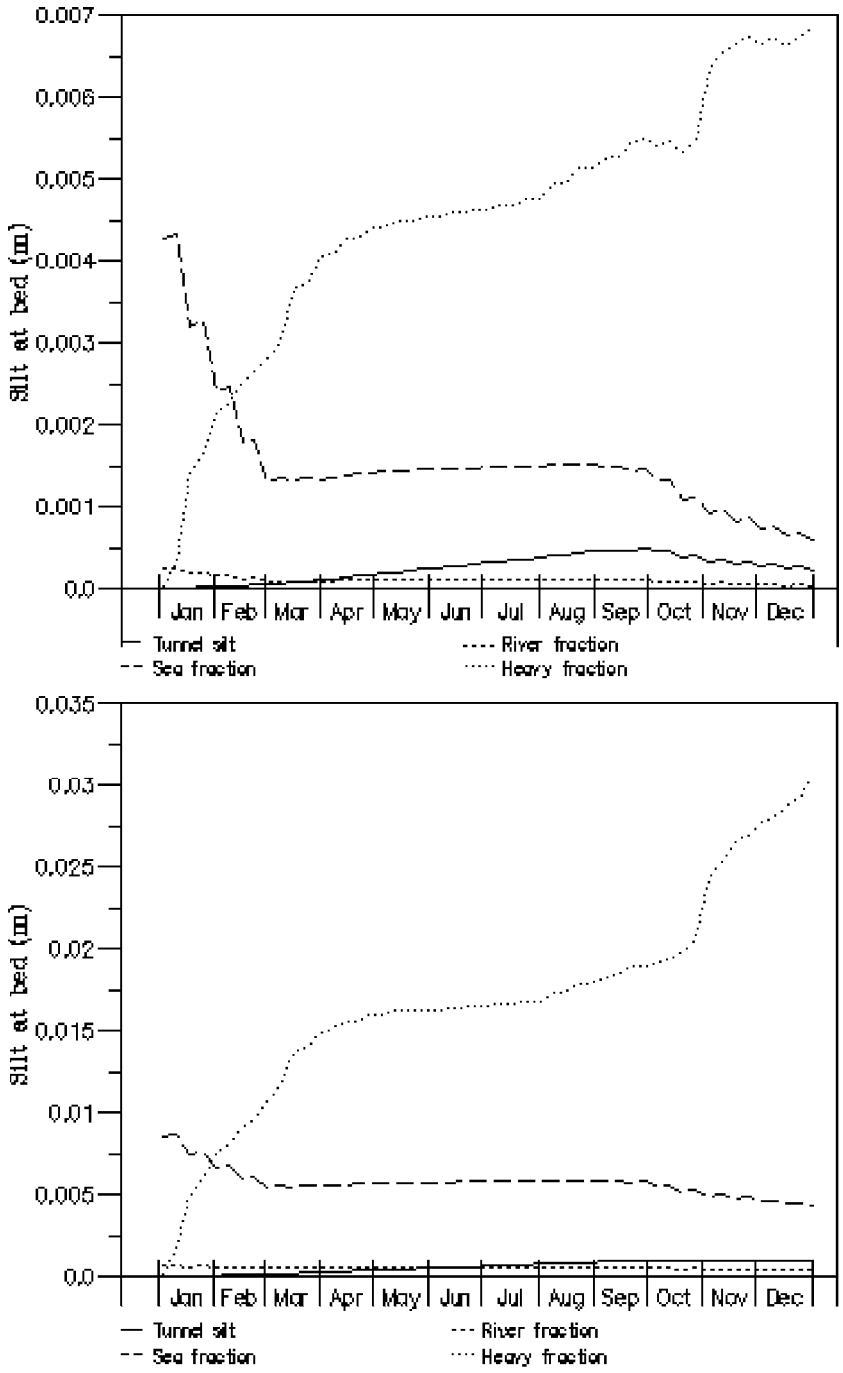

Figure 6.9 Composition of the bed for two locations at Molenplaat. Silt at the bed expressed in height (m) was obtained from the model using a density of 2650 kg/m^3. Top of figure is for centre of Molenplaat, bottom of figure for a location at the southeast border of the Molenplaat.

From the figures showing accumulation of bottom sediment, it follows that:

- The amount of silt from the tunnel boring that deposits at the bed is small compared to the natural deposits. An exception is the south coastline close to the dumping location;
- The amount of silt at Molenplaat is dominated by the sedimentation of the heavy fraction in the model; The amount of the tunnel material which accumulates is small compared to the natural sediment.

6.2.4 Transport analysis

An assessment was made of the transport fluxes of SPM in the estuary for the above given scenario (and for the natural background). The model grid was first aggregated into the 14 SAWES segments of the Western Scheldt (Van Maldegem, 1992; see Figure 2.1). An additional segment was added (No. 15) for the sea part of the model, not included in the model of Van Maldegem. Fluxes between SAWES segments and sedimentation per segment were determined for the T1 scenario simulations (Table 6.1 and 6.2). Separate analysis was made for the first and second half of the year.

Table 6.1 Transport of dumped tunnel silt between the SAWES model grid segments (Ktons)

Transport from→ to:	January - June	July- December	Total
segment 2→ upstream	7.1	9.6	16.7
segment 3→2	7.1	9.7	16.8
segment 4→3	7.8	10.3	18.1
segment 5→4	8.1	10.6	18.7
segment 6→5	11.2	13.9	25.2
segment 7→6	13.3	15.2	28.5
segment 8→7	17.1	18.6	35.7
segment 9→8	23.2	22.3	45.6
segment 10→9	28.0	25.2	53.2
segment 11→10	36.5	32.5	69.0
segment 12→11	53.4	36.5	89.9
segment 13→12	64.2	42.1	106.3
Segment 13	↑ **503 Kton dumped** ↓	↑ **503 Kton dumped** ↓	↑ **1006 Kton dumped** ↓
segment 13→14	384.8	423.6	808.4
segment 14→15	357.6	405.6	763.2
segment 15→ sea	347.2	401.5	748.7

From the dumping location (in Segment 13), approximately 80% of the dumped tunnel material is transported towards the sea (to segments 14), and 10% is transported upstream (to segment 12). The percentages are slightly different for the first and second half of the year. Eventually, 75% of the dumped material is transported out to the North Sea. Less than 2% of the dumped material is transported upstream beyond the model boundary.

Transport of the all the silt fractions between the SAWES model segments is shown in Figure 6.12

Table 6.2 Net sedimentation of tunnel silt (Ktons) per SAWES model grid segment

SAWES Segment Number	January - June	July- December	Total year
2 (part)	0.0	0.0	0.0
3	0.6	0.4	1.0
4	0.2	0.2	0.4
5	2.8	3.0	5.8
6	1.6	0.9	2.5
7	3.4	3.1	6.5
8	5.5	3.4	8.9
9	3.6	2.5	6.1
10	6.6	6.8	13.4
11	12.6	3.5	16.1
12	6.1	5.4	11.5
13 *	43.5	37.0	80.5
14	20.3	17.7	38.0
15 (new segment)	5.1	2.8	7.9
Total	111.9	86.8	198.7

* Silt is dumped in segment 13

Of the total amount of silt dumped, approximately 20% is sedimented in the Western Scheldt. Most of the sedimentation occurs near the dump location (segments 13-14). The amount which is not sedimented and not transported out of the system, remains in the Western Scheldt, and results in increased silt concentrations (4% of the total mass dumped). The total mass balance of for the tunnel silt and the other silt fractions over a whole year for the tunnel dumping scenario are given in Table 6.3.

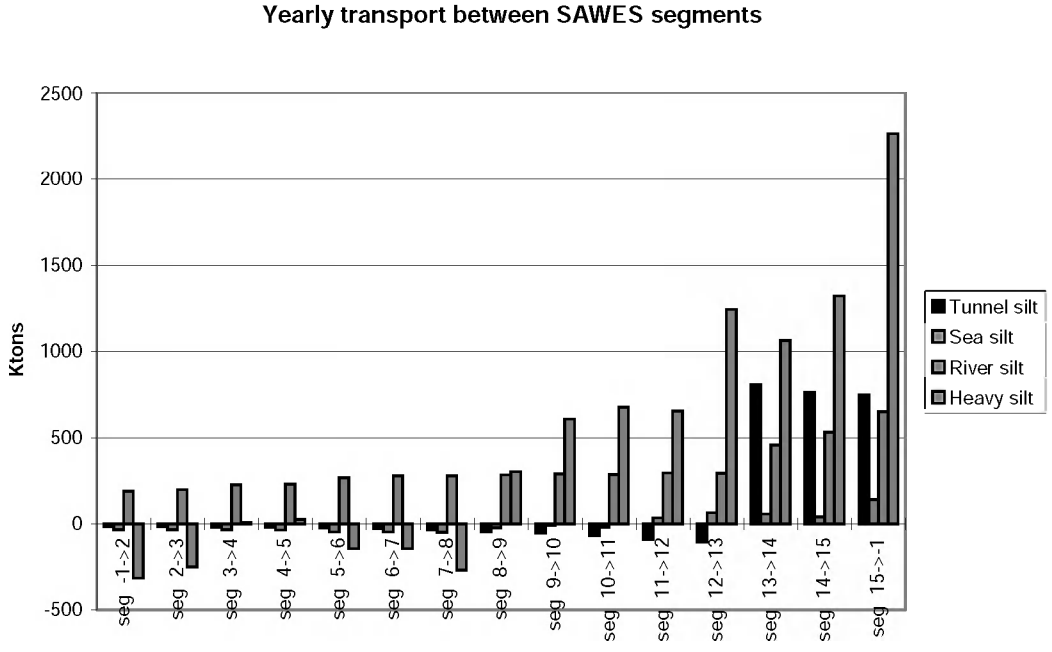

Figure 6.10 Transport of different silt fractions between the SAWES segments of the Western Scheldt

Table 6.3 Total mass balance for different silt fraction over the whole Western Scheldt for the complete year (Ktons).

Total Year	Tunnel silt	River silt	Sea Silt	Heavy silt
Loads (dumping)	1006	414.3	0.0	0.0
Outflow at river boundary	16.7 (1%)	-189.1	33.3	314.3
Outflow to sea	748.7 (75%)	649.0	140.9	2262.0
net sedimentation	198.8 (20%)	-71.7	-200.0	-3601.8
Change of Mass in system	41.3 (4%)	26.1	25.8	1025.5

6.3 Conclusions

The amount of tunnel silt dumped may lead to an observable increase of SPM levels around Terneuzen and in an area of roughly 25 km around Terneuzen. This increase in SPM is only significant with respect to SPM background levels for the summer period. For the winter period, this increase is smaller than the natural fluctuations due to tide and wind, and can therefore probably not be discriminated from the natural background of SPM.

Remote Sensing techniques will most likely be able to detect a significant increase in SPM levels during summer. However, support of modelling results will be necessary to identify what SPM concentration increases can be expected in what areas during the tidal phases which correspond to the exact times of the images. Also a plume of SPM starting at the dump location and moving from west to east with tidal motion must be observable with remote sensing techniques. However, for winter periods this is again not possible since:

- natural backgrounds are too high for detection of the SPM plume;
- the cloud cover percentage and low sun angel are unfavourable for the use of remote sensing in these periods;

Unfortunately, the SPM continuous monitoring locations seem not be placed at representative locations:

- The Terneuzen monitoring location is almost at the dumping site, and therefore will measure only local effects and not say anything about the transport of dumped silt;
- The Baalhoek and Vlissingen stations are too far away for detecting a significant increase in SPM during summer;

With this respect, the remote sensing technique is probably (*for the summer period*) the most promising technique available for detecting the SPM increase from tunnel silt.

Any consequences for the environment are not discussed in this report, but are addressed separately in Baptist and Peters (1999). Main issues are probably related to primary production and consequences for fishery due to an increase in turbidity. This increase is not only influenced by the relative increase of SPM concentrations, but also very much affected by the inherent optical properties (especially the scattering efficiency) of the dumped silt, and its contaminants like 'bentonite'. These properties must be identified as soon as possible when the dumping starts, in order to make a correct judgement of the dumping effects for the local environment.

The present dumping can only serve as a test case, for the true T1-scenario. Most important limitations with respect to its validity are:

- the basic simulation was for 1998 (using e.g. 1998 wind conditions) and not for the real T1 period;
- the exact amount of dumped material (and its physical properties) are not known yet;
- the model is a simplification of the natural situation. Predictions still need to be justified/falsified by measurements during the dumping.

7 Conclusions and Recommendations

7.1 Conclusions

The RESTWES study has focused on characterising the SPM conditions in the Western Scheldt, specifically the 1998 baseline conditions (T0) prior to dumping of tunnel boring material 'Boomse Klei' from the Western Scheldt tunnel construction. This study has shown that the T0 situation can be optimally characterized based on three sources of information, namely:

- in-situ data
- remote sensing
- water quality model

Based on these three sources of information, a number of important characteristics of the suspended particulate matter have been described, including the dynamic behaviour as well as the spatial variability. Also important processes affecting the SPM concentrations are identified, such as the spring-neap tidal cycle. This work also indicates the strengths and weaknesses of the individual information sources for describing SPM in the Western Scheldt. Specific conclusions drawn from each data source are presented.

In-situ Data
The long-term monthly averaged data indicate seasonal trends in SPM concentration which occur over the whole estuary: high winter concentrations and low summer concentrations. There is a gradient in concentrations over the length of the Western Scheldt, with lowest concentrations in the east at the mouth of the estuary, and highest concentrations near the Belgian border.

Typical winter concentrations are 40-60 ± 40 mg/l. The concentrations are lowest at the sea side, due to influx of North Sea water with relatively low SPM concentrations. Highest concentrations are measured at Saeftinghe, where the average monthly concentrations for January - March are 80-90 ± 40 mg/l.

Typical summer concentrations at all locations in the Western Scheldt are 10-20 ± 10 mg/l. Again, concentrations are lowest at the sea side, and highest near the Belgian border (e.g. Saaftinghe) where summer concentrations are slightly higher than 20 mg/l.

Continuous data from locations Vlissingen, Terneuzen and Baalhoek indicate a consistent 14 day spring-neap cycle, with an additional 12 hour cycle caused by the tidal period. Some additional patterns in the data occur due to storm events (high wind), and possibly other localized conditions (e.g. dumping of dredged sediment or localized bottom sediment erosion). Continuous data at Terneuzen for October - December 1998 show concentrations between 60-150 mg/l, varying regularly over the spring-neap cycle.

Continuous data at Baalhoek over the same period show a much larger concentration range (25-250 mg/l), with much more extreme concentration variations over short time periods. The difference in these signals may be due to very localized effects.

Remote Sensing Data

Remote sensing maps of SPM can be prepared from SPOT satellite reflectance data, using an optical model. The optical model was developed based on inherent optical properties of Western Scheldt sediment as measured during a field campaign in March 1999 (see Peters, et al., 1999). Retrieved SPM concentrations could be mapped in steps of 3 mg/l at the lowest concentration range with errors (roughly estimated) from approximately 5 up to 33%.

The remote sensing images are 'instantaneous pictures' of the suspended matter concentration in the estuary, and the 9 processed images show a high level of spatial detail which is not available in either the in-situ data or the model results. One example is the elevated SPM concentrations seen at the Vlakte van Raan, or along the Belgian coast at the south side of the mouth of the Western Scheldt. With sufficient remote sensing images, detailed SPM concentrations and patterns can be seen over time. However, due to variations in SPM over tidal and spring-neap cycles (as seen in the continuous in-situ data), the exact moment of a remote sensing images (e.g. period in the tidal cycle) must be known in order to make proper analysis.

NOAA satellite images

The possibility of using NOAA satellite images for model boundary conditions has been investigated. Because NOAA has 2 daytime images per day, the images are in principle available at a high enough frequency to be used as boundary conditions for the water quality model. However, the resolution of the data (approximately 1 x 1 km) and problems of signal saturation at high concentrations, and calibrating the images, results in insufficient detail and accuracy for use as model boundary conditions. NOAA however, does give information on the main patterns in SPM that can be seen (at low spatial resolution).

Water Quality Model

The dynamic water quality model combines the high temporal scale of the (continuous) in-situ data with the large spatial scale of remote sensing data. The model is the only information source which can give information on SPM at all times at all locations in the Western Scheldt. The water quality model integrates the main trends, patterns and causal effects that are analyzed in the in-situ and RS data.

An integration of in-situ and remote sensing data with the water quality model has been made with data model integration using the method of a cost function. With the cost function, the available information from both in-situ and remote sensing data are incorporated as best as possible into the model. Seasonal patterns, spring-neap cycle, dumping of sediment from harbour dredging activities and wind effects are all incorporated. The model gives a mass conservative spatial representation of SPM, can calculate transport of material and can predict concentrations from dumping.

Due to restrictions in data of inputs, boundaries and forcings, the present model application is limited in its ability to simulate detailed patterns in SPM concentration as seen in the remote sensing, and very short term variations in SPM concentrations as seen in the continuous in-situ data. It can be concluded that these are effects caused by localized conditions and effects which are not included in the general model processes.

Predictions of the T1 situation

Predictions for the T1 situation were made assuming a discharge of 1 million tons of fine silt over a year at one location (near Terneuzen).

Concentration increases
The dumping of tunnel sediment creates a 'plume' of increased concentration which fluctuates around the dumping location, moving upstream and downstream with the tide. The predictions show a maximum SPM concentration of 30-40 mg/l in the immediate vicinity of the dumping location.

A concentration increase of 25 mg/l is seen in a limited area, which can extend a few kilometers from the dumping location. A concentration increase of ~10 mg/l is seen in a large area, extending upstream to Baalhoek (~17 km). At Vlissingen, a concentration increase of, on average, 2mg/l is predicted.

Because a constant discharge of tunnel sediment has been assumed, the predicted *increase* in SPM concentration is constant over the year. Due to the natural seasonal variation in SPM, the concentration increase may not be 'visible' in the fall and winter months (when background concentrations and natural variability are high). The SPM concentration increase will most likely be 'visible' in the summer months, when background concentrations and natural variability are low.

Transport of the tunnel sediment
The concern about the effects of dumped sediment on specific regions of ecological or economical concern (nature areas, sand mining regions, fishing/shellfish areas) requires an analysis of *transport* and fluxes of material, i.e. 'Where does the dumped material end up?'

The water quality model can provide this information on the transport of the dumped tunnel sediment. For the transport analysis, the model results were aggregated to the 14 segments of the SAWES Western Scheldt model (also a 15th segment was added at the mouth of the estuary). Transport between segments, and sedimentation per segment were calculated.

Analysis of the sediment transport shows that of the total amount of silt dumped (1 Mton), approximately 75% is transport out to the North Sea, and 20% is sedimented in the Western Scheldt. Most of the sedimentation occurs near the dump location (SAWES segments 13-14). About 10% of the dumped sediment is transported upstream from the dump site towards Belgium. Most of this eventually sediments within the Western Scheldt.

7.2 Recommendations for T1 monitoring

General recommendation:
Data from all three information sources (in-situ, remote sensing and model) have proved to be valuable in characterizing the state of the total suspended matter in the Western Scheldt. Each of the sources has its own value and provides unique information which cannot be substituted by one of the other sources. As a general recommendation, it is urged that all three sources be used in characterizing the T1 phases, i.e. operational monitoring.

The expected increase in SPM concentrations due to the dumping will be 25 mg/l or less, except for the region immediately near the dumping location. During much of the year, this concentration increase will be difficult to observe, as it falls within the natural variation in SPM concentrations. However, in the summer months, an increase of 25 mg/l SPM is significant compared to both the average concentrations and the expected variability. Therefore, more detailed monitoring of the T1 situation should take place during the summer months. For example, more remote sensing images could be procured during the summer months.

Recommendations for Remote Sensing
Although the current study has proven that remote sensing can provide high resolution spatial SPM data with sufficient accuracy for integrated methods of sediment monitoring in the Western Scheldt, the method can be improved:

- In such a tidal estuary where fresh water interacts with salt waters, the spatial variation of SIOPs (specific inherent optical properties) was probably under sampled (5 locations were sampled on one day: 10 March 1999). This should be addressed in further sampling campaign(s), which would also provide insight as to the temporal and spatial variation in SIOPs for such dynamic systems.
- During the present study, variations in chlorophyll (TCHL) and coloured dissolved organic matter (CDOM) were neglected in the calculation of SPM concentrations. In view of the possible effects of variations in TCHL and CDOM concentrations on SPM retrieval (especially during the summer months), it is advised to study the optical properties and concentrations at some times during the year.
- The approach to atmospherically correct the remote sensing data proved to be feasible. In future, a downwelling irradiance spectroradiometrical measurement at e.g. a fixed point would increase the accuracy.
- For the monitoring of effects by tunnel material dumping on the sediment budget it would be advisable to study the IOPs (inherent optical properties) of Western Scheldt water containing various concentrations of the dumped material ("Boomse Klei"). It is possible that the Boomse Klei has a unique optical signal which will allow it to be distinguished from other sediment in the Western Scheldt.

Alternative satellite systems, such as Landsat-5 and 7 can provide additional temporal coverage at almost the same resolution. For providing boundary conditions (SPM concentrations e.g. in the North Sea outside the Estuary) to the water quality model, the suitability of low resolution remote sensing (e.g. SeaWiFS and IRS/P3 MOS products) should be investigated.

During the T1 phase, the remote sensing images may be able to show the direction of transport of dumped sediment, and qualitatively how much material moves in which direction. However, the remote sensing data cannot give quantitative results on sediment fluxes.

Recommendations for in-situ data: data from continuous monitoring stations:
For monitoring in the T1 situation, both the availability and the format of the continuous monitoring data are important. Data should be available in near real-time (i.e. within a few weeks of the observation). It is recommended that the data be made available in plain ascii format, as continuous records of time and observation. In the data files currently available, the data records are interrupted by blank lines and headers, thus the files require processing before they can be used for analysis.

Recommendations for data on dredging from harbours:
An analysis of data concerning sediment dumping from harbours for 1997 and 1998 indicates that the total amount of dumped material (fine sediment) from harbour dredging activities may be significant, possibly on the order of 1-1.5 million tons. This is of the same order of magnitude as the total amount of dumping expected from the tunnel material. However, this material is dumped over short time spans, so that localized impacts may be very high.

Available data from 1997 and 1998 showed approximately a factor 6 difference in total amounts of dumped material, and this raises some questions as to the accuracy of the data. It is recommended that the existing procedures for data management and data processing of harbor dredging data needs significant improvement. For operational monitoring of the T1 situation, it is necessary that data are available in near real-time. These data need to be processed and should provide a summary of: location, amount (tons) dumped, and time period dumped (dates); (see Table 4.2 as example).

Recommendations for data on spreading of tunnel boring material.
For operational monitoring of the T1 situation, it is necessary that data on spreading of tunnel material are available in near real-time. These data need to be processed and should provide a summary of: amount (tons), location, and time period dumped (weeks). When dumping data for 1998 are

Recommendations for modelling
The hydrodynamic model which forms the input to the water quality model must be re-run so that the period of the spring-neap cycle is exactly 14.756 days. In this case, the calculated results will be in phase with measured concentrations and can be directly compared. Currently, a shift in the timing of the model results has to be made in order to have a correct

For monitoring the T1 situation, the model can either be run in forecast mode, or hindcast mode.

In *forecast* mode, the model can be used to make predictions about the transport and fate of the dumped tunnel sediment (i.e. what will happen to the sediment that is dumped in the next month?). To make a prediction, assumptions about the model inputs need to be made (see Text box), specifically:

- Hydrodynamics
- Wind
- Boundary Conditions
- Dumping of harbor dredging sediment and tunnel sediment

A recent remote sensing SPM map can be used to provide the starting conditions for the model calculation.

In the *hindcast* mode, the model can be used to assess the transport and fate of tunnel sediment that has *already* been dumped (i.e. Where has the sediment gone that was dumped in the last 2 months?). To make this assessment of past dumping, real data can be used to supply the necessary model inputs: hydrodynamics, wind, boundary conditions, and dumping of harbor dredging sediment and tunnel sediment.

Remote sensing SPM maps can be used to provide the model boundary conditions, and can also be used to validate the model results.

8 References

Baptist, M.J. and S.W.M. Peters, 1999. RESTWES Ecology: Use of remote sensing for classification of intertidal areas, and preliminary ecological assessment of tunnel boring material in the Western Scheldt. WL|Delft Hydraulics, Report Z2472.30.

Boere P., 1987. 'Valsnelheids- en vertikaal slibtransportmetingen in de Westerscheldemond en berekenignen van de horizontale slibtransporten in de Oosterschelde', Balansnota 1987-30, Rijkswaterstaat, Tidal Waters Division Note GWAO.87.113, 69pp.

Brummelhuis P.G.J. ten, Vos R.J. and Gerritsen H., 1998. 'Skill assessment of SPM transport models using the adjoint technique', submitted to Estuarine, Coastal and Shelf Sciences (17 p).

Burt T.N., 1986. 'Field settling velocities of estuary muds', In: Metha A.J. (ed.). Estuarine Cohesive Sediment Dynamics. Lecture notes on Coastal and estuarine Studies, Vol. 14, Springer -Verlag Berlin, Heidelberg, New York: pp126-150.

Buchart H. and Baumert H., 1998. 'The formation of estaurine turbidity maxima due to density effects in the salt wedge. A hydrodynamic process study. J. Phys. Oceanogr. 28, p310-321.

De Bie L.M. and Benijts F. 'Invloed van enekel randvoorwaarden op de mobiliseerbaarheid van nutrienten en polluenten in baggerspecie: uitloogproeven op laboschaal.

Ecoflat; 1999. 'Final Workshop, 17 - 18 March 1999', A.Blauw (WL|Delft Hydraulics, The Netherlands) and F. Twisk (RIKZ Middelburg, The Netherlands), Private Communication.

Fettweis M., 1995. 'Modelling currents and sediment transport phenomena in shelf seas and estuaries', PhD. Thesis, KU Leuven.

Fettweis M., M. Sas and J. Monbaliu; 1998. 'Seasonal, Neap-Spring and Tidal Variation of Cohesive Sediment Concentration in the Scheldt Estuary, Belgium', Est.Coast.Shelf Sc. 47, p21-36.

Gerritsen H., Boon J.G., van der Kaaij T. and Vos R.J., 1999. 'Integrated modelling of SPM in the North Sea', submitted to Estuarine, Coastal and Shelf Sciences (22 p).

Haan, J.F. de, J.M.M. Kokke, A.G. Dekker and M. Rijkeboer, 1998. Remote sensing algorithm development; Toolkit for water quality continued. Operationalisation of tools for the analysis and processing of remote sensing data of coastal and inland waters. NRSP-2. 98-12. Netherlands Remote Sensing Board (BCRS), Rijkswaterstaat Survey Department, Delft, the Netherlands.

Herman P.M.J. and Carlo Heip,1998. MATURE: Biogeochemistry of the Maximum Turbidity zone in estuaries. A summary report', NIOO, 1998, pre-print.

Hoogenboom, H.J., A.G. Dekker and J.F. de Haan, 1998.InverSion: Assessment of water composition from spectral reflectance. A feasibility study of the use to the matrix inversion method. NRSP-2. 98-15. Netherlands Remote Sensing Board (BCRS), Rijkswaterstaat Survey Department, Delft, the Netherlands.

Hoogenboom, H.J., 1999. RESTWES: Integrated monitoring of sediment in the Western Scheldt; Part I: Data acquisition. RIKZ Draft report.

Hydrografische kaart voor kust- en binnenwateren, Koninklijke Marine dienst der Hydrografie, kaart 1803, editie 1997

Kokke J.M.M.,1996. 'Kartering van het percentage slib op droogvallende delen in de Westerschelde met Landsat Thematic Mapper', Maart 1996, RWS-MD.

Kromkamp J. and R. Wouts R., 1998. 'Particulate Matter North Sea Plus', BCRS report NUSP-98-04, July 1998.

MUMM, 1998 (Management Unit of the North Sea Mathematical Models), Brussels, Belgium, e-mail address for dumping figures: Brigitte.Lauwaert@mumm.ac.be.

Pasterkamp, R., M. Rijkeboer, and S.W.M. Peters, 1999. Preliminary report on RESTWES in-situ observations 10-3-1999. IvM report W-99/12.

Peters, S.W.M., R. Pasterkamp, M. Rijkeboer and A.G. Dekker, 1999. RESTWES: Retrieval of total suspended matter concentrations from SPOT images. Institute for Environmental Studies, Free University Amsterdam, report W-99/.

Prangsma G.J. and Roozekrans J.N., 1989. 'Using NOAA AVHRR imagery in assessing water quality parameters', Int. J. Remote Sensing, 10, p811-818.

RWS, 1998. Milieu-effectrapport Boorspecie Westerscheldetunnel, Hoofdrapport. Rijkswaterstaat Directie Zeeland, Bouwdienst Rijkswaterstaat.

Ten Brinke W.B.M. 'Slib in het estuarium van de Schelde: paden en lotgevallen', deel 1 & 2, RU Utrecht, Fysische Geografie,

Ten Brummelhuis P.G.J. , Vos R.J. and Gerritsen H., 1999. 'Skill assessment of SPM transport models using the adjoint technique', submitted to Estuarine, Coastal and Shelf Sciences (17 p).

Thoolen P., M. Baptist M. and P. Herman, 1997. 'Comparing patterns in macrofauna structure at different scales: within tidal flats, between tidal flats and between estuaries', Beon Rapport nr. 98-14, ISSN 0924-6576, December 1997.

Torfs H., 1995. 'Erosion of Mud/Sand mixtures', PhD. Thesis, K.U. Leuven, Belgium.

Van Alphen, J., 1987. Slibvoorkomerns op het Nederlands en Belgisch deel van het Continentaal Plat. RWS-Directie Noordzee, Nota nr. NZ-N-87.09.

Van Essen K., and Hartholt H.,1999. 'Mediane slibwaarde van de Westerschelde bodem', RIKZ-den Haag.

Van Eck G.Th.M. and N.M. de Rooij, 1990. 'Development of a water quality and bio-accumulation model for the Western Scheldt Estuary', in 'Coastal and Estuarine Studies, volume 36, p95-104, W. Michaelis (Ed.), Springer-Verlag.

Van Maldegem, D.C., 1992. De Slibbalans van het Schelde-Estuarium. Rijkswaterstaat, SAWES Nota 91.08, November 1992.

Van Maldegem D.C., Mulder H.P.J., Langerak A., 1993. 'A cohesive sediment balance for the Schedlt Estuary', Neth. J. Ecology 27, 247-256.

Van Leussen W., 1994.'Estuarine Macroflocs and their role in Fine-grained sediment transport. ' Thesis, RU Utrecht.

Van der Slikke M.J., 1997. 'Grootscahlige zandbalans van de Westerscheldemonding (1969-1993), een inventarisatie van de dieptegegevens (1800-1996)', IMAU, RU Utrecht, November 1997.

Van Raaphorst W., Phillipart C.J.M., Smit J.P.C., Dijkstra F.J. and Malshaert J.F.P., 1998. 'Distribution of suspended particulate matter in the North Sea as inferred from NOAA/AVHRR reflectance images and in situ observations', J. Sea Research, 39, p197-215.

Verlaan P.A.J., 1998. 'Marine vs fluvial bottom mud in the Scheldt estuary', Estuarine, Coastal and Shelf Science, 46, p1-11.

Verlaan P.A.J., M. Donze and P.Kuik, 1998. 'Marine vs fluvial Suspended Matter in the Scheldt estuary', Estuarine, Coastal and Shelf Science, 46,000-000.

Verlaan P.A.J., S.V. Meijerink, V.J. Maartense and M. Donze, 'Slibtransport in de Schelde over de Belgisch-Nederlandse grens', H2O,

Vos R.J., and Schuttelaar M., 1995. 'RESTWAQ: Data assessment, data-model integration and application to the Southern North Sea', BCRS report 95-19, Delft.

Vos R.J., Borsboom M.J.A. and Tan K.,1996. 'DELWAQ FAST SOLVERS II, New Krylov methods for solving linear and non-linear equations', WL|Delft Hydraulics Report.

Vos R.J., Boon J.G. , Baart A.C., Schuttelaar M., Villars M.T. Van Pagee H., Althuis Y.A. and Roozekrans J.N., 1997. 'The combined use of remote sensing imagery and water quality models in the Southern North Sea', Proceedings of the Fourth International Conference on Remote Sensing for Marine Coastal Environments', Orlando, Florida, 1997, p. II-23 - II-32.

Vos R.J. and Schuttelaar M., 1996. 'An integrated data-model system to support monitoring and assessment of marine systems', (1996 Conference, The Hague, The Netherlands), in Operational Oceanography, The Challenge for European Co-operation, Elsevier Oceanography Series 62, p.507-515, 1997.

Vos R. and Ten Brummelhuis P., 1997. 'Goodness-of-Fit criteria for the simultaneous assimilation of Remote Sensing and in-situ data in SPM transport models', prepared for CEC-DGXII-MAST-3 program and Netherlands Board of Remote Sensing (BCRS), WL | Delft Hydraulics report Z2025.

Vos R.J., Villars M., Roozekrans J.N., Peters S.W.M. and van Raaphorst W., 1998. 'RESTWAQ 2, Part I: Integrated monitoring of total suspended matter in the Dutch coastal zone', BCRS report 98-08, Delft, The Netherlands.

Vos R.J., Dekker A.G., Peters S.W.M., van Rossum G.A. and Hooijkaas L.J., 1998. RESTWAQ-2, PART II, 'Comparison of remote sensing data, in-situ data and model results for the Southern Frisian Lakes', BCRS report 98-08b, Delft, The Netherlands.

Vos R.J., van der Kaaij, Brummelhuis P.G.J. ten and Gerritsen H., 1999. 'Integrated data-modelling approach for SPM transport on a regional scale', submitted to Coastal Engineering (26 p).

WL|Delft Hydraulics, 1997. DELWAQ Technical Reference Manual. Version 4.20.

Wollast R., 1998. 'The Scheldt Estuary', in 'Pollution of the North Sea, An assessment', W. Salomons (ed.), Springer-Verlag, Heidelberg, p183-193.

A Model set-up and processes

In this Appendix, details of the water quality model set-up, model processes and process parameters are given.

A.1 Aspects of model set-up

A.1.1 Numerical parameters

The minimum residence time in the grid cells of the water quality computational grid was analysed. The smallest value is on the order of a few seconds, though for most segments it is larger than 30 seconds. For computational stability, this implies that an implicit solution procedure must be used. An efficient and robust iterative solver was employed (Vos et al., 1996) that can handle aggregated (partially unstructured) grids. However, since a first order discretized upwind scheme is employed numerical dispersion is introduced. Therefore, no further (horizontal) dispersion is added in the water quality simulations. Time-steps of 15 minutes were employed for the grid with 4341 segment for 11 substances, leading to calculation times for the final simulations for 1998 of 4.3 hours on a Silicon Graphics Origin 2000 workstation with (10) 250 MHz superscalar processor. Since for model calibration many simulations (~50 simulations) are required, longer simulation times are not acceptable.

A.1.2 Substances modelled

The substance of interest in the study is Suspended Particulate Matter (SPM), which is the total amount of fine suspended material (< 63 μm). In the present simulations, the organic fraction of SPM (phytoplankton and detritus) is not considered explicitly, but is included implicitly in the modelled sediment fractions.

In the water quality model for the T_0-scenarios (no dumped material from tunnel silt), 11 substances were modelled. The first 5 of these substances are in the water column, the latter 3 substances are in (two) bottom layers of sediments. These 11 substances are:

1. Continuity (-), to confirm mass conservation;
2. Salinity (ppt), to check the hydrodynamic calculation and check mixing of sea and river water;
3. Inorganic Matter fraction 1(IM1, mg/l). This fraction is for sea silt.
4. Inorganic Matter fraction 2 (IM2, mg/l). This fraction is for river silt.
5. Inorganic Matter fraction 3 (IM3, mg/l). This is a heavy silt fraction.
6. Inorganic Matter fraction1 in sediment layer 1 (IM1S1, g)
7. Inorganic Matter fraction2 in sediment layer 1 (IM2S1, g)
8. Inorganic Matter fraction3 in sediment layer 1 (IM3S1, g)

9. Inorganic Matter fraction1 in sediment layer 2 (IM1S2, g)
10. Inorganic Matter fraction2 in sediment layer 2 (IM2S2, g)
11. Inorganic Matter fraction2 in sediment layer 2 (IM3S2, g)

A.1.3 Discharges from harbour dredgings

Available data on loads from dumping of dredged harbour material indicate that these dumpings are quite significant. The main dumping locations are Terneuzen, Breskens, Vlissingen, Perkpolder and Walsoorden. Locations for these dumping sites, (RijksDriehoek coordinate, and Water Quality model grid number) are given in Table A1. Values for dumped dry silt for 1997 and 1998 are given in the main text, Table 4.1 and 4.2.

Table A.1 Location of dumping sites for dredged harbour silt

Location	x- coordinate	y-coordinate	WQ grid number
Terneuzen	45847	374546	2541
Breskens	27000	381300	2757
Vlissingen	36000	385000	394
Perkpolder	60000	380000	4362
Kruiningen	60575	383529	1591
Walsoorden	60940	377900	3529

The available data for 1998 dumpings provided information about the wet volume of dredged material dumped per location. This data on wet volume had to be converted to the modelled parameter, i.e. dry weight of silt.

The formula for conversion of wet volume dredged material to dry weight of silt (< 63 µm) is as follows:

$$G^{silt}_{dry}(ton) = V_{beun}(m^3)\frac{f_{beun} f^{total}_{dry} f_{silt}}{\left(\frac{f^{total}_{dry}}{\rho_{dry}(ton/m^3)} + \frac{(1 - f^{total}_{dry})}{\rho_{water}(ton/m^3)}\right)}$$

with:

G^{silt}_{dry} = dry weight of silt fraction (< 63 µm) in tons
V_{beun} = wet volume of the ship ('beun') in m^3
f_{beun} = correction factor for shape of ship (~0.6)
f^{total}_{dry} = fraction of dry material for wet weight (~0.41)
f_{silt} = fraction of dry weight that is silt (~0.5)
ρ_{dry} = density of dry material in tons/m^3 (~2.2)
ρ_{wet} = density of water in tons/m^3 (=1.035)

Using the above given estimates for the conversion factors this leads to:

$$G^{silt}_{dry}(ton) = 0.162\ V_{beun}(m^3)$$

A.2 Selection of model processes and initial parameter settings

In modelling the processes of sedimentation and resuspension, a number of parameters for the process equations must be specified. The Delft3D-WAQ package allows for a large variety of these processes (WL | Delft Hydraulics, 1997). A proper selection, and proper choices of parameter settings for the Western Scheldt had to be made. Some of these parameters can not be chosen easily, and require a sensitivity analysis first.

This section will describe the important processes in the present model. It describes further the choices made for model parameters as a start for the final model calibration. Initial conditions are described.

Summary of model processes and parameters:

- Critical input parameters for the sedimentation of sediments according to Krone are the *settling velocities*, and the *critical shear stress for sedimentation*. Values are specified below. For calibration only the settling velocity of the heavy fraction is important.
- Critical input parameters for the erosion of sediments according to Partheniades are the *critical shear stress for bed erosion*. For calculation of the shear stresses induced by flow the bottom roughness (according to Manning), is affected by the *Manning coefficient*. During the model set up the critical shear stress for erosion was varied, whereas the Manning parameter was kept constant at default values (0.026). Important for bed erosion was the use of two layers, each having a very different critical shear stress for erosion:
  1. A first layer (S1) with critical shear stresses important for bed erosion is. Fit for shallow areas with bio-stabilisation in spring and summer.
  2. A second layer (S2) with much higher critical shear stress between 4.0 and 5.0 Pa. This is for introduction of spring-neap SPM differences.

  Exact values were part of a sensitivity analysis described below. The values are also varying over the year with the seasons. Note that the values are much higher than those typical for pure sand (~0.25 Pa, Torfs H., 1995), referring to the fact that we are dealing with *cohesive sediments.*
- Another important parameter is the erosion rate ($kg/m^2/sec$). As a start a value of 4320 $kg/m^2/sec$ was taken.
- Critical input parameters for Bijker formulations for wind induced erosion by waves are *wind Fetch* (m) and *wind speed* (m/s). Wind speed was taken from (quadratically) daily averaged values from the KNMI station at Vlissingen. The Fetch is a critical parameter of the model and was derived during the model set up with test models (see this section). Two fetches were used:
  1. A Fetch (0.125 km) for generation of short capillary waves at the tidal flats. Such waves only have effect at very shallow waters. This fetch was used for all areas with an average water depth $H < 2$ m.
  2. A Fetch (6 km) for generation of waves in the order of a few km that might erode curves, and flats at the sides of the estuary. This value was used for all area with average water depth $H > 2$m.

Values for these Fetches were derived by a small sensitivity analysis, described below (Process 2 and Process 3).

The model includes a series of processes that are considered to be important for the SPM content of the Western Scheldt estuary. Specifically, four processes are responsible for the distribution and fate of SPM which enters the Western Scheldt from the initial conditions, from the boundaries or from dumpings:

1. Setting of sediments;
2. Erosion from tidal flats by flow and wind induced waves;
3. Erosion from gullies by tidal flow;
4. Erosion from gullies by wind induced waves

The processes as relevant to the Western Scheldt are described below. Complete formulations are given in the DELWAQ Technical Reference Manual (WL|Delft Hydraulics, 1997).

A summary of model parameters for the final model set up is given in Tables B.1 and B.2.

Process 1: Settling of sediments

Three fractions of sediment, each having different settling velocities were modelled. Settling velocities for the sea fraction and river fraction are concentration dependent according to Boere (1987) and Burt (1986):

$$v_{sed} = k^0_{sed}\left(\frac{c}{1000}\right)^n$$

with:
- v_{sed} = settling velocity in (m/day)
- K^0 = settling constant
- c = silt concentration in mg/l
- n = flocculation parameter (-)

Fraction 1: K^0=50; n=0.67 (n from Boere 1987, measured at neap tide for Western Scheldt)
Fraction 2: K^0=50, n=1.37 (n from Burt, 1986, measured in River Scheldt)

K^0 was determined from (Figure 6.7 in) van Leussen (1989). Settling velocities are given in Figure A.1. Enhanced settling due to salinity gradients is not used. A critical shear stress for sedimentation was set to 0.1 Pa.

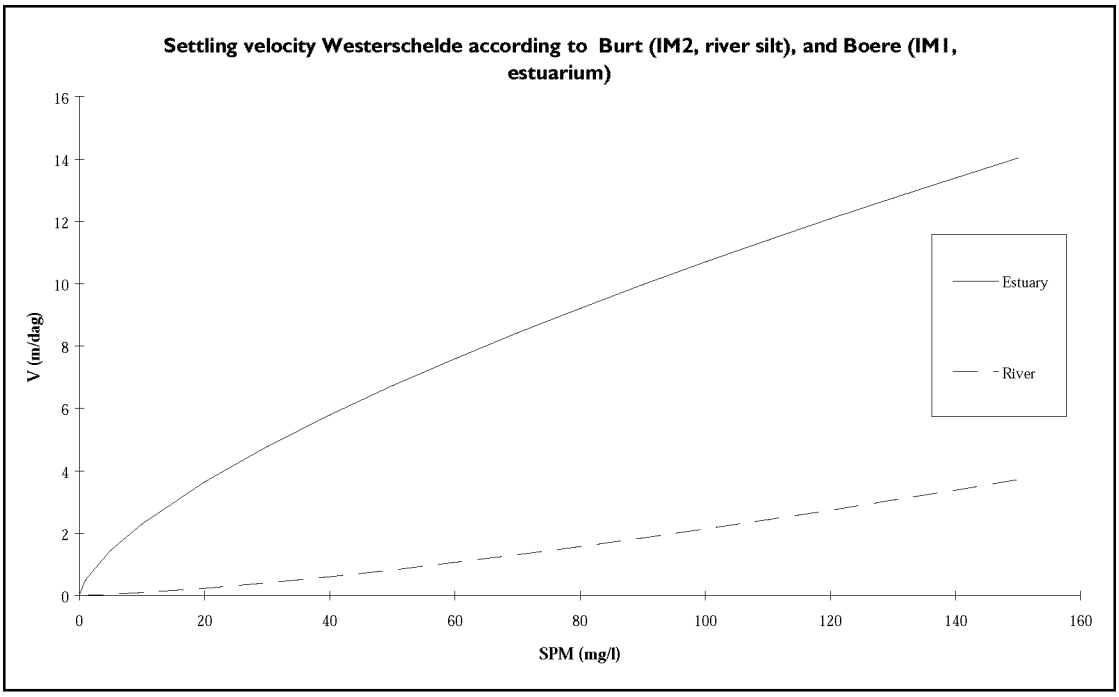

Figure A.1 Settling velocities for two sediment fractions.

Also a third fraction was modelled with a constant settling velocity of 100 m/day, and a high critical shear stress for sedimentation of 4.0Pa. Both these values were varied somewhat during the model set up, but it was concluded that the amplitude for spring-neap variation at Terneuzen was bets represented with the values given here. This gives a spring-neap cycle variation of SPM.

Process 2: Erosion from tidal flats by flow and wind induced waves

The model was first initialised[5] to give a stable (top) sediment layer (S1) at the tidal flats for no wind (no waves). This happens at a critical shear stress value for erosion of 0.8 Pa. The resulting bottom distribution for the top layer was used for all later runs and is given in Figure A.2. This (top) sediment layer has no sediment outside the tidal flats. At the tidal flats the first layer is never fully eroded during the winter seasons, so the second layer never can be eroded over there. In the areas outside the tidal flats, a second bottom layer (S2) with much higher critical shear stresses (4.0-5.0 Pa, being much more stable) was used.

[5] *Also the initial distribution of IM1 and IM2 in the water column was derived from this simulation. This value is much less criticial for the results than the bottom composition due to the relatively fast refreshment of the system by the sea water and river water.*

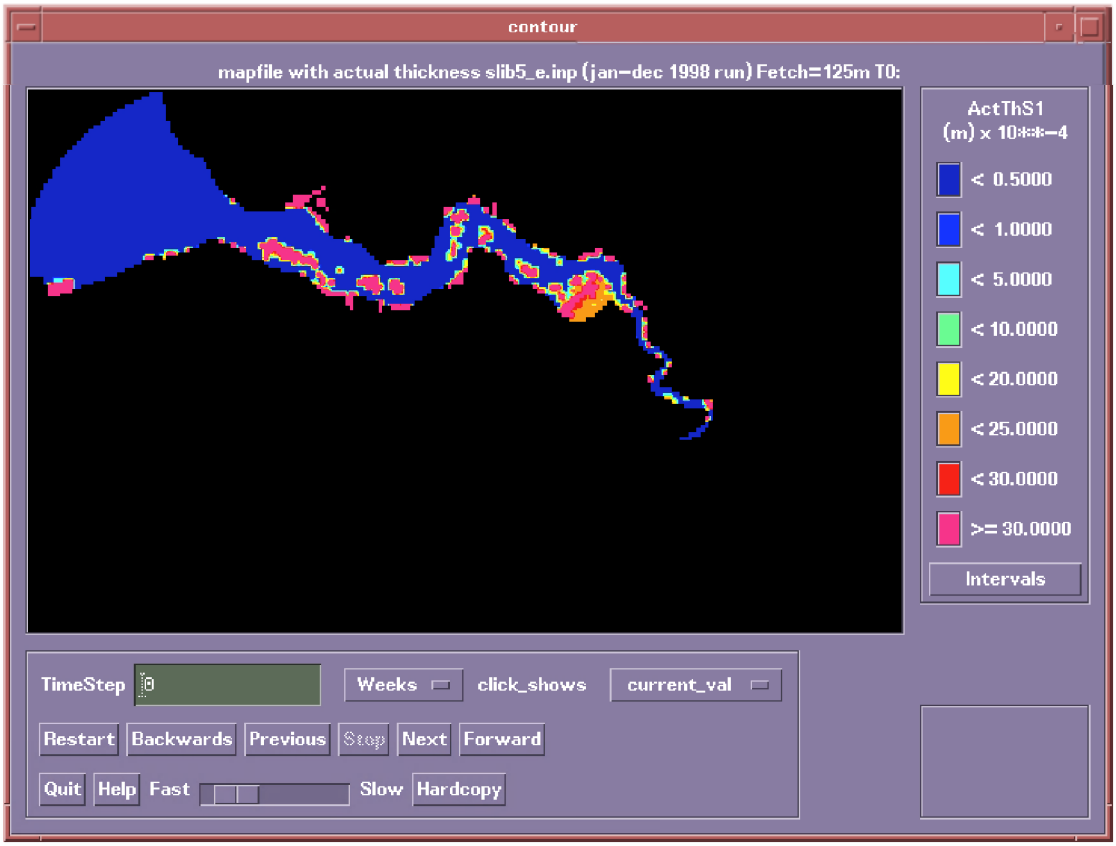

Figure A.2 Initial thickness of the bottom layer (thickness for of two sediment fractions) used for 1-1-1998 (also figure 4.5).

The effect of stabilisation of the tidal flats by diatoms in spring-summer was simulated by choosing a time-varying function for critical shear stress for erosion (see Figure A.3). In winter this value is lower than 0.8Pa (0.6 Pa) , in summer it is above the critical shear stress for erosion (1.5 Pa). The chosen function of Figure A.3 was multiplied by 1.5 as a second test, but that lead to worse results.

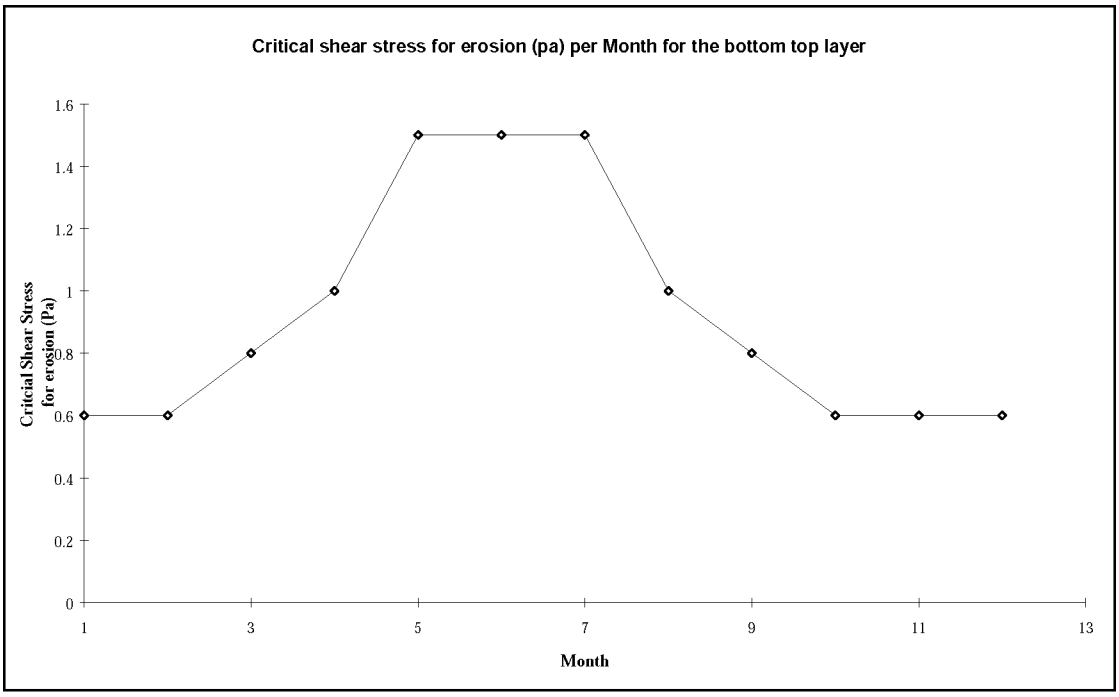

Figure A.3 Critical shear stress for erosion of the top sediment layer (S1)

The shear stress according to Bijker for a tidal flat with a water layer of 0.075 m is given in Figure A.4. It might be noted that a large Fetch (1 km) erodes the tidal flat fully already at low wind speeds. The short fetches react much more strongly to wind speeds higher than 10 m/s.

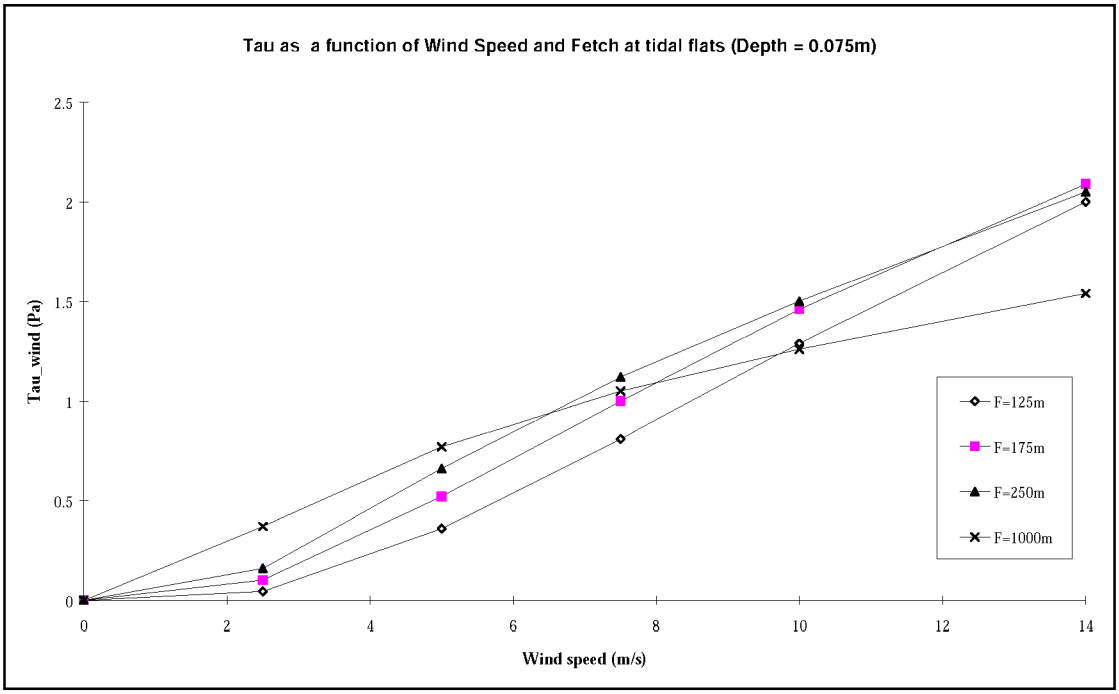

Figure A.4 Bottom shear stress as a function of wind speed at a tidal flat

The additional shear stress at tidal flats may go up to a few Pascals at high wind speeds (see Figure A.4). The use of these capillary waves (wave periods < 1 sec) leads to high concentration peaks of SPM (SPM) during periods with high wind speeds (especially those above 10 m/s).

In Figure A.5, the calculated SPM concentration at Baalhoek is shown (model segment 3408) for different fetch values, ranging from 1m (almost no wind effect), to 1000m. In these simulations, the critical shear stress for erosion from sediment layer 1 was as in Figure A.3, and for sediment layer two was 4.0 Pa. These values lead to an initial choice for the Fetch at tidal flats of 125m.

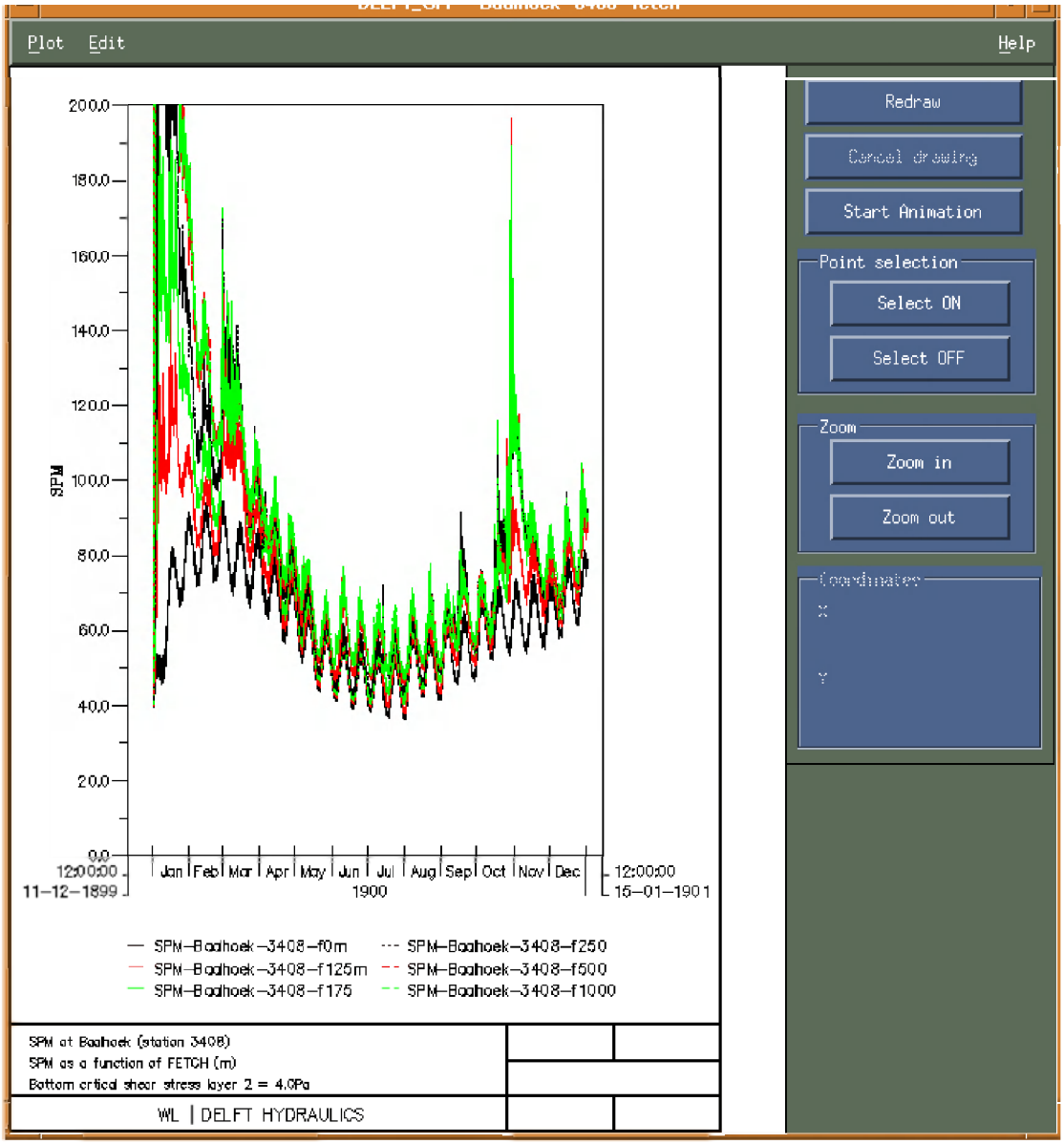

Figure A.5 SPM concentrations at Baalhoek as a function of 6 Fetches:
Fetch = 1m (black), Fetch = 125m (red), Fetch = 175m (green), Fetch = 250m (red), Fetch = 500m (red), Fetch =1000m (green).

Wind from KNMI show stormy periods for January, end of February, and end of October-begin of November. These periods are recognised as SPM peaks in Figure A.5. The erosion by waves at tidal flats was finally simulated by applying a short Fetch of 125 m (second red line in Figure A.5) that generates capillary waves (T ~ 0.5 sec, H ~ 0.045m).

Process 3: Erosion from gullies by tidal flow

Gullies may release some sediment at high shear stresses. Hereto, a second layer with a high critical shear stress for erosion was added to the model. In order to simulate a distinct SPM difference between spring and neap tides (that have much different shear stress due to flow), a critical shear stress of 4.0-5.0 Pa works fine, since then only during spring tide, the bottom erodes. These rather high critical shear stresses may result from mixtures of sand with a rather low silt content. For such mixtures silt can be very effective in stabilising the bottom.

The spring-neap variation is best visualised in Figures A.6a and A.6b for the tidally averaged neap and spring tide respectively (peak values at ebb or flood are higher).

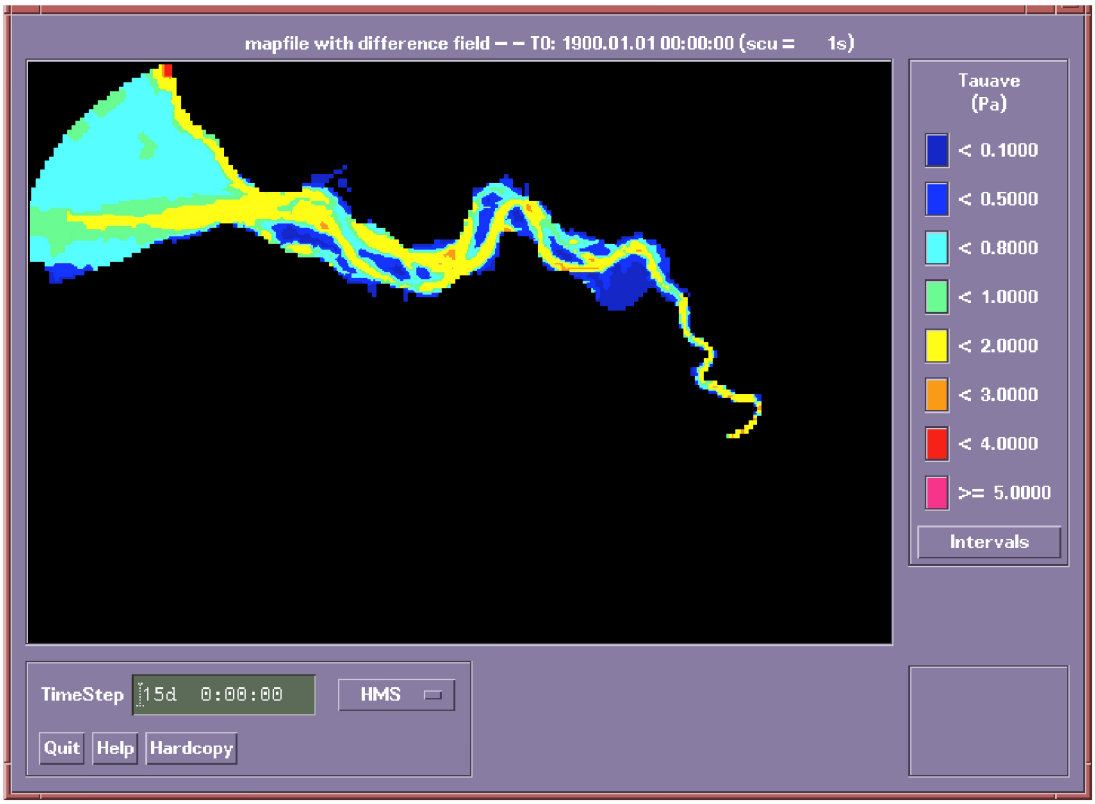

Figure A.6.a The *average* bed shear stress over 7 model days without wind for the *neap period* (from day 7-14 of the hydrodynamic data base).

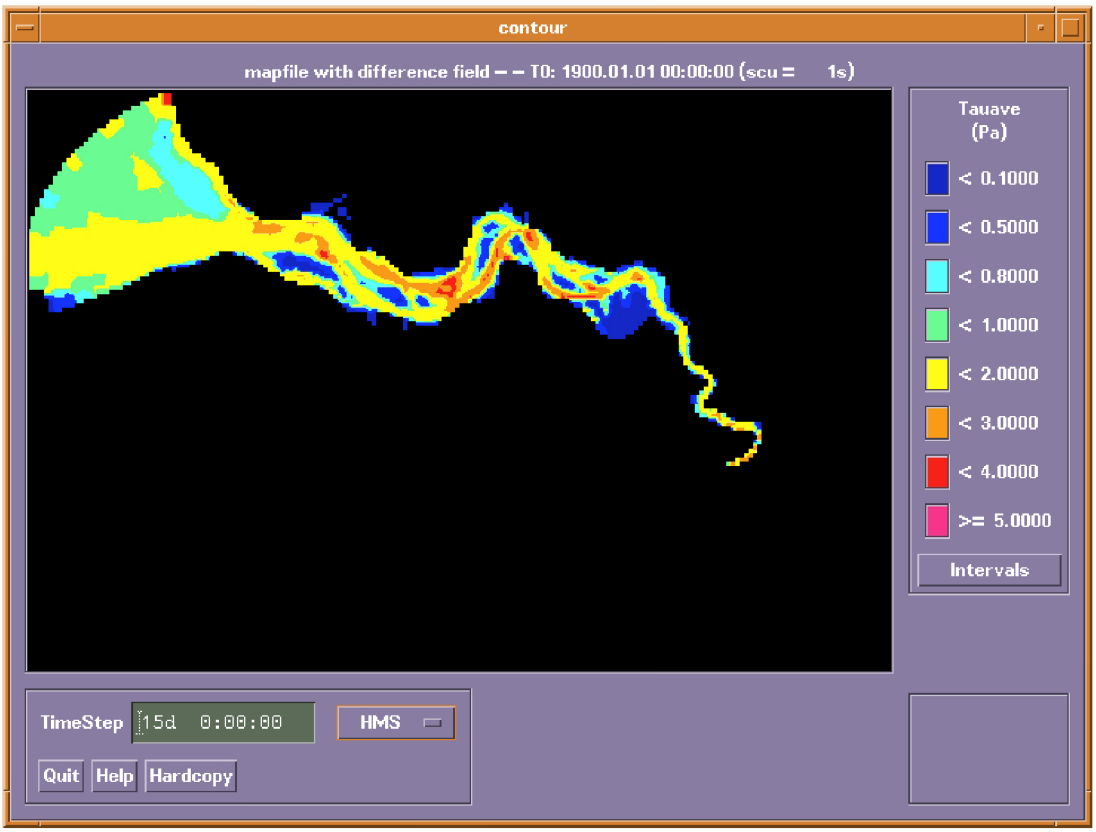

Figure A.6.b The average bed shear stress over 4 model days without wind for the spring period (from day 1-5 of the hydrodynamic data base).

In Figure A.7, a small sensitivity analysis is given for the value of the critical shear stress of the second bottom layer at station Terneuzen. The spring-neap variation is clearly present all over the year, but unfortunately the summer SPM concentrations are too high compared to those of van Maldegem (1992). At Terneuzen, van Maldegem finds on average 20 mg/l whereas simulations with 4.0 Pa and a Fetch of 125m show about 40 mg/l at Terneuzen.

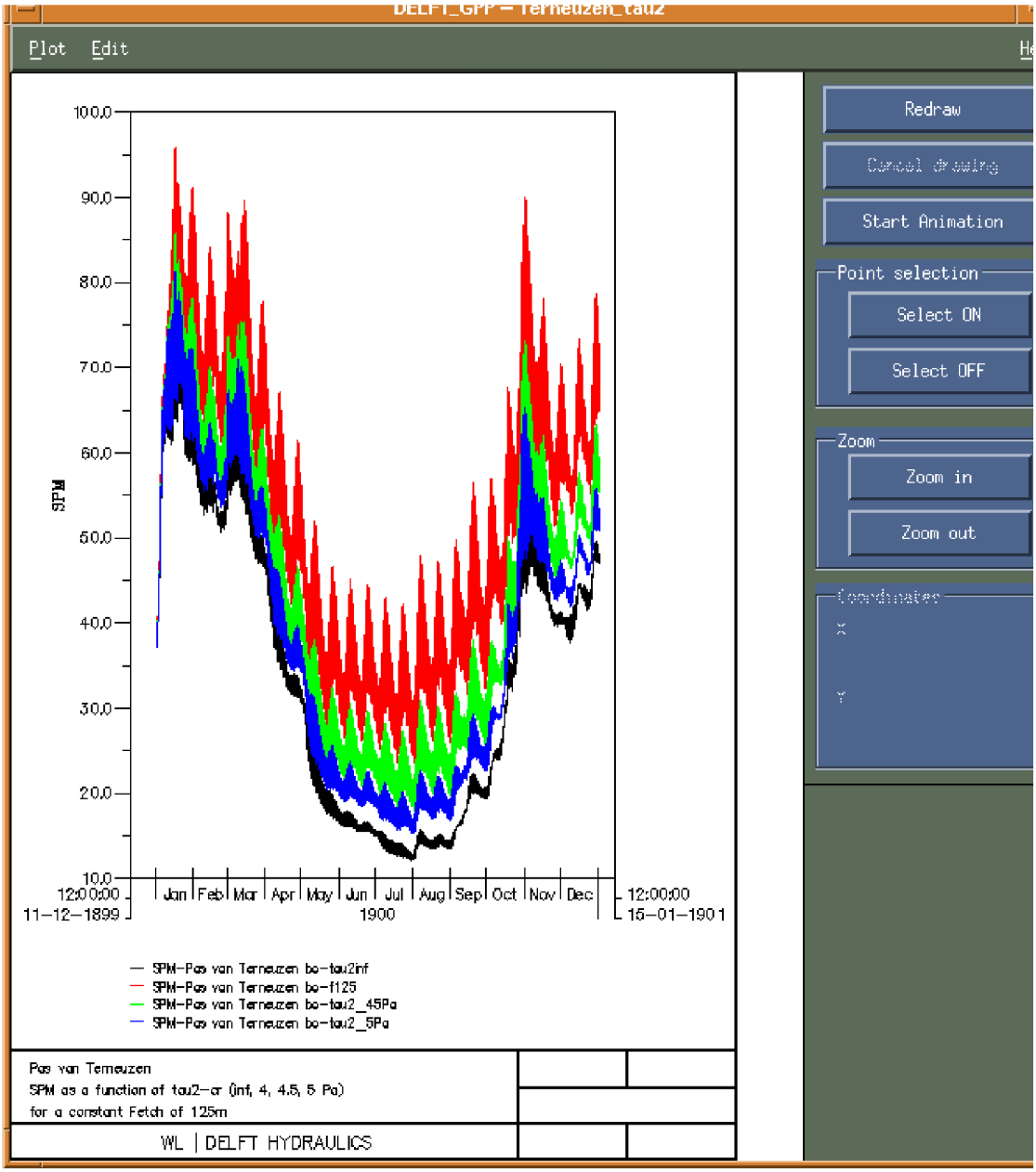

Figure A.7 SPM concentrations at 'Pas van Terneuzen' for several values of the critical shear stress for erosion of the second bottom layer at a constant Fetch of 125m.

Figure A.7 shows that a value of 5.0 Pascal is much better for this station in summer. Therefore, the final model set up employs a time-varying function for the critical shear stress of the second layer. In Figure A.8, 3 such functions are given:

- For layers S1 (see also Figure A.3);
- For layer S2 with low values and much erosion in March and September (function 1);
- For layer S2 with higher values and less erosion in March and September (function 2);

During final model calibration a selection was made for either function 1, or function 2. Function 1 was chosen as a start.

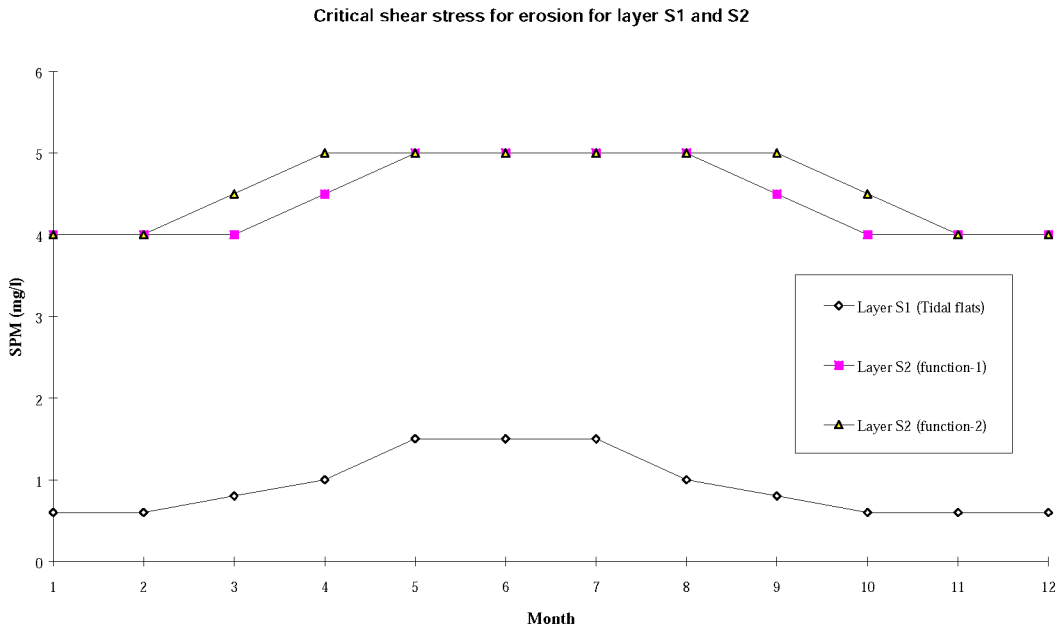

Figure A.8 Time-dependency of critical shear stress for layers S1 and S2

Process 4: Erosion form gullies by wind induced waves

Capillary waves do not attribute in the gullies to erosion. Here waves with longer periods may be applied (T~ 2.5s, H~ 1m) for erosion. Waves of a Fetch of 10km can very well erode the shallow sides of the gullies (H<2.5m) at high wind speeds. This is clearly shown in Figure A.9 where the shear stress at the bed is plotted as a function of Depth for a constant Fetch of 10 km. It is evident from Figure A.9 that in areas with depths between 2.5m and 5m, waves induced by wind speeds beyond 10m/s can lead to significant bottom erosion.

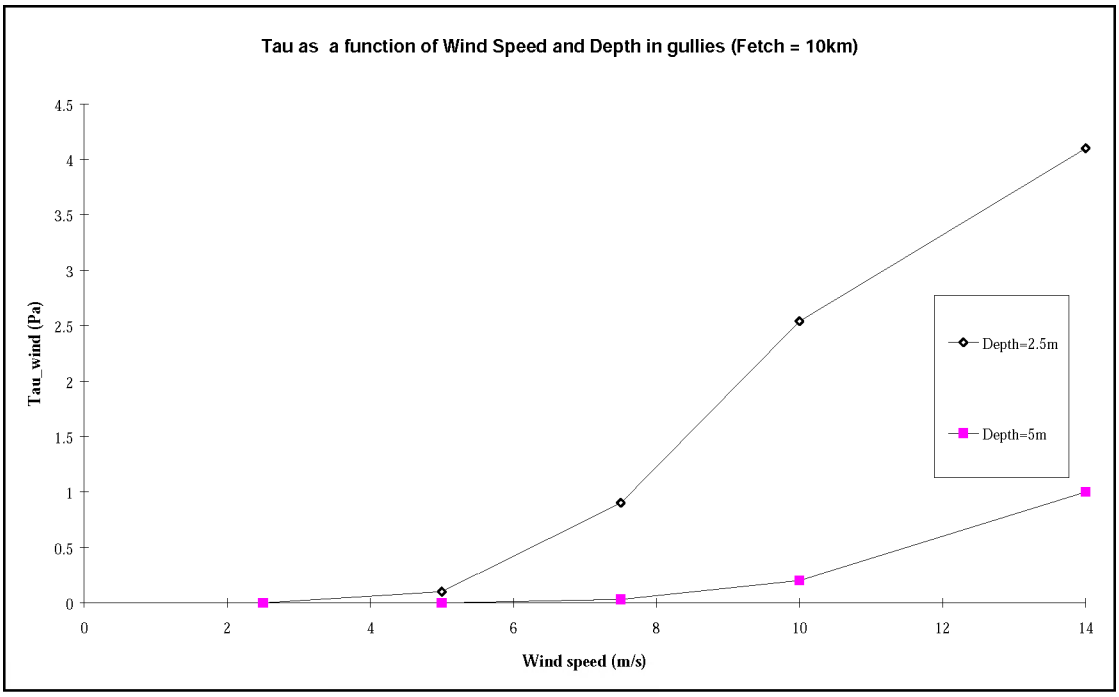

Figure A.9 Bottom shear stress (Pa) as a function of water depth for a Fetch of 10 km.

In the model, for areas of depth between 2.5m and 5m the shear stress due too flow is low (< 1.0Pa). Adding waves with a Fetch of 10 km may lead to additional erosion during windy periods from sides of the gullies. Such waves have periods of ~2.5 s and heights of ~1m.

In order to generate such erosion effects (which can be recognised sometimes on remote sensing images), the Fetch was initialised in the model as being 10 km for computational segments with a (tidally averaged) water depth greater than 2.0 m. For segments with a water depth (average) less than 2.0m (i.e. all tidal flats), a Fetch of 125m was retained. Finally, also a Fetch of 5 km was used, but this had no effect on the SPM concentrations.

In Figure A.10 the effect of the different Fetch values on calculated SPM at Baalhoek are shown. The reference calculation (bottom line) had a uniform Fetch of 125m for all segments.

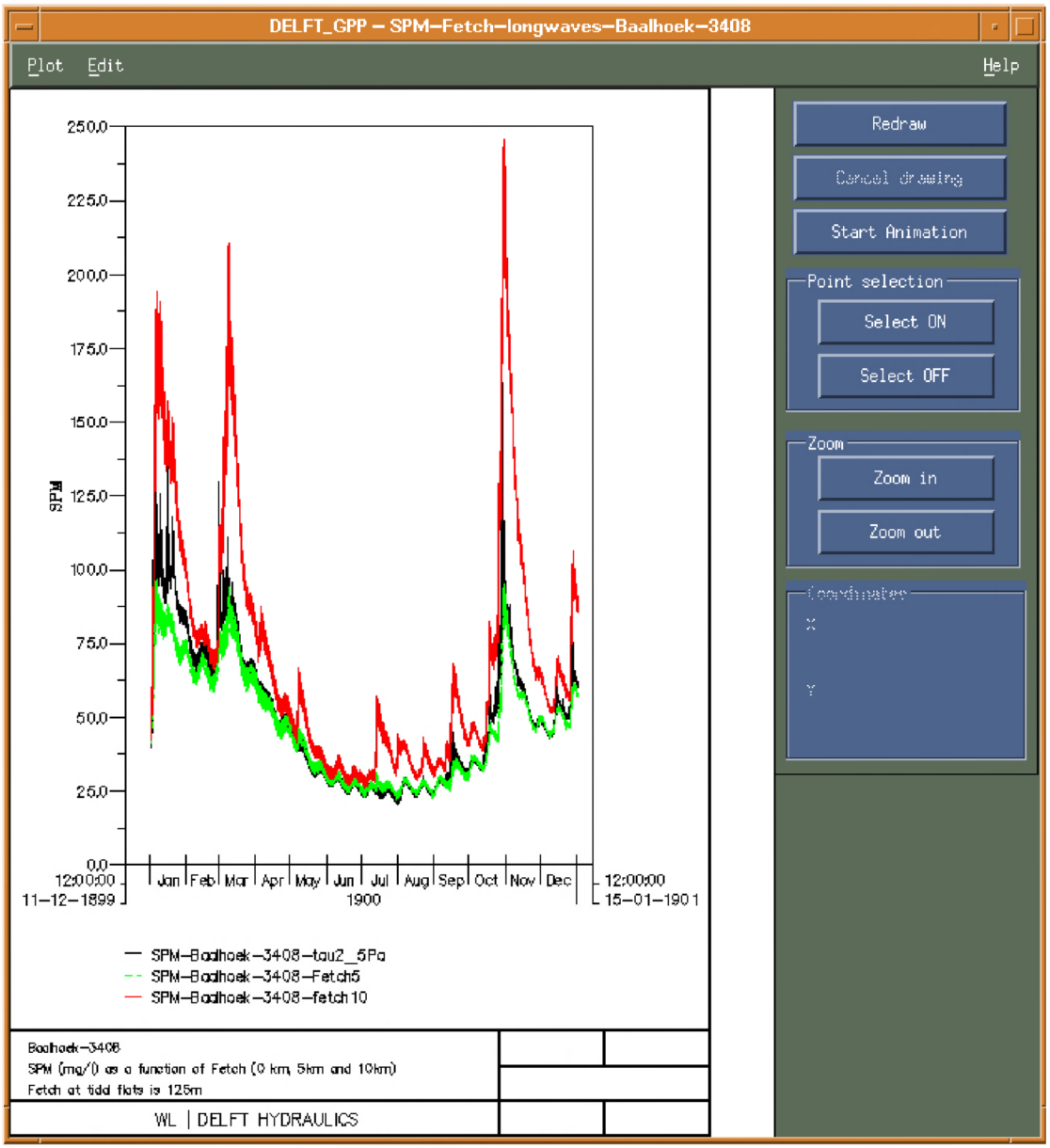

Figure A.10 The effect of waves with long Fetch at Baalhoek (only applied for segments with depth > 2.0m).

Note in Figure A.10 the strong increase of SPM in stormy periods (especially October-November 1998), and the increase of the spring-neap variation in SPM for some periods with moderate winds (especially July-September). The final choice from this small sensitivity analysis is a value of 6 km for the Fetch at all segments with a depth larger 2 meters.

B Cost Function for Model Calibration

In this Appendix, the procedures followed in calibration of the water quality model are presented. Specifically, details are given to the cost-function, in which information from both in-situ and remote sensing data were used to optimally tune model parameters. Through application of the cost function, the remote sensing data has been incorporated into the water quality model.

B.1 Introduction

In section 4.3 and Appendix A the set up of the water quality model is described. This model was set up by initialisation of some of the model parameters in test models. The results of these test models were often derived from *qualitative comparison with a single data set (either the Terneuzen set or the Baalhoek set).* Remote sensing data were not used, and no validation was done for the spring and summer period. This was felt to be a serious shortcoming.

The SPM model now needs a proper calibration on *all available data simultaneously* and this is done in this section. These calibration data ('observables') are:

1. Continuous in-situ data for SPM (mg/l) at Baalhoek, Terneuzen and Vlissingen (see Chapter 2).
2. Twenty year monthly mean averages for SPM for 8 locations (see Chapter 2).
3. 9 processed images from remote sensing, transformed to the aggregated SCALWEST model grid (see section 3.3.2).

It is evident that a proper and objective calibration for such large amounts of data is hardly possible by visual inspection. Therefore, quantitative methods for model calibration are required. Such methods were developed and tested successfully by Vos and ten Brummelhuis et al. in the PROMISE project (Vos and Ten Brummelhuis 1997, Ten Brummelhuis et al., 1999) for the North Sea, and in the RESTWAQ-2 project (1998, PART I) for the Dutch coastal zone. The formal methodology is described in Vos and Ten Brummelhuis (1997). A simplified version of this methodology was applied in this study, as described in section B.2.

An adjoint method was recently developed by Ten Brummelhuis (1999) for automatic calibration and structured sensitivity analysis with the Delft3D-WAQ code of cohesive sediments. This procedure was not applied in the present project due to limitations of computer power, and limitations in budgets and time-schedule for operationalisation of this model code for the Western Scheldt. For future applications it might be desirable to use this adjoint for a more extensive and reliable model calibration.

B.2 Cost functions for data-model integration

Cost functions are used for model calibration. A cost function (or Goodness-of-Fit criteria) measures quantitatively the misfit between model results and measurements ('observables'). Inputs for the cost functions are besides observables, *their uncertainties*. Is the model result is within the uncertainty range of the measured data, data and model are supposed to be in agreement and not misfit is counted. A simple Goodness-of-fit function that satisfies this criteria is:

$$J(\alpha_1,\alpha_2,....) = \sum_{i=1}^{n}\left(\max,\left\{\left[ABS(C_i^{\mathrm{mod}}(\alpha_1,\alpha_2,....) - C_i^{obs}) - S_i^{obs}\right],0.0\right\}\right)^2$$

with:

$J(\alpha_1,\alpha_2,....)$ = cost function of Goodness of Fit for a model with parameters α_i;

$C_i^{\mathrm{mod}}(\alpha_1,\alpha_2,....)$ = model concentration of SPM for a model with parameters α_i;

C_i^{obs} = observed SPM concentrations;

S_i^{obs} = uncertainty range ('band with') for observed SPM concentrations;

B.2.1 Use of remote sensing data in the cost function

For comparison of the Remote Sensing data and the model data, the model data closest to the remote sensing data in time, and within one meter difference of water level at Terneuzen were selected and compared to the remote sensing data. This was done after aggregation of the model data and remote sensing data for 9 zones in the model. These zones are given in Figure B.1. Only averaged concentrations per zone are compared.

The zone partitioning only leads to a simplified quantification of the difference between the model and the remote sensing data. With the present zones, mainly the gradient in SPM from West to East in the estuary is fitted. For instance, the detailed patterns of SPM in zone number 1 (zone at sea boundary), containing the sharp gradients between Paardemarkt, Scheur van Wielingen, Vlakte van Raan, Scheur van Deurlo and Oostgat as observed in some of the (winter) remote sensing images are not taken into account. Optimisation of such details can be done by introducing more zones here. This was not done in this study, but may be an issue for future optimisations of the calibration. The remote sensing cost function is:

$$J^{RS}(\alpha_1,\alpha_2,....) = \sum_{im=1}^{9}\sum_{z=1}^{9} w_{im,z}\left(\max,\left\{\left[ABS(\overline{C}_{im,z}^{\mathrm{mod}}(\alpha_1,\alpha_2,....) - \overline{C}_{im,z}^{RS}) - \overline{S}_{im,z}^{RS}\right],0.0\right\}\right)^2$$

Here the subscripts im and z are for the image-number and zone number respectively,. The overbar indicates the time- and spatial averaging for each zone. The pre-factor 'w' has been introduced in order to eliminate certain zones for certain images. This factor is either '1' or '0'.

The band width 'S' was taken to be 10% of the observed concentration, except for the 1 October image where it was assumed to be 50%. This estimate was estimated from the accuracy of processing of the level 1 SPOT images (section 3.3.1).

The zones of van Maldegem (1992) could have been used as well, instead of the 9 zones defined here. However, they are similar to the 9 zones used here, except that zone 1 is not included by van Maldegem, and that the Belgium Scheldt contains more zones than shown in Figure B.1. The objective of the zones is to quantify the gradient in SPM concentration in the Western Scheldt from West to East.

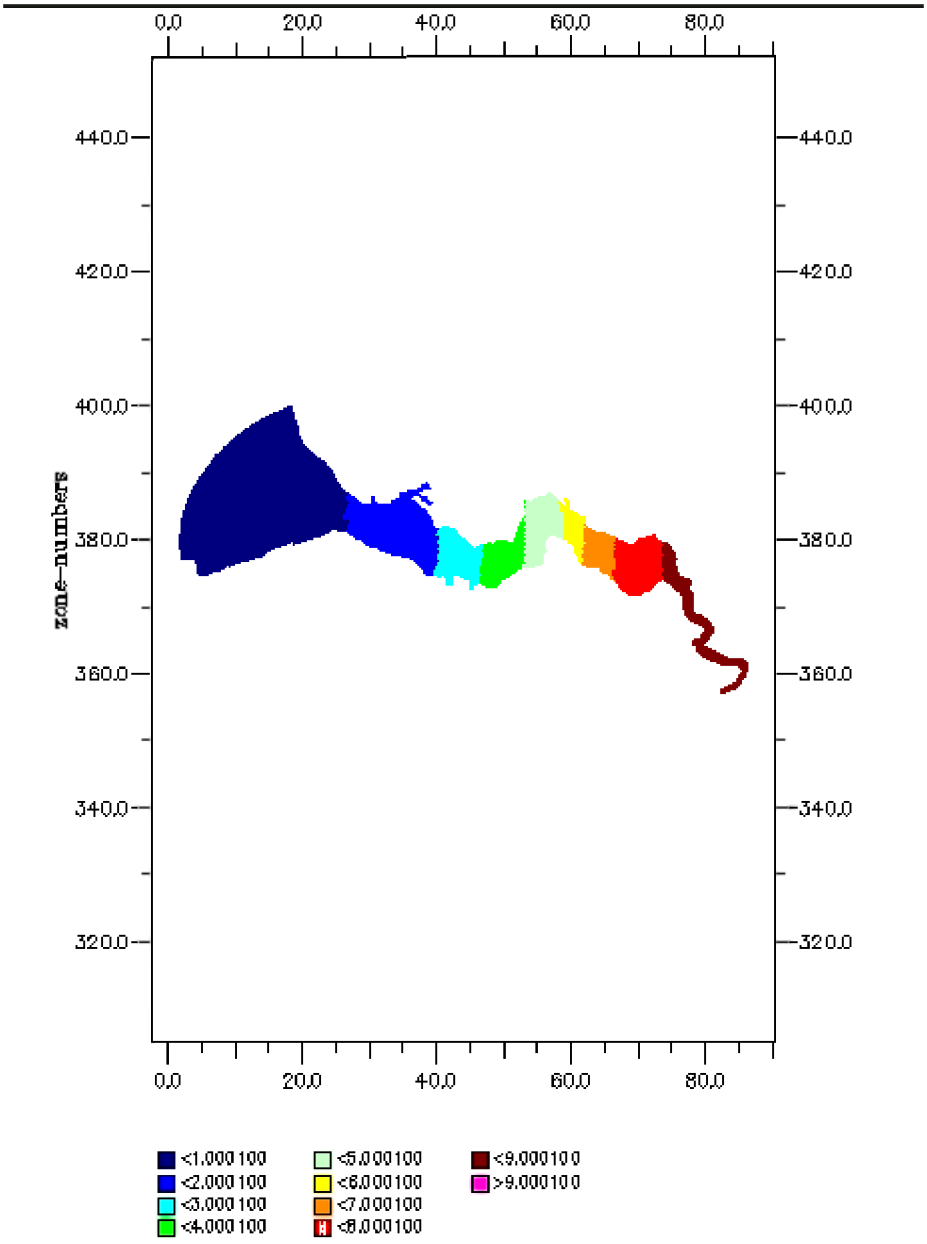

Figure B.1 Zone partitioning for comparison of Remote Sensing SPM data with model results. Only averaged concentrations per zone are compared.
(<1.000100 = zone 1; < 2.000100 = zone 2; etc.)

B.2.2 Use of in-situ data in cost functions

The model concentrations of SPM and in-situ data were monthly averaged before the difference between the model and the data was calculated. For the continuous in-situ data, this leads to reduction of much of the information in the cost function. However, we found that use of daily averages did not give very different results. Nevertheless, the cost function is not sensitive for a misfit in the oscillations of spring-neap tide and lunar tide. Such cost-functions still need to be developed in the future. This can be done by explicitly using the amplitude and phase of these oscillations in the cost functions (beside the SPM concentrations), obtained from a Fourier analysis of modelled and observed time-series of SPM.

The cost function for in-situ data of the twenty year monthly averages by Van Maldegem is:

$$J^{IS-1}(\alpha_1,\alpha_2,....) = \sum_{m=1}^{12}\sum_{s=1}^{8} \left(\max,\left\{\left[ABS(\overline{C}_{m,s}^{\mathrm{mod}}(\alpha_1,\alpha_2,....) - \overline{C}_{m,s}^{IS-1}) - \overline{S}_{m,s}^{IS-1}\right],0.0\right\}\right)^2$$

Here the subscripts m and s are for the month (Jan-Dec), and station number respectively (1= boei Oostgat, 2= Honte, 3=Splitsingspunt Wielingen, 4 = Pas van Terneuzen, 5=Overloop van Hansweert, 6=Zuidergat boei 49, 7=Zuidergat boei 59A, 8=Saaftinge boei 76). The overbar indicates the time-averaging for each month. The uncertainties S were set equal to the standard deviations that Van Maldegem derived from his time-series.

The cost function for in-situ data for the continuous stations is:

$$J^{IS-2}(\alpha_1,\alpha_2,....) = \sum_{m=1}^{12}\sum_{s=1}^{3} w_{m,s}\left(\max,\left\{\left[ABS(\overline{C}_{m,s}^{\mathrm{mod}}(\alpha_1,\alpha_2,....) - \overline{C}_{m,s}^{IS-2}) - \overline{S}_{m,s}^{IS-2}\right],0.0\right\}\right)^2$$

Here the subscripts m and s are for the month (Jan-Dec), and station number respectively. The stations are 1= Vlissingen, 2= Terneuzen, and 3= Baalhoek. The pre-factor 'w' has been introduced in order to eliminate certain months for which there are no data. This factor is either '1' or '0'. The uncertainties S were taken to be 20% of the observed averages.

B.2.3 Total Cost function

For final set up of the model, the cost functions J^{RS}, J^{IS-1} and J^{IS-2} must be summed. However, this will lead to unrealistic results since the cost functions are not of the same order of magnitude and need some normalisation. The final cost function has been obtained by normalising the value of each cost function with a constant factor:

$$J^{Total}(\alpha_1,\alpha_2,....) = \frac{J^{RS}}{R_1} + \frac{J^{IS-1}}{R_2} + \frac{J^{RS-2}}{R_3}$$

with the factors R_i then normalisation factors. These were chosen to be equal to the non-normalized cost-function results for one of the simulations (this was chosen to be simulation 'b', see section 4.4.4). Note that for each type of cost function, the 'normalised' value is J^i/R_i.

B.3 Variable model parameters

The variable process parameters have been described in section 4.3. An overview of process parameters and their initial settings that were optimised during the model calibration is given in Table B.1. In Table B.2 values for the other parameters (that were not optimised) are given. Most of these parameters were initialised during the model set up with a sensitivity analysis in test models (see section 4.3 and Appendix A).

Table B.1 Model parameters and inputs that were varied during the calibration. Initial values are given for simulation b (filename: slib7_b.inp')

Parameter	Description	Unit	Initial value (run b)	Alternatives evaluated
TauCRS2DM	Critical shear stress layer 2	Pa	Function 1, Fig A.8	Function 2 Fig A.8, or constant 5 Pa
Bottom-comp.S2	Ratio of (IM3/DM) in layer 2 at start	%	95	50
Sea Boundary IM1	Concentrations of IM1 at sea boundary	mg/l	Function Figure 4.3a with 10% higher values	Function, Figure 4.3a
ZResDM	Erosion rate for layers 1 and 2	g/m2/s	17280	8640
Dumpings	Amounts for Dutch harbour dumpings	Mton	zero	1997 or 1998
VSedIM2	Settling velocity IM2	m/day	Function, Fig A.1	100% increase

Table B.2 Model parameters and inputs that were fixed during the calibration. Values have been derived during the model set up (see section 4.3 and Appendix A).

Parameter	Description	Unit	Fixed value	Notes
TauCRS1DM	Critical shear stress layer S1	Pa	Function, Fig A.3	Derived during model set up
Fetch for H< 2m	Fetch for waves for depth < 2m	m	125	Derived during model set up
Fetch for H> 2m	Fetch for waves for depth > 2m	m	6000	Derived during model set up
TauCSIM1	Critical shear stress sedimentation IM1	Pa	0.1	common value
TauCSIM2	Critical shear stress sedimentation IM2	Pa	0.1	common value
TauCSIM3	Critical shear stress sedimentation IM3	Pa	4	Derived during model set up
Manning	Manning coefficient for Chezy form.	-	0.026	common value
VSedIM1	Settling velocity IM1	m/day	Function, Fig A.1	literature
VSedIM3	Settling velocity IM3	m/day	100	Derived during model set up
Bottom-comp.S1	Initial bottom for layer 1 at start	-	Figure A.2 / 4.5	Derived during model set up
River Boundary IM2	Concentrations of IM2 at Antwerp	mg/l	Function, Figure 4.3b	Derived during model set up

B.4 Calibration results

Finally, 11 simulations were done with variations of the parameters given in Table B.1. These simulations are defined in Table B.3 and numbered 'a' to 'k'.

Simulation 'b' was the reference simulation. In first instance 'a' was the reference since it was in good agreement with the data for Terneuzen. However, since 'a' was much worse when compared with the other data, 'b' was selected as a further reference in the study.

Dumpings were added for simulations 'i', 'j' and 'k'. This is not really a variation. It is noted that the 1997 data were not appropriate, and the 1998 data for the dumpings were only obtained at the last minute of the project.

Table B.3 Parameter values for parameters for runs. Simulation 'b' is the reference run and is defined in Tables B.1 and B.2. Not more than 3 parameters are varied per simulation

Run	Parameter	Value	Parameter-2	Value-2	Parameter-3	Value-3
a	Bottom-comp.S2	50%	-			
c	TauCRS2DM	5 Pa (constant)	-			
d	Sea Bound. IM1	10% lower	-			
e	TauCRS2DM	Function 2	-			
f	VSedIM2	200%				
g	TauCRS2DM	Function 2	Sea Bound.IM1	Function, Figure 4.3a		
h	TauCRS2DM	Function 2	Sea Bound.IM1	Function, Figure 4.3a	ZRESDM	50%
I	Bottom-comp.S2	50%	Dumpings	1997 data		
j	Dumpings	1997 data				
k	TauCRS2DM	Function 2	Sea Bound.IM1	Function, Figure 4.3a	Dumpings	1998 data

B.4.1 Normalised Cost functions

Results for the 'normalised' cost functions and the totals were obtained with the FORTRAN program 'seashis4' and are given in Table B.4. The normalisation factors were those of the non-normalized results of simulation 'b' and are R_1 = 18521.4; R_2= 27334.3 and R_3=1125.8.

Table B.4 Results of the normalised cost-functions for model simulations for parameter optimisation. Best results are 'bold'.

	Remote Sensing data	20 year In-Situ data	Continuous In-situ data	
Simulation	J-RS/R1	J-IS1/R2	J-IS2/R3	Total cost function
a	8.31	2.90	16.08	27.30
b	1	1	1	3
c	**0.03**	**0.16**	3.08	3.27
d	0.81	0.81	1.02	2.65
e	0.73	0.75	0.85	2.32
f	0.95	0.95	1.00	2.89
g	0.59	0.60	1.01	**2.20**
h	0.09	0.26	2.29	2.64
I	22.65	7.63	98.5	128.78
j	10.36	19.62	44.3	74.28
k	0.83	0.73	**0.65**	2.21

In Figures B.2 - B.4, a comparison is made for models a-h for the continuous monitoring stations at Terneuzen, Baalhoek and Vlissingen respectively.

B.4.2 Discussion of the results

- Simulation 'a' was initially optimised on the continuous data for Station Terneuzen. For that station the agreement was very good, as is shown in Figure B.2 (red line is model 'a'). However, the cost function is dramatically bad for all other data! For RS data, the monthly averaged in-situ data (Van Maldegem) and the Baalhoek continuous in-situ data SPM values are systematically too high.
- Simulation 'c' is best for the Remote Sensing data and for the monthly averages of Van Maldegem. However, this model performs poorly when compared to the continuous in-situ stations. For these stations, the calculated SPM values are systematically too low and do not show any spring-neap variation, due to a too high critical shear stress for erosion of layer 2. A comparison of model results for Baalhoek confirms this (Figure B.3);
- The results for remote sensing data and the monthly averaged data of Van Maldegem lead to the same parameter settings. This is in agreement with the fact that these two data sets are in good agreement (see section 3.3).
- The continuous monitoring data are best fitted with simulation 'k'. Simulation 'g' already performs well, but adding the dumpings for 1998 to 'g' improves the fit at Terneuzen. This is explained from the fact that the dumpings only take place at Terneuzen (where modelled SPM was low) and not at Baalhoek (where modelled SPM was good), whereas at Vlissingen these dumping do not have much effect.
- The simulations with dumpings from 1997 data have a very poor performance as indicated by the cost function, implying that these dumping figures are out the realm of all data, even the twenty yearly averaged data. Also, the exact timings of the 1997 dumpings were not well known, only general indications of the dumping months.
- Simulation 'g' is best for all simulations, whereas 'k' (equal to 'g' + 1998 dumpings) almost has similar performance. Since 'k' includes the dumpings it was selected as the final result.
- The Terneuzen continuous data, and to a lesser extent the Vlissingen data have higher SPM concentrations for the winter periods than most of the model simulations. The twenty year mean monthly averages indicate lower concentrations for winter. Probably, the twenty year men monthly averages do not contain much of the storm effects incorporated in the in-situ data, and therefore may lead to underestimated monthly averaged SPM concentrations for winter periods.
- The remote sensing image for 11 January 1998 (the only remote sensing winter image) indicates that the modelled SPM is too high in the estuary (the zone near the sea boundary is perfectly fitted for the average SPM).
- All other remote sensing images show lower SPM concentrations in the estuary than the model does for spring and summer.

B.5 Conclusions on Model Calibration

A dynamic water quality model for SPM has been set up for the Western Scheldt estuary. It was calibrated on in-situ data and remote sensing data simultaneously, taking into account estimates (a band width) for errors in the data. During the final model calibration 5 model

parameters were varied, and the effect of adding dumpings of harbour silt was tested (see Table B.1). Model 'k' was selected as best result and serves as the basis for a T1-scenario simulation (dumping of silt for 1999 from Tunnel boring).

The process of model calibration and data model integration points out some discrepancies in the available data. Data from the continuous monitoring station at Terneuzen fitted well with only one model simulation (the initial model 'a') that was derived from the model set up. However, *this initial model has a poor performance for all other data.* This indicated that:

1. the model set up had to be adjusted with rather large parameter shifts for agreement with other data.
2. pitfalls that may occur when calibrating the model on one local station only. *There is a need of various data sources, from various techniques and from various locations for model calibration.*
3. the station Terneuzen is situated at a position where the total SPM might be dominated by a local source of SPM. This will need further discussion. Note that the 12 hour frequency peak in SPM observed at Baalhoek also indicates that at this station there is a large effect of local SPM fluctuations.

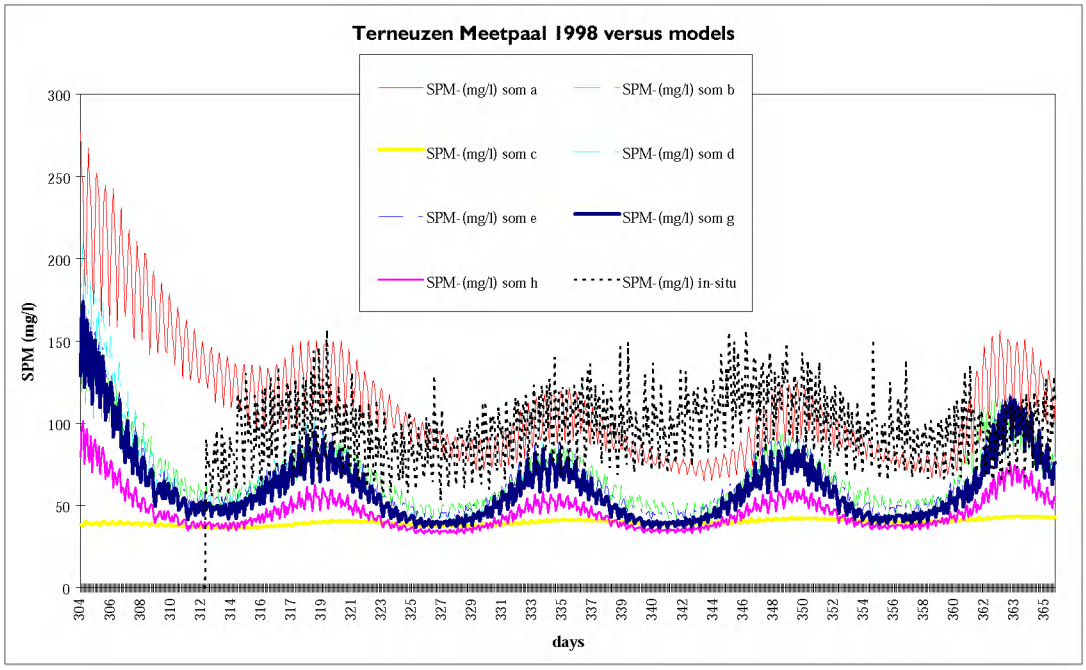

Figure B.2 Comparison of model results for models a-h at Terneuzen. Black-dotted line is in-situ data from continuous monitoring data (shifted over +8 days).

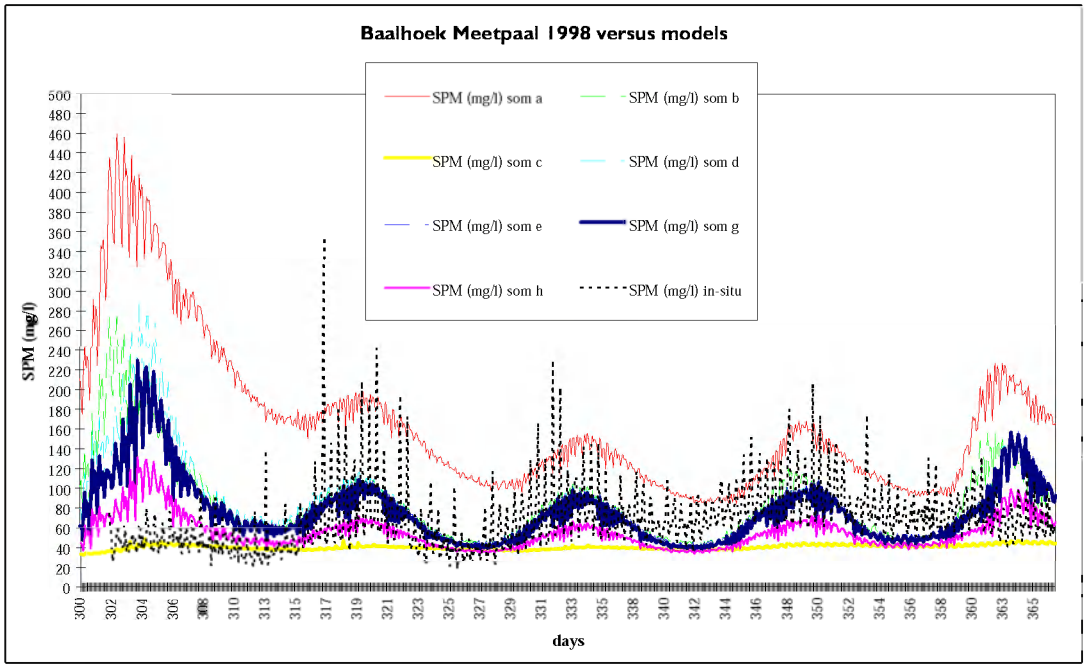

Figure B.3 Comparison of model results for models a-h at Baalhoek. Black-dotted line is in-situ data from continuous monitoring data (shifted over +8 days).

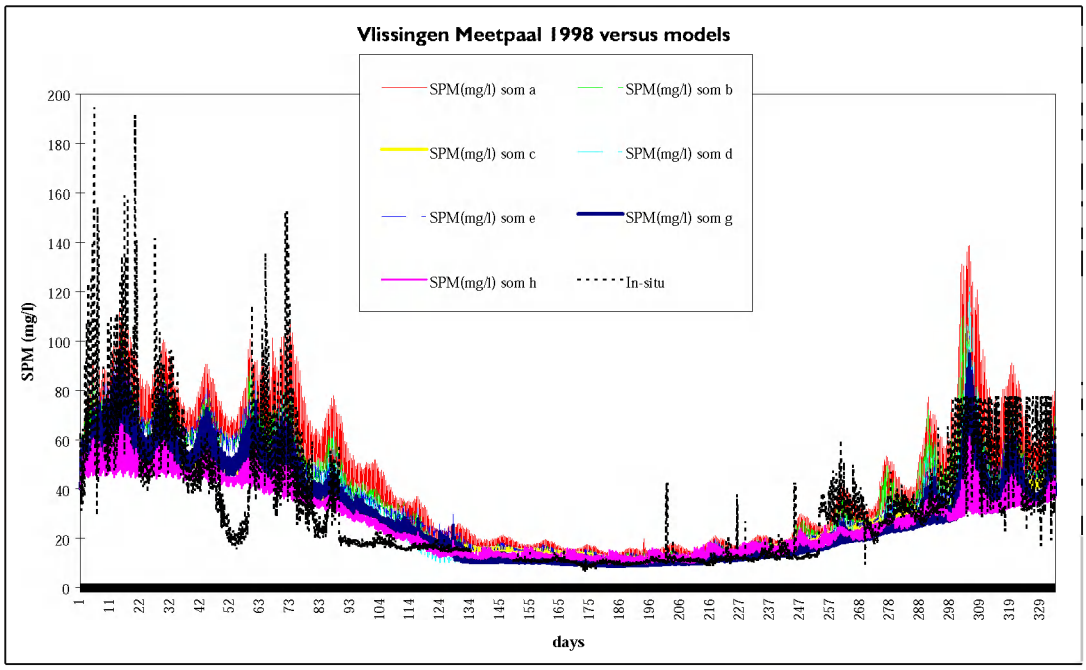

Figure B.4 Comparison of model results for models a-h at Vlissingen. Black-dotted line is in-situ data from continuous monitoring data (shifted over +8 days).